Iranian Journal of Veterinary Science and Technology

IJVST

Number 3
Volume 17
Year 2025
ijvst.um.ac.ir

IRANIAN JOURNAL OF VETERINARY SCIENCE AND TECHNOLOGY

ISSN (Print): 2008-465X
ISSN (Online): 2423-6306
Serial number: 40

دانشگاه فردوسی مشهد
Ferdowsi University of Mashhad

In the Name of God, the Compassionate, the Merciful

Iranian Journal *of* Veterinary Science and Technology

Editorial Office:
Faculty of Veterinary Medicine,
Ferdowsi University of Mashhad,
Azadi Square, Mashhad, IRAN
P.O. Box: 1793; Postal Code: 9177948974

Tel: +98 51 3880 3742 ***Fax:*** +98 51 3876 3852
Web: ijvst.um.ac.ir ***Email:*** ijvst@um.ac.ir

FERDOWSI UNIVERSITY OF MASHHAD PRESS

GENERAL INFORMATION

ISSN Print Edition: 2008-465X
ISSN Online Edition: 2423-6306

Journal Homepage:
ijvst.um.ac.ir

Abstracting and Indexing:
Scopus, ISI Master Journal List, Zoological Record; EMBASE, EBSCO, MIAR, Scientific Information Database (SID); Islamic World Science Citation Database (ISC); Magiran; Google Scholar; Centre for Agriculture and Biosciences International (CABI), DOAJ.

This journal has achieved the rating of:
- "Scientific-Research", by Commission of Evaluation of Iranian Scientific Journals, the Ministry of Science, Research and Technology, from Vol.7, No. 1, July 2015 onward.
- "International", by Commission of Evaluation of Iranian Scientific Journals, the Ministry of Science, Research and Technology, from Vol.13, No. 2, 2021 onward.

Publication Date:
Iranian Journal of Veterinary Science and Technology (IJVST) is published 4 times a year. Volume 14 with 4 issues appear in 2022.

SCOPE

Iranian Journal of Veterinary Science and Technology (IJVST) publishes important research advances in veterinary medicine and subject areas relevant to veterinary medicine including anatomy, physiology, pharmacology, bacteriology, biochemistry, biotechnology, food hygiene, public health, immunology, molecular biology, parasitology, pathology, virology, large and small animal medicine, poultry diseases, diseases of equine species, and aquaculture. Articles can comprise research findings in basic sciences, as well as applied veterinary findings and experimental studies and their impact on diagnosis, treatment, and prevention of diseases. IJVST publishes four kinds of manuscripts: Research Article, Review Article, Short Communication, and Case Report.

ON THE COVER

A microscopic view of the preen gland in a young chicken (6–9 months old). (see page 33).

Editorial Office:
Faculty of Veterinary Medicine,
Ferdowsi University of Mashhad,
Azadi Square, Mashhad, IRAN
P.O. Box: 1793; Postal Code: 9177948974

Tel: +98 51 3880 3742 ***Fax:*** +98 51 3876 3852
Web: ijvst.um.ac.ir ***Email:*** ijvst@um.ac.ir

FERDOWSI UNIVERSITY OF MASHHAD PRESS

TABLE OF CONTENTS

Mannir Dahiru Usman , Clarance Suh Yah , Victoria Folakemi Akinjogunla , Tauheed Abubakar Muazu, Abdulrazak Lawal, Yusuf ABUBAKAR, Khalid Shuaibu Hassan, Jamiu Olatoye Salako, Christian Anuoluwapo Olaseni

Biochemical and Molecular Characterization of Pseudomonas putida, P. fluorescens and P. aeruginosa Isolate from Oreochromis niloticus (TILAPIA) and Clarias gariepinus (AFRICAN CATFISH) 1

Maya Boukerrou, Rania Ridouh, Alaa Eddine Djeghar, Faiza Tekkouk-Zemmouchi, Baaissa Babelhadj, Allowen Evin, Claude Guintard

Osteo-Morphometry in Ouled-Djellal White Arab Sheep: Age-Related Correlations between Mandible, Skull and Body Measurements 8

Soheila Shirkhani, Behrooz Fathi

***Peganum harmala* extract delayed the lethal effect of viper snake *Echis carinatus* venom in mice** 21

Alhaji Zubair Jaji, Latifah Ozohu Abdulkarim, Furo Nathan Ahmadu, Esther Solomon Kigir, Kenechukwu Tobechukwu Onwuama, AbdulGaniu Olawale Ibrahim , Shaibu Mohammed Atabo, Sulaiman Olawoye Salamia, Wanmi Nathaniela

Changes in the Uropygial (preen) gland in Fulani ecotype chicken (gallus gallus domestica) a post-hatch study 29

Olubunmi Titilayo Ojoawo , Jelili Akinwole Akinlade, Opeyemi Agbeniyi, Opeyemi Oladipupo Hammed, Rom-Kalilu Fiwasade Adejoke

Preliminary Evaluation of the Therapeutic Effects of Neem Leaf Extract and Ivermectin in West African Dwarf Goats with Clinical Mange 38

Siamak Alizadeh, Mohammadreza Hosseinchi, Raman Esmaeilnejad

Radioanatomical Study of the Rose-Ringed Parakeet (Psittacula Krameri) Head Based on the Findings of Computed Tomography Scanning 47

IRANIAN JOURNAL OF VETERINARY SCIENCE AND TECHNOLOGY

Editorial Office:
Faculty of Veterinary Medicine, Ferdowsi University of Mashhad,
Azadi Square, Mashhad, IRAN
P.O. Box: 1793; Postal Code: 9177948974

Tel: +98 51 3880 3742 ***Fax:*** +98 51 3876 3852
Web: ijvst.um.ac.ir ***Email:*** ijvst@um.ac.ir

TABLE OF CONTENTS

Nader Ahmadi Saleh Baberi, Reyhaneh Ghasemi, Navid Emami, Hajar SohrabiNia

Low agreement between serological and molecular tests for the diagnosis of cattle brucellosis *61*

Mohammad Ahmadi Ashtiyani, Jalal Shayegh, Ali Rezapour, Habib MotieGhader

Oral Squamous Cell Carcinoma in a Budyonny horse: A case report 69

Errata *74*

Persian abstracts *76*

Author index *80*

Guide for authors *82*

IRANIAN JOURNAL OF VETERINARY SCIENCE AND TECHNOLOGY

Editorial Office:
Faculty of Veterinary Medicine, Ferdowsi University of Mashhad,
Azadi Square, Mashhad, IRAN
P.O. Box: 1793; Postal Code: 9177948974

Tel: +98 51 3880 3742 ***Fax:*** +98 51 3876 3852
Web: ijvst.um.ac.ir ***Email:*** ijvst@um.ac.ir

Iranian Journal of Veterinary Science and Technology

Received: 2024- Nov-14
Accepted after revision: 2025- May-31
Published online: 2025- Sep-01

Biochemical and Molecular Characterization of *Pseudomonas putida, P. fluorescens* and *P. aeruginosa* Isolate from *Oreochromis niloticus* (TILAPIA) and *Clarias gariepinus* (AFRICAN CATFISH)

Mannir Dahiru Usman [a], Clarance Suh Yah [b], Victoria Folakemi Akinjogunla [c], Tauheed Abubakar Muazu [d], Abdulrazak Lawal [e], Yusuf ABUBAKAR [f], Khalid Shuaibu Hassan [g], Jamiu Olatoye Salako [h], Christian Anuoluwapo Olaseni [h]

[a] Department of Veterinary Medicine, Bayero University Kano, Nigeria.
[b] Faculty of Health Science Research Office (HSSO). Faculty of Health Sciences, University of the Witwatersrand, Johannesburg, South Africa.
[c] Department of Fisheries and Aquaculture, Bayero University Kano, Nigeria.
[d] Department of Veterinary Anatomy, Bayero University Kano, Nigeria.
[e] Department of Veterinary Public health and Preventive Medicine, Bayero University Kano, Nigeria.
[f] Department of Veterinary Public health and Preventive Medicine, Federal University of Agriculture Zuru, Nigeria.
[g] Centre for Dryland Agriculture, Bayero University Kano, Nigeria.
[h] Department of Fisheries and Aquaculture, Bayero University Kano, Nigeria.

ABSTRACT

Bacterial pathogens are a major cause of economic losses in aquaculture and pose serious threat to public health. This study investigates the phenotypic and the genomic characteristics of pathogenic *Pseudomonas* species in two finfish species, *Oreochromis niloticus* (Tilapia) and *Clarias gariepinus* (African catfish), sourced from the Galadima fish market in Kano metropolis, Nigeria. Twenty fish samples, including 10 Tilapia and 10 African catfish were randomly selected and tissue samples (liver, spleen, intestine and gills) were collected for analysis. *Pseudomonas* spp. were screened via culturing and isolation techniques and biochemical tests. Molecular identification was carried out based on 16S rRNA gene sequence analysis. Out of all the samples analyzed, 6 % tested positive for *Pseudomonas* spp., including *P. putida* (5 %), *P. aeruginosa* (1.25 %), and *P. fluorescens* (1.25 %). This study confirms the presence of potentially pathogenic *Pseudomonas* species in commercially important finfish species from the Galadima fish market in Kano, Nigeria. These findings highlight the need for regular monitoring and molecular surveillance of bacterial pathogens in aquaculture products to prevent economic losses and safeguard public health.

Keywords

Tilapia, African catfish, Sequencing, Bacteria

Number of Figures: 3
Number of Tables: 6
Number of References:: 27
Number of Pages: 7

Abbreviations

PCR: Polymerase chain reaction
NCBI: National Center for Biotechnology Information
MR: Methyl red, VP: Voges Proskauer
BLAST: Basic local alignment search tool

Corresponding author:
Mannir Dahiru Usman
Email: mdusman.vmed@buk.edu.ng
Tel:+23(480)6558-1870

Introduction

Aquaculture is currently the fastest-growing sector of food-animal production globally [1] . In 2022, global aquaculture production reached approximately 130.9 million tons, significantly contributing to food security, especially in food-insecure regions [2]. The industry also supports the livelihood of millions of people worldwide [3]. According to World Bank (2024) classification, the total share of fisheries and aquaculture harvested by non-high-income countries in recent decades has increased from about 33 % in the 1950s to 84 % in 2022, Of this total production, the upper-middle-income countries contributed 56 %, lower-middle-income countries 26 %, high-income countries 16 % and low-income countries 2 % [3]. Global fish production is estimated to reach approximately 196 million tons by 2025 accounting for about 17.3 % of the total consumption of animal protein worldwide. In 2017, fish represented about 6.8% of the total animal protein consumption, with a per capita consumption estimate of 20.3 kg. This provides about 20 % of average per capita animal protein diet for nearly 3.3 billion people, and contributes at least 10 % of such protein intake for 5.6 billion people [4].

Finfish species such as tilapia and catfish are affordable sources of animal protein, and by-products [5]. They also serves as a source of income for low-income populations in rural, developing or undeveloped areas [6]. These species are known generally to occupy various habitats (freshwater, brackish or marine) and come in diverse shapes, sizes and biological adaptations.

Despite these benefits, infectious diseases remain a major setback to the aquaculture industry. They result in great economic losses due to fish mortality, poor marketability, increased treatment cost and potential zoonotic disease transmission [7].

Among bacteria pathogens *Pseudomonas* species stand out as gram-negative opportunistic bacteria, with high adaptability to survive in various environmental conditions, including the aquaculture environment [8]. Numerous species of *Pseudomonas* are known to be pathogenic for Aquatic and other animals including humans [9]. Pseudomonadiasis is one of the most prevalent diseases in global aquaculture [10], causing severe economic losses and decreased fish farming efficiency [11]. It has been reported to be among the most common diseases of fish, causing almost 100 % mortality in some cases [12]. Although many Pseudomonas spp have been described as opportunistic pathogens, several species including *P. putida, P. fluorescence, P. aeruginosa, P. anguilliseptica, P. baetica, P. chlororaphis, P. koreensis, P. luteola, P. plecoglossicida,* and *P. pseudoalcaligenes* were identified to be the primary pathogens of several disease cases of farmed fish [8, 9]..

In regions like Nigeria, limited information about the exact pathogen responsible for fish diseases hampers the implementation of effective preventative and control measures [7, 10]. Therefore, species-specific detection of *Pseudomonas* may help for establishing a more complete understanding of their pathological significance [13]. Molecular detection could also guide researchers to gain a clear understanding of the ecological impact of the pathogen and also overcome the deficiencies of the traditional approaches.

Given the limited literature and data on the molecular characterization of important microorganisms of fish and environmental health concerns from the study area, this study is the first of its kind in Kano, Nigeria. The present study aim to describe the phenotypic and genomic characteristics of pathogenic *Pseudomonas* species isolated from two fish species, Oreochromis niloticus and *Clarias gariepinus*, sold at the Galadima fish market in Kano metropolis, Nigeria.

Result

Pseudomonas species isolation rates

In this study, three Pseudomonas species (*P. fluorescens* P. *aeruginosa* and *P. putida*) reported to be fish pathogens were isolated and characterized. The overall isolation rate of pathogenic *Pseudomonas* from all the samples was 6 (7.5 %) after molecular characterization (5 % *P. putida*, 1.25 % *P. aeruginosa* and 1.25 % *P. fluorescens*) (Table 1).

Table 1.
Summary of the total isolation rate after Molecular characterization

Isolate	*Clarias gariepinus*	*Oreochromis niloticus*	Total (%)
P. putida	3	1	4 (5)
P. fluorescens	1	0	1 (1.25)
P. aeruginosa	1	0	1 (1.25)
Total	5	1	7.5

Pseudomonas fish species-specific isolation rates

The isolation rate from the African catfish (Clarias gariepinus) was 5 (12.5 %) while the specific isolation rates from the gills, liver, spleen and intestine were 3 (40 %), 0 %, 0 (0 %), 2 (20 %) respectively (Table 2). The isolation rate from the Tilapia (*Oreochromis niloticus*) was 1 (2.5 %) while the specific isolation rate from the gills, liver, spleen and intestine

were 0 %, 0 %, 1 (10) %, 0 % respectively (Table 2). Table 2 shows the isolation rate in different parts of *C. gariepinus* and *O. niloticus* from the market. There was significant difference in the isolation rate between *C. gariepinus* and *O. niloticus* ($p < 0.05$).

Table 2.
The percentage of Pseudomonas isolation in fish species from Galadima market, Kano Nigeria at the level of Biochemical characterization

Organs examined	*Clarias gariepinus*		*Oreochromis niloticus*	
	Isolation rate (out of 10)	%	Isolation rate (out of 10)	%
Gills	4	40	1	10
Liver	0	0	0	0
Spleen	1	10	1	10
Intestine	2	20	0	0
Total (out of 40)	7	17.5	2	5

Organ-Specific isolation rates of Pseudomonas

There were a significant difference in the isolation rate between the various body parts across both fish species ($p < 0.05$). The gills of *C. gariepinus* exhibited the highest rate of contamination, with an isolation rate of 30%. The gills and intestine are the only parts of the *C. gariepinus* contaminated, the intestine followed with a 20 % isolation rate. For the spleen, the isolation rate from the *C. gariepinus* was 0 % and 10 % from the *O. niloticus*. No *Pseudomonas* species were isolated in all the liver samples from both *C. gariepinus* and *O. niloticus*. Overall, the gills and intestines were the primary sites of *Pseudomonas* presence in *C. gariepinus*, while the spleen was the only contaminated site in O. niloticus. The gills samples from *C. gariepinus* had a higher isolation rate (30 %) than the O. niloticus (0 %). Similarly, the intestine of *C. gariepinus* had a higher isolation rate (20 %) than the *O. niloticus* (10 %). However, the spleen samples from *O. niloticus* had a higher isolation rate (10 %) than the *C. gariepinus* (%) (Table 3).

Table 3.
The percentage of Pseudomonas isolation in fish species from Galadima market, Kano Nigeria after Molecular characterization

Organs examined	*Clarias gariepinus*		*Oreochromis niloticus*	
	Isolation rate	%	Isolation rate	%
Gills	3	30	0	0
Liver	0	0	0	0
Spleen	0	0	1	10
Intestine	2	20	0	0
Total	5	12.5	1	2.5

Discussion

Fish and fishery products are vital for global nutrition and food security. Nonetheless, they are highly perishable, with quality influenced by species differences, feeding habits, and environmental conditions [15]. Improperly processed or raw fish can act as vehicle for pathogenic microorganisms, posing notable public health risks [16]. Among these, *Pseudomonas* spp are recongnised as important opportunistic pathogens in fish, with the potential to cause disease in humans while also serving as indicators of fish quality and safety [9]. In this study we established to species level the occurrence of the fish pathogen (*Pseudomonas* spp) of public health importance with an overall prevalence of 6 %.

Masbouba [17] reported a higher isolation rates, 36.9 % for *P. fluorescens* and 29.1 % for *P. aureginosa*, from diseased *Clarias gariepinus*. The elevated isolation rates in that study may be attributed to sampling clinically infected fish from an outbreak on a farm. Olayemi *et al.* [18] isolated *P. aerugenosa* from the gills of *C. gariepinus* in Ile-Ife, Nigeria.

The presence of *Pseudomonas* in the spleen, intestine and gills of fish (*C. gariepinus* and *O. niloticus*) sampled from the Galadima fish market in Kano metropolis showed bacterial contamination. This cause for concern, as *P. putida* and *P. fluorescens* are known to cause septicemia in fish. Their infections often resemble motile Aeromonas septicemia especially in stressed fish stocks [19,20]. As fish serve as an affordable source of protein, such contamination poses a serious health hazard to humans and may serve as zoonosis risks to consumers [21].

Interestingly, the findings of this study differs considerably from those of a similar investigation in Khartoum, where isolation rates of Pseudomonas from gills and intestines were 63 % and 31 % respectively [22]. The differences in isolation and characterization methodologies, sample origin, hygienic practices and the different sources of water and its quality may have contributed to the differing results. Moreover, the higher isolation rates in the

previous study may be associated with clinical infections in fish populations.

Fisheries are vital to food security, livelihoods, and economic growth in many Africa nations, including Nigeria [21, 23]. The study's findings indicate that fish in Kano region are susceptible to Pseudomonas infections. These infections have the potential to degrade fish quality, higher growth rates, increase mortality, and ultimately reduce profit margins for fish farmers. Additionally, managing such infections often requires antibiotic treatment, which raises production costs [24].

Pseudomonas species are particularly concerning due to their resistance to multiple antibiotics. In Nigeria, the regulation of antibiotic use in aquaculture is weak, increasing the risk of antimicrobial resistance (AMR) [25]. This issue threatens not just local aquaculture sustainability but also feeds into the global AMR crisis. The situation becomes even more alarming when Pseudomonas infections are transmitted to humans [26]. The risk escalates when Pseudomonas infections are transmitted to humans, *P. aeruginosa* is an opportunistic human pathogen and can pose serious health risks, especially to immunocompromised individuals, through the handling or consumption of contaminated fish [27].

In conclusion, the detection of *P. putida*, *P. aeruginosa* and *P. fluorescens* in fish from Kano, Nigeria, underscores the need for improved public awareness and deeper understanding of pathogenic bacterial infections in aquaculture. Enforcing strict hygienic control protocols, implementing preventive strategies, and promoting effective biosecurity practices are essential steps toward safeguarding healthy aquaculture environments

Materials and Methods

Study Area

This study was conducted at Galadima market, located in Fagge Local Government Area of Kano state, Nigeria (Latitude 12.0127° N and longitude 8.5344° E) [14]. Galadima Market is the largest hub for fresh fish in the region, where farmers supply fresh fish for wholesale and retails from the wild and in captivity (aquaculture) for consumption.

Study design

The aim of this research was to isolate *Pseudomonas* species of medical importance from two major fish species freshly brought for sale at the Galadima fish market in the Kano metropolis. A total of 80 tissue samples were collected, comprising the gills, liver, spleen, and intestine, from 20 fish specimens (10 *Clarias gariepinus* and 10 Oreochromis niloticus). Their morphometric measurements were also recorded (Table 4). Samples were cultured on Nutrient agar and and bacterial isolates were subjected to biochemical characterization followed by molecular identification through DNA sequencing.

Culture and Bacterial isolation

Culture, isolation and identification of bacteria were carried out based on the method described by [8]. Each sample was inoculated on Nutrient agar and incubated at 37°C for 24 hours. The growths were subjected to Gram staining and biochemical test for further identification.

The inoculation Media was prepared based on the manufacturer's instructions. A sterilized spatula was used to cauterize the surface of the sample. The cauterized surface was then cut using sterilized scissors. A swab stick was then inserted deep into the cut tissue sample to collect samples for primary smear preparation. Secondary and tertiary smear were made using a sterilized wire loop. The samples were incubated at 37oc for 24 hours. Plates were examined for bacterial growth, subcultured and re-incubated at 37°C for another 24 hours. Colonial morphology was then studied (Figure I). All isolates were preserved and later sent to South Africa for DNA sequencing.

Biochemical characterisation

Biochemical tests were conducted after the colony morphology assessment, assessment to further characterize the isolates (Figure 2). Standard conventional biochemical assays, included Gram staining, urease, citrate, catalase activities and oxidase, Indole, Methyl red (MR), Voges Proskauer (VP) and motility tests were carried out [8]. The test tubes containing the test media were labeled and arranged properly in a test tube rack, each was inoculated with an inoculum of the isolates and incubated at 37oc for 24 hours. After incubation, reagents such as Kovac's, VP1 and VP2 were added to the incubated peptone water for both Indole and MRVP tests respectively Reaction were recorded accordingly (Table 5) and DNA was extracted from confirmed isolates for sequencing.

Table 4.
Morphometric measurements of the Oreochromis niloticus and Clarias gariepinus collected from Galadima Fish Market, Kano State, Nigeria.

S/N	Fish Species	Total Length (cm) ± SD	Total Weight (g) ± SD	Standard Length (cm) ± SD
1	Oreochromis niloticus (range)	39.07 ± 5.52 (26.1 - 49.6)	589.23 ± 233.9 (140 - 1150)	36.27 ± 5.23 (22.15 - 47.2)
2	Clarias gariepinus (range)	41.29 ± 3.44 (35.0 - 48.2)	658.94 ± 174.2 (353.2 - 1020.5)	39.0 ± 3.45 (33.3 - 46.0)

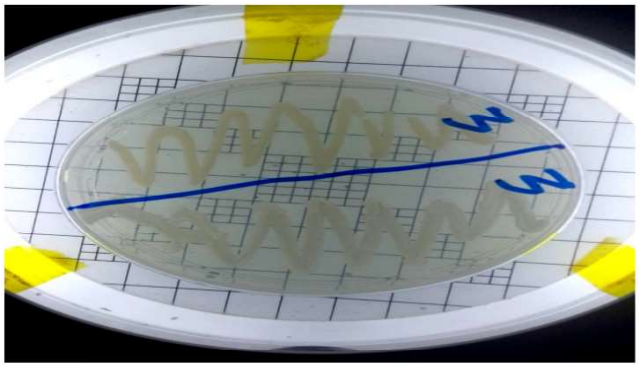

Figure 1.
Pseudomonas on nutrient agar

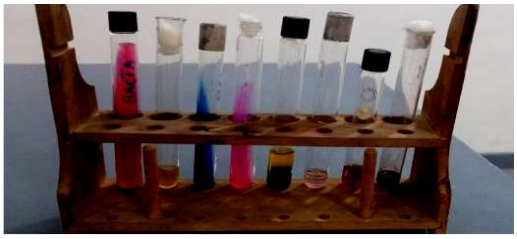

Figure 2.
Biochemical identification of Pseudomonas species

Table 5.
Biochemical tests and reactions

S/N	Test	Pseudomonas spp
1	Gram reaction	-
2	Oxidase	+
3	Indole	-
4	Methyl red	-
4	Voges-proskauer	-
5	Citrate	+
6	Catalase	+
7	Urease	-
8	Motility	+

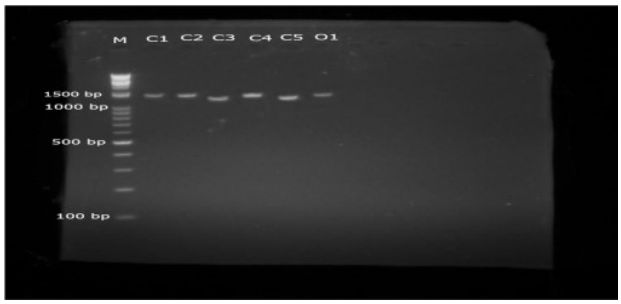

Figure 3.
Gel image showing position and base pairs for the different Pseudomonas species. Keys: C= *Clarias gariepinus*; O= *Oreochromis niloticus*; M= *Molecular ladder*: C1 = *P. putida*, C2= *P. putida*, C3= *P. fluorescen*, C4= *P. putida*, C5= *P. aeruginosa*, O1 = *P. putida*.

Extraction of genomic DNA, amplification by PCR and Sequencing

The confirmed isolates were sent to Inqaba Biotec™ (Pretoria, South Africa) for PCR, agarose gel electrophoresis and Sanger sequencing. Genomic DNA was extracted using the QIAamp DNA kit (Qiagen, Germany). DNA concentration and purity were assessed before molecular analysis. Primer selection, PCR amplification, purification of the amplified products, DNA sequencing and the sequence analysis were performed as described by Duman et al., 2021 [8].

PCR amplication targeted universal primer 16S rRNA (small subunit ribosomal RNA) gene using the primers listed in Table 6.

Figure 3 is a gel image showing position and base pairs for the different *Pseudomonas* species.

Species level identification was performed using sequencing of DNA dependent RNA polymerase subunits. The sequences obtained from the sequencing were analyzed and aligned. By BLAST the homologous searches were done from the results of the sequencing. The nucleotide sequence of the PCR product showed 99.29, 99.22, 94.81 % and 94.72 *Pseudomonas* putida, 96.52 % *Pseudomonas* aeruginosa and 94.72 % *Pseudomonas* fluorescens respectively. The results revealed similarity levels to published *Pseudomonas* species sequences in the NCBI database.

Authors' Contributions

A, B, and C conceived, designed and supervised the experiment
A, B, D, E, H and I collected and prepared the samples for the experiment
C, D, E, F, G, H and I conducted the experiment
D, G and F analysed and interpreted the results
A, B, C, F and E led the writing of the manuscript.

All authors contributed significantly to the success of the experiment, analysis and manuscript writing.

Table 6.
Universal Primers

Universal primer set used for PCR amplification	Target	Sequence (5' to 3')
16S-27F	16S rDNA sequence	AGAGTTTGATCMTGGCTCAG
16S-1492R	16S rDNA sequence	CGGTTACCTTGTTACGACTT

Acknowledgements

The authors acknowledge and thank the management and staff of the Biotechnology Laboratory, Center for Dryland Agriculture, Bayero University, Kano Nigeria.

Competing Interests

The authors declare that there is no conflict of interest.

Reference

1. 1. FAO. 2024. G20 backs FAO's Blue Transformation for sustainable fisheries and aquaculture, highlights family farming. FAO Newsroom, 2024.

2. Usman MD, Wakawa AM, Musa A, MT Ahmad, Ahmad KH, Muazu TA, Musa AZ, Atabo, SM. Occurrence of hemolytic Escherichia coli, antimicrobials residue in cultured Clarias gariepinus and assessment of antimicrobial use among catfish farmers in Kano metropolis, Nigeria. Journal of Sustainable Veterinary & Allied Sciences. 2022;2(2):105-113. Doi:10.54328/covm.josvas.2022.068.

3. FAO 2024a. FishStat. Global production by production source 1950-2022. [Accessed on 29 March 2024]. In: FishStatJ. Available at: www.fao.org/fishery/en/statistics/software/fishstatj. License: CC-BY-4.0.

4. Sudheesh PS, Al-Ghabshi A, Al-Mazrooei N, Al-Habsi S. Comparative Pathogenomics of Bacteria Causing Infectious Diseases in Fish. International Journal of Evolutionary Biology. 2012 May; 2012(1):45726. Doi:10.1155/2012/457264.

5. Akinjogunla VF, Shu'iabu U. Ichthyofauna Composition and Operative Artisanal Fishing Activities in Ajiwa Irrigation Dam, Katsina State, Northern Nigeria. Journal of Innovative Research in Life Sciences. 2022;4(1):45-53.

6. Akinjogunla VF, Yah CS, Akinjogunla OJ, Ayanwale AV, Adefiranye OO, Ejikeme CE. A Comparative Assessment of Morphometrics and Microbial Assemblages of Crassostrea gasar (Oyster) from Riparian Swampy Areas, off Lagos Lagoon, Nigeria. Tropical Journal for Natural Products Research. 2023 ;7(10):2837–2845. Doi: 10.26538/tjnpr/v7i10.39.

7. Usman MD, Wakawa AM, Musa A, Ahmad KH, Isiaku A. Occurrence of multi-drug resistant Enterobacteriaceae in cultured Clarias gariepinus (African catfish) in Kano metropolis, Nigeria. Sokoto Journal of Veterinary Sciences. 2021 ;19(2):106-111. Doi:10.4314/sokjvs.v19i2.5.

8. Magdy IH, El-Hady MA, Ahmed HA, Elmeadawy SA, Kenwy AM. A contribution on Pseudomonas aeruginosa infection in African catfish (Clarias gariepinus). 2014 ;575-588.

9. Duman M, Mulet M, Altun S, Saticioglu IB, Ozdemir B, Ajmi N, Lalucat J and García-Valdés E. The diversity of Pseudomonas species isolated from fish farms in Turkey. Aquaculture. 2021;535:736369. Doi:10.1016/j.aquaculture.2021.736369.

10. Irshath AA, Rajan AP, Vimal S, Prabhakaran VS, Ganesan R. Bacterial pathogenesis in various fish diseases: recent advances and specific challenges in vaccine development. Vaccines. 2023;11(2):470. Doi:10.3390/vaccines11020470.

11. Shabana BM, Elkenany RM, Younis G. Sequencing and multiple antimicrobial resistance of Pseudomonas fluorescens isolated from Nile tilapia fish in Egypt. Brazilian Journal of Biology. 2022;84:257144.Doi:10.1590/1519-6984.257144.

12. Thomas J, Thanigaivel S, Vijayakumar S, Acharya K, Shinge D, Seelan TSJ, Mukherjee A, Chandrasekaran N. Pathogenecity of Pseudomonas aeruginosa in Oreochromis mossambicus and treatment using lime oil nanoemulsion. Colloids and Surfaces B: Biointerfaces. 2014;116:372-377. Doi:10.1016/j.colsurfb.2014.01.019.

13. Tripathy S, Kumar N, Mohanty S, Samanta M, Mandal RN, Maiti NK. Characterisation of Pseudomonas aeruginosa isolated from freshwater culture systems. Microbiological Research. 2007;162(4):391-396. Doi:10.1016/j.micres.2006.08.005.

14. National Population Census. National Population Commission Office, Kano. Kano State, Nigeria. 2006

15. Derome N, Filteau M. A continuously changing selective context on microbial communities associated with fish, from egg to fork. Evolutionary Applications. 2020;13(6):1298-319. Doi:10.1111/eva.13027.

16. Jennings S, Stentiford GD, Leocadio AM, Jeffery KR, Metcalfe JD, Katsiadaki I, Auchterlonie NA, Mangi SC, Pinnegar JK, Ellis T, Peeler EJ. Aquatic food security: insights into challenges and solutions from an analysis of interactions between fisheries, aquaculture, food safety, human health, fish and human welfare, economy and environment. Fish and Fisheries. 2016;17(4):893-938. Doi:10.1111/faf.12152.

17. Masbouba IM. Studies on Pseudomonas Infection in Fish in Kafr El - Sheikh Province. Unpublished M V Sc. Thesis, Tanta University. 2004

18. Olayemi OO, Adenike K, Ayinde AD. Evaluation of antimicrobial potential of a galactose-specific lectin in the skin mucus of African catfish (Clarias gariepinus, Burchell, 1822) against some aquatic microorganisms. Research Journal of Microbiology. 2015;10(4):132. Doi:10.3923/jm.2015.132.144.

19. Attia MM, Abdelsalam M, Elgendy MY, Sherif AH. Dactylogyrus extensus and Pseudomonas fluorescens dual infection in farmed common carp (Cyprinus carpio). Microbial Pathogenesis. 2022;1;173:105867. Doi:10.1016/j.micpath.2022.105867.

20. Mishra SS, Das R, Sahoo SN, Swain P. Biotechnological tools in diagnosis and control of emerging fish and shellfish diseases. InGenomics and biotechnological advances in veterinary, poultry, and fisheries. 2020;1;311-360. Doi:10.1016/B978-0-12-816352-8.00014-X.

21. Luqman M, Hassan HU, Ghaffar RA, Bilal M, Kanwal R, Raza

MA, Kabir M, Fadladdin YA, Ali A, Rafiq N, Ibáñez-Arancibia E. Post-harvest bacterial contamination of fish, their assessment and control strategies. Brazilian Journal of Biology. 2024 ;1;3;84:e282002. Doi:10.1590/1519-6984.282002.

22. Yagoub SO. Isolation of Enterobacteriaceae and Pseudomonas spp. from raw fish sold in fish market in Khartoum state. Journal of Bacteriology Research. 2009;1(7):85-8.

23. Maulu S, Musuka CG, Molefe M, Ngoepe TK, Gabriel NN, Mphande J, Phiri M, Muhala V, Macuiane MA, Ndebele-Murisa MR, Hasimuna OJ. Contribution of fish to food and nutrition security in Southern Africa: challenges and opportunities in fish production. Frontiers in Nutrition. 2024; 11:1424740.

24. Chubado A. The role of fisheries resources in economic development and job creation in Nigeria. J Aqua Fish. 2021; 2(5):1-1.

25. Irshath AA, Rajan AP, Vimal S, Prabhakaran VS, Ganesan R. Bacterial pathogenesis in various fish diseases: recent advances and specific challenges in vaccine development. Vaccines. 2023;11(2):470. Doi: 10.3390/vaccines11020470.

26. Dauda AB, Nababa AS, Oshoke JO, Salele HA, Odetokun IA, Bello OM, Dasuki A. Antibiotics Use and Awareness of Risks Associated with Antimicrobial Resistance Among Fish Farmers in Katsina State, Nigeria.

27. Magdy IH, El-Hady MA, Ahmed HA, Elmeadawy SA, Kenwy AM. A contribution on Pseudomonas aeruginosa infection in African catfish (Clarias gariepinus).

How to cite this article
Usman MD, Yah ClS , Akinjogunla VF, Muazu TA, Lawal A, Abubakar Y, Hassan KhSh, Salako JO, OlaseniLASENI Ch O. Biochemical and Molecular Characterization of *Pseudomonas putida, P. fluorescens* and *P. aeruginosa* Isolate from *Oreochromis niloticus* (TILAPIA) and *Clarias gariepinus* (AFRICAN CATFISH). Iran J Vet Sci Technol. 2025; 17(3): 1-7.
DOI: https://doi.org/10.22067/ijvst.2025.90677.1437
URL:https://ijvst.um.ac.ir/article_46816.html

Iranian Journal of Veterinary Science and Technology

Received: 2025- Mar-18
Accepted after revision: 2025- Jul-22
Published online: 2025-Jul-23

RESEARCH ARTICLE

DOI: 10.22067/ijvst.2025.92718.1491

Osteo-Morphometry in Ouled-Djellal White Arab Sheep: Age-Related Correlations between Mandible, Skull and Body Measurements

Maya Boukerrou[a], Rania Ridouh[a], Alaa Eddine Djeghar[a], Faiza Tekkouk-Zemmouchi[a], Baaissa Babelhadj[b,c], Allowen Evin[d], Claude Guintard[e]

[a] Gestion Santé et Productions Animales Research Laboratory, Institut des Sciences Vétérinaires El-Khroub, Université Constantine 1 Frères Mentouri, Constantine 25000, Algeria.
[b] Department of Biological Sciences, Laboratory of Ecosystems Protection in Arid and Semi-Arid Zones, Faculty of Natural and Life Sciences, University of Kasdi Merbah, Ghardaïa road 30000 Ouargla, Algeria.
[c] Ecole normale supérieure de Ouargla, Algeria.
[d] Institute of Evolutionary Science-Montpellier (ISEM), University of Montpellier, CNRS, EPHE, IRD, Montpellier, France.
[e] Comparative Anatomy Unit, National Veterinary School of Nantes, Vet Agro Bio Nantes-Oniris, route de Gâchet, CS 40706, 44307 Nantes cedex 03, France.

ABSTRACT

The Ouled Djellal White Arab sheep is the predominant breed in the Algerian steppes and high plains, known for its adaptability and meat production. This study examines correlations between mandibular, body, and craniometric measurements in two age groups to establish a reference dataset for archaeozoological applications. Thirty female Ouled Djellal sheep, evenly divided into young adults (2–4 years) and adults (>4 years), were examined. Eight body measurements were recorded pre-slaughter, followed by eight mandibular and sixteen craniometric measurements after bone preparation, with four indices subsequently calculated. Significant correlations were observed between mandibular and body measurements, and between mandibular and craniometric parameters. Correlations were more numerous and stronger in adults (ranging from 0.47 to 0.70) than in young adults (from 0.41 to 0.67). While differences in covariation strength were observed between age groups, some correlations, such as those between thoracic perimeter (TP) and mental foramen length (ML6), and between head length (hL) and aboral height of the ascending branch (MH1) persisted across age groups. Dentition-related measurements correlated more frequently in adults, reflecting skeletal maturity, whereas variability in young adults indicated ongoing growth. These findings highlight the importance of age considerations in morphometric analysis and provide reference data for estimating body size and cranial dimensions from mandible measurements, contributing to archaeozoological studies of North African ancient specimens.

Keywords

Archaeozoology, correlations, craniometry, sheep

Abbreviations

ANCOVA : Analysis of Covariance

Number of Figures: 7
Number of Tables: 6
Number of References:: 24
Number of Pages: 13

Corresponding author: *Maya Boukerrou*
Email: maya.boukerrou@doc.umc.edu.dz
Tel:+213 (7) 7598-5249

Introduction

Algerian White Arab sheep, or Ouled Djellal, is the predominant sheep breed in the Algerian steppes and high plains, representing approximately 63% of the national flock, estimated at around 12 million head. Native to the Ouled Djellal region, this breed is characterized by its slim build, refined head, and high-quality white wool. It is well adapted to arid environments and suited to a nomadic lifestyle [1, 2].

Archaeological research in Algeria, despite being in its early stages, has led to the discovery of several sites, revealing animal bone remains from periods spanning the Paleolithic to the Neolithic. Notable examples include Oued Boucherit in Sétif (dated 2.4–1.7 million years ago) [3], Tighennif in Mascara (around 700,000 years ago) [4], and Gueldaman Cave GLD1 near Akbou, Béjaïa (dated to 5052-4885 B.C.) [5]. These sites have provided a variety of animal remains, including sheep mandibles and skull fragments. Such archaeozoological findings enable researchers to explore the attributes of ancient fauna. However one major challenge persists: the absence of robust reference database from living animals, particularly for body measurements. Estimation body measurements from archaeological bones relies on comparative datasets that include both body measurements and osteometric data from known specimens. Such reference datasets are scarce and currently absent for North African sheep populations.

This research is part of a series of osteobiometric studies on native Algerian ruminants, including sheep [6, 7], goats [8, 9], and camels [10, 11]. Building upon this work, the current study aims to examine correlations between the body measurements taken from live Ouled Djellal sheep and osteometric parameters of their skulls and mandibles. These correlations were compared between young adults and adults. The ultimate aim is to establish a reliable reference framework of one of the main breeds of Algeria, thereby enabling archaeozoologists to estimate body size and cranial dimensions from mandibular remains recovered in archaeological sites.

Result

Univariate analysis

The mandibular parameters MH1, MH7, MH8, and RM1 showed statistically significant differences between the age groups ($p < 0.05$; Table 1 and Figure 1). Average values for MH1 and MH8 were higher in adults, whereas MH7 and RM1 were higher in young adults. Notably, the average RM1 index was lower in adults than in young adults.

Bivariate analysis

Correlations by Age

Significant correlations between mandibular and body measurements, as well as between mandibular and craniometric parameters, were more numerous and stronger in adults than in young adults (Tables 2 and 3). When significant, correlation coefficient for adults ranged from 0.47 to 0.70, while for young adults they ranged from 0.41 to 0.67.

To evaluate whether age groups differed in their covariation patterns, a series of two-way ANCOVAs was conducted (Table 2). Some of these relationships remained stable across both age groups, such as those between thoracic perimeter (TP) and ML6, as well as between head length (hL) and MH1. However, 5 out of 20 mandibular body parameter pairs and and 10 out of 44 mandibular craniometric parameters pairs (Table 2) showed non homogeneous relationship between young adults and adults. In these case, correlation were analyzed separately. Examples include: Adults: correlations between head length (hL) and ML9, head width (hW) and MH9, as well as between MH8 and CL20, and MH9 and CL31. Young adults: correlations between scapulo-ischial length (SIL) and mandible weight (MW), as well as between CB8 and MB1. In general, measurements related to dentition (ML9, MH9, MH8) were more commonly observed in adults.

The four strongest and most significant correlations are illustrated in Figure 2, showing examples from both mandibular and body parameter pairs (Figures 2A,2B), as well as mandibular and craniometric parameters (Figures 2C,2D) for both age groups.

Correlations in the total population

Most correlations between mandiblar and body measurements were consistent between the two age groups (Table 2 and Table 3). Out of 99 correlations, only 14 differed significantly between age groups (Table 4). These correlations were considered low, with coefficients ranging from 0.10 to 0.39 or moderate from 0.40 to 0.59.

Analysis of mandible and skull measurements revealed several significant correlations between mandibular and craniometric parameters (Table 5). The strongest correlation was between mandible weight (MW) and skull weight (SW), with a correlation coefficient of 0.85.

The mental foramen length (ML6) and the aboral height of the ascending branch (MH1) were most frequently correlated with craniometric parameters. ML6 showed the strongest correlations with both skull lengths and height CH6, while MH1 was primarily correlated with cranial widths, but also with certain lengths and height CH6.

Table 1.
Descriptive statistics of mandibular parameters

Groups	Statistical parameters	ML6	ML8	ML9	MB1	MH1	MH7	MH8	MH9	MW	RM1	RM2
Young adults N=15	m	165,05	58,50	24,22	61,71	82,97	41,33	24,26	19,71	83,20	25,10	74,45
	Min	155,36	52,68	19,43	52,44	76,88	37,36	21,41	16,57	70,00	22,19	59,66
	Max	180,15	62,66	28,24	68,18	88,35	47,37	26,06	22,15	94,00	30,18	82,58
	σ	6,99	3,05	1,95	5,00	3,47	2,92	1,45	1,81	6,56	2,26	6,10
	CV%	4,23	5,21	8,04	8,10	4,18	7,07	5,99	9,20	7,88	9,00	8,19
Adults N=15	m	166,74	57,09	24,12	62,16	88,54	38,88	25,55	20,65	85,80	23,35	70,33
	Min	152,66	51,27	21,66	52,82	83,34	35,79	23,70	18,04	67,00	21,31	62,69
	Max	178,39	63,10	26,52	70,35	96,88	42,50	27,63	24,19		26,61	83,59
	σ	6,62	3,28	1,40	5,02	4,26	1,93	1,19	2,01	14,17	1,48	6,46
	CV%	3,97	5,74	5,81	8,07	4,81	4,95	4,64	9,72	16,51	6,35	9,18
total Population N=30	m	165,89	57,79	24,17	61,94	85,76	40,10	24,90	20,18	84,50	24,22	72,39
	Min	152,66	51,27	19,43	52,44	76,88	47,37	21,41	16,57	67,00	21,31	59,66
	Max	180,15	63,10	28,24	70,35	96,88	2,73	27,63	24,19		30,18	83,59
	σ	6,74	3,19	1,67	4,93	4,75	35,79	1,46	1,94	10,93	2,08	6,52
	CV%	4,06	5,52	6,90	7,95	5,54	6,81	5,86	9,61	12,93	8,58	9,00
p YA-A		0,389	0,25	0,885	0,87	0,001	0,033	0,033	0,325	0 ,95	0,019	0,067

m: mean, Min: minimum, Max: maximum, σ: standard deviation, CV%: coefficient of variation in %.
p YA-A corresponds to the p-value for the Wilcoxon-Mann-Whitney test comparing young adults and adults.

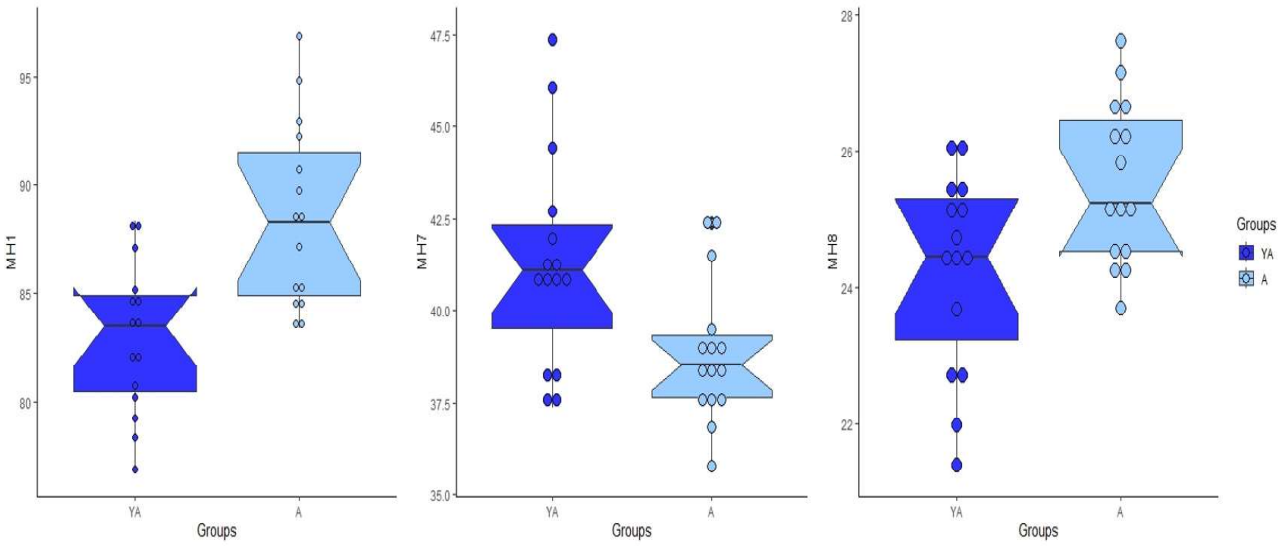

Figure 1.
Boxplots illustrating the variation in the mandibular variables MH1 (left), MH7 (middle), and MH8 (right) between Young Adults (YA) and Adults (A). Descriptions of these variables can be found in Table 6.

Table 2.
Correlations between mandibular and body parameters by age.

VAR 1	VAR 2	Total population	Adults	Young adults	p-value
LW	MH1	0.28	0.66	0.20	0.208
LW	MH8	0.29	0.17	0.65	0.335
SIL	MW	-0.07	0.20	-0.55	0.026
WH	MH8	0.13	0.73	0.16	0.137
TP	ML6	0.51	0.46	0.60	0.973
TP	MH1	0.38	0.66	0.30	0.298
TP	MH8	0.33	0.18	0.62	0.44
CP	MH1	0.48	0.64	0.35	0.292
CP	MH9	0.42	0.52	0.25	0.335
CP	MW	0.41	0.63	-0.26	0.042
hL	ML6	0.48	0.45	0.58	0.575
hL	ML9	0.34	0.61	0.09	0.02
hL	MH1	0.54	0.65	0.46	0.226
hW	MH9	0.20	0.57	-0.33	0.016
hW	MH1	0.48	0.50	0.52	0.912
hW	MW	0.50	0.63	0.52	0.679
eL	MH1	0.22	0.52	0.19	0.43
eW	MH1	0.29	0.62	0.29	0.516
eW	MH8	0.31	0.51	0.33	0.48
eW	MW	0.16	0.47	-0.40	0.033

p-value represent the difference between the young adults and the adults using two-way ANCOVA test.

Table 3.
Correlations between mandibular and craniometric parameters by age.

VAR 1	VAR 2	Total population	Adults	Young adults	p-value
CL1	ML6	0.76	0.80	0.72	0.352
CL1	MH1	0.63	0.77	0.56	0.538
CL2	ML6	0.81	0.82	0.80	0.481
CL2	MH1	0.63	0.76	0.57	0.621
CL7	ML6	0.75	0.76	0.76	0.24
CL7	MH1	0.58	0.50	0.60	0.952
CL10	ML6	0.55	0.51	0.56	0.917
CL10	ML9	0.32	0.50	0.21	0.231
CL10	MH1	0.42	0.28	0.56	0.378
CL20	MB1	0.45	0.50	0.39	0.616
CL20	MH8	-0.001	-0.38	0.48	0.032

Table 3 cont.

VAR 1	VAR 2	Total population	Adults	Young adults	p-value
CL31	ML6	0.46	0.60	0.52	0.779
CL31	ML8	0.65	0.57	0.68	0.577
CL31	MH7	0.47	0.53	0.27	0.273
CL31	MH9	0.04	0.54	0.28	0.033
CL31	MW	0.34	0.65	0.04	0.364
CL34	ML6	0.44	0.61	0.31	0.305
CL34	MB1	0.25	0.53	0.04	0.115
CB2	MH1	0.29	0.19	0.69	0.15
CB2	MH7	0.26	0.54	0.10	0.096
CB2	MH9	0.29	0.51	0.04	0.192
CB3	MH1	0.56	0.34	0.62	0.128
CB8	MH1	0.34	0.51	0.22	0.769
CB8	MB1	-0.23	0.21	0.57	0.024
CB8	MW	-0.04	0.19	0.46	0.044
CB8	RM2	-0.41	0.07	0.67	0.037
CB10	MH1	0.65	0.67	0.82	0.203
CB10	MH7	0.06	0.56	0.14	0.045
CB10	MH9	0.38	0.65	0.07	0.148
CB10	MW	0.33	0.61	0.20	0.087
CB14	MH1	0.68	0.56	0.69	0.453
CB14	MW	0.39	0.70	0.28	0.026
CB18	MH1	0.55	0.35	0.52	0.307
CB18	MW	0.09	0.32	0.41	0.049
CB19	MH1	0.60	0.62	0.60	0.947
CB19	MW	0.37	0.50	0.04	0.455
CH5	MH1	0.04	0.02	0.67	0.127
CH6	ML6	0.76	0.71	0.83	0.944
CH6	MB1	0.59	0.67	0.49	0.426
CH6	MH1	0.39	0.36	0.60	0.43
SW	ML8	0.14	0.45	0.53	0.02
SW	MH1	0.49	0.64	0.28	0.074
SW	MH7	0.19	0.63	0.16	0.003
SW	MW	0.85	0.92	0.50	0.062

p-value represent the difference between the young adults and the adults using two-way ANCOVA test.

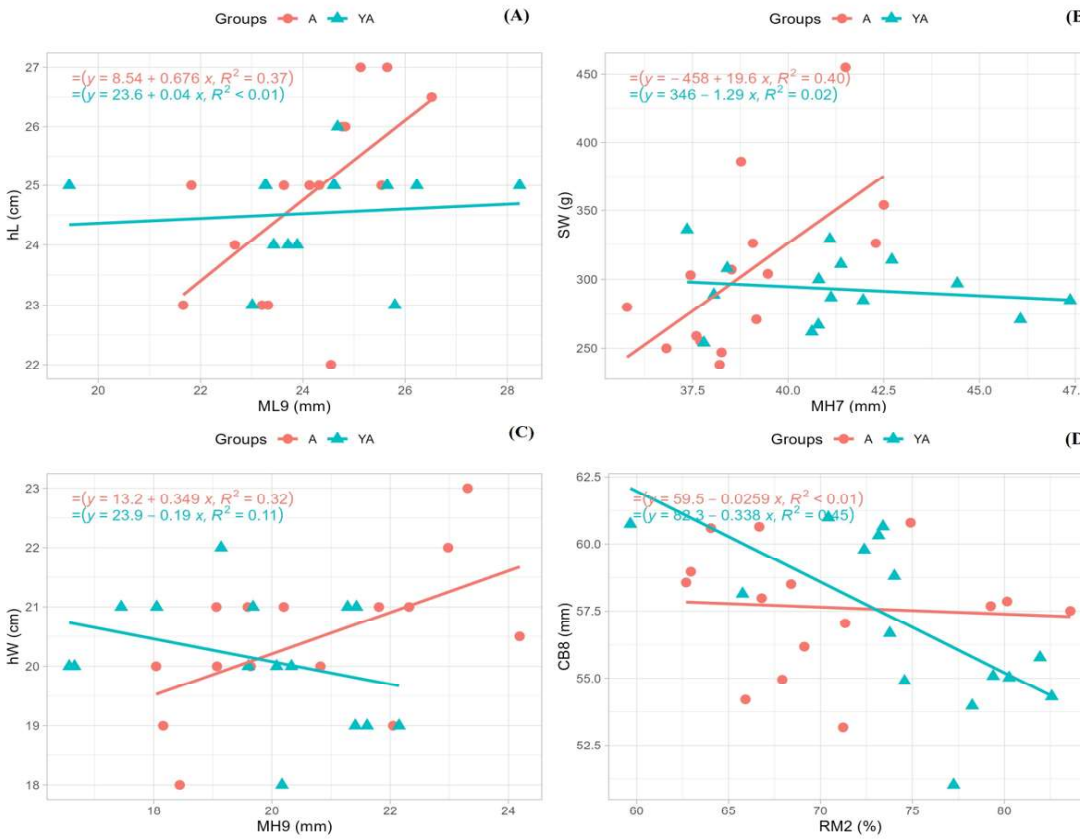

Figure 2.
Example of a scatter plots with linear regression between mandibular and body parameters: A. hL=f(ML9), B. hW=f(MH9) and between mandibular and craniometric parameters: C. SW = f(MH7), D. CB8 = f(RM2) for adults and young adults. Only the strongest correlations are shown.

Table 4.
Correlations between mandibular and body measurement for all specimens. Only the significant correlations ($p < 0.05$) are shown.

Body measurements	Mandibular measurements	Coefficient (r)	p-value
Head length	MH1	0.54	0.0022
Thoracic Perimeter	ML6	0.51	0.0042
Head width	MW	0.50	0.0044
Cannon perimeter	MH1	0.48	0.0068
Head length	ML6	0.48	0.0073
Head width	MH1	0.48	0.0066
Cannon perimeter	MH9	0.42	0.021
Scapulo-ischial length	RM1	0.41	0.022
Cannon perimeter	MW	0.41	0.024
Cannon perimeter	ML6	0.39	0.032
Live weight	ML9	0.38	0.038
Thoracic Perimeter	MH1	0.38	0.040
Scapulo-ischial length	MH7	0.38	0.038
Live weight	MH7	0.37	0.043

p-value represent the difference between the young adults and the adults using two-way ANCOVA test.

The four strongest and most significant correlations are illustrated in Figure 3, showing pairs of mandibular-body (Figure 3A,3B), and mandibular-craniometric relationships (Figure 3C,3D).

Table 5.
Correlations between mandibular and craniometric measurement for all specimens. Only the significant correlations ($p < 0.05$) are shown.

Mandibular measurements	Craniometric measurements	Coefficient (r)	*p*-value
MW	SW	0.85	2.17e-09
ML6	CL2	0.81	5.90e-08
ML6	CH6	0.76	9.46e-07
ML6	CL1	0.76	1.14e-06
ML6	CL7	0.75	2.20e-06
MH1	CB14	0.68	3.30e-05
ML8	CL31	0.65	0.00011
MH1	CB10	0.65	9.74e-05
MH1	CL1	0.63	0.00016
MH1	CL2	0.63	0.00021
MH1	CB19	0.60	0.00041
MB1	CH6	0.59	0.00065
MH1	CL7	0.58	0.00086
MH1	CB3	0.56	0.0013
MH1	CB18	0.55	0.0015
ML6	CL10	0.55	0.00181
MH1	SW	0.49	0.00578
MH7	CL31	0.48	0.00805
ML6	CL20	0.47	0.00802
MB1	CL7	0.46	0.00985
ML6	CL31	0.46	0.0100
MB1	CL20	0.45	0.0137
ML6	CB10	0.44	0.0139
MH9	CB10	0.38	0.0384
MW	CB19	0.37	0.0451
MB1	CL2	0.37	0.0445

Discussion

This study examined the correlations between mandibular and craniometric osteometric measurement, and body measurements on the living animals in Ouled Djellal sheep, focusing on age-related effects, it revealed that the average mandibular height behind M3 (MH7) was greater in young adults. This can be attributed to the association of MH7 with the eruption of third molar (M3): after M3 eruption is complete in adults, the mandibular body tends to lower (Figure 4). Similar findings were noted by Ridouh [12] in the native Algerian goat and by Dib, Babelhadj [11] in the Tergui dromedary. In contrast, the higher value of MH8 in adults may related to the eruption of premolars prier to adulthood.

When comparing the Ouled Djellal sheep with other breeds, the mental foramen length (ML6) in our sample (165.89 mm) is greater than that in other sheep breeds, including Yankassa (165 mm) [13], Konya Merino (163.44 mm) [14], Barbados Black Belly (160.9 mm), Awassi Females (155.22 mm) [15], French breeds (152 mm) [16], Mehraban (137.4 mm) [17], Morkaraman (122.29 mm), Tuj (118.85 mm) [18], and Iranian Native sheep (112.9 mm) [19]. This indicates that Ouled Djellal females have relatively longer mandibles compared to most other breeds.

Regarding mandibular angle width (MB1), the Ouled Djellal (61.94 mm) exhibits a mean value close to that of Sharri females (61.64 mm) [20] and Awassi females (60.22 mm) [15]. yet exceeded values reported for Norduz females (45.14 mm) [21], Konya Merino (56.88 mm) [14], Tuj (43.61 mm), Morkaraman (43.2 mm) [18], and French breeds (58 mm) [16]. This suggests broader mandibles in Ouled Djellal females.

The height of the ascending branch (MH1) is particularly higher in Ouled Djellal females (85.76 mm), than French breeds (80 mm) [16], Mehraban (77.5 mm) [22], Konya Merino (76.11 mm) [14], Barbados Black Belly (70.8 mm) [23], Zell sheep females (69.81 mm) [24], Iranian native sheep (62.6 mm) [19], Morkaraman (62.08 mm) [18], Norduz females (61.98 mm) [21], and Tuj (60.86 mm) [18]. This further supports the Ouled Djellal females are distinguished by the greater height of their mandibular branches.

Comparing our findings with to Ami's [6] results on Ouled Djellal from the same region, the mean values of ML6 (153.20 mm), MB1 (59.6 mm) and MH1 (79.86 mm) were lower in Ami's study. This difference may be due to the presence of juvenile individuals in Ami's dataset.

Since these three parameters (ML6, MB1, MH1) represent the mandibular dimensions along its main

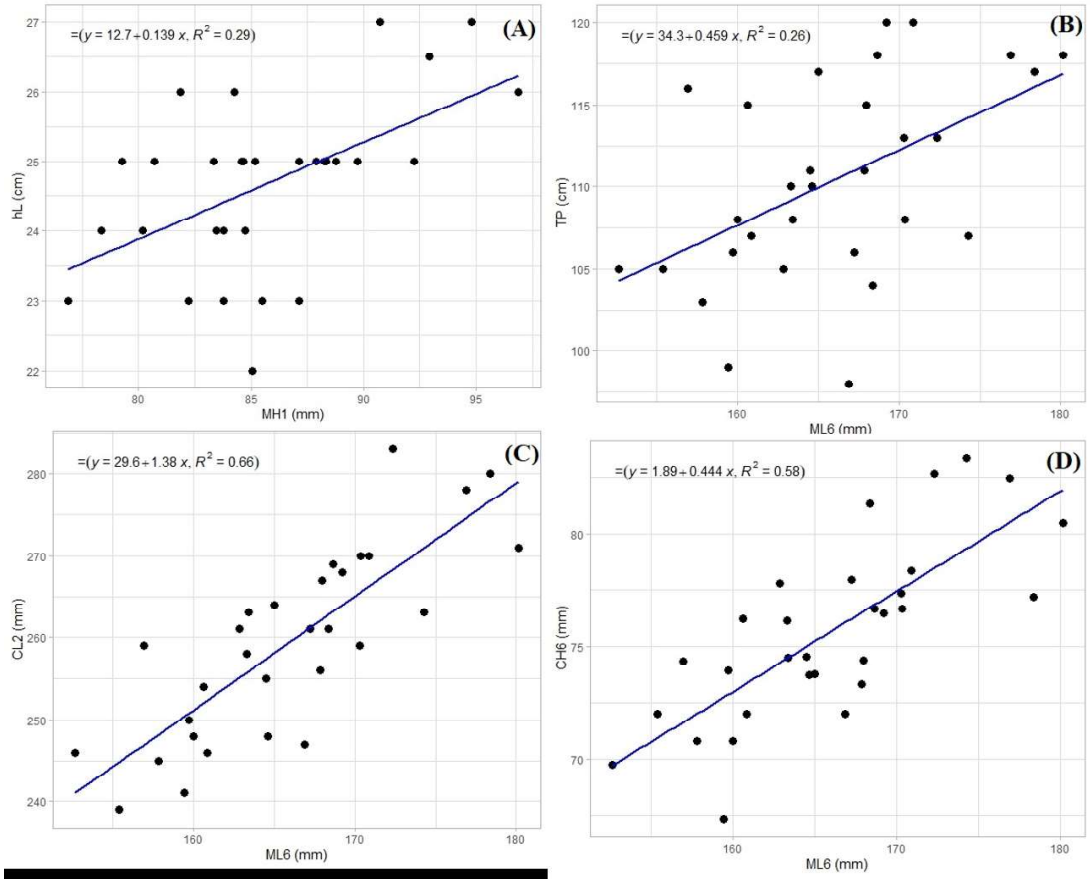

Figure 3.
Example of scatter plots with linear regression between mandibular and body parameters: A. hL=f(MH1), B. TP=f(ML6) and between mandibular and craniometric parameters: C. CL2 = f(ML6), D. CH6 = f(ML6) for all specimens. Only the strongest correlations are shown.

Figure 4.
Mandibular corpus height behind the third molar (MH7) in young adults (top) and adults (bottom)

axes, our results suggest that the mandibles in our study population are overall relatively larger than other sheep breeds.

The lower RM1 values in adults, suggest thinner mandibular bodies compared to young adults. Additionally, both RM1 (24.22%) and RM2 (72.39%) in our study were lower than those reported by Ami [6] for Ouled Djellal (26.06% and 74.63%), and by Guintard and Fouché [16] for French breeds (25% and 73%). These findings indicate that the mandibles in our study possess more slender bodies.

Moreover, the correlation patterns were stronger and more consistent in adults than young adults. In young adults, varying growth rates between zootechnical and bone parameters suggest that osteological development is still ongoing. In contrast, adults exhibit a stable and fully mature form across both zootechnical and osteological measures, which likely explains the stronger consistency in correlations at this stage.

Furthermore, the relatively weak correlations in the total population can be attributed to several factors, such as age, dentition stage, nutrition, and environmental conditions, all of which influence the growth and development of sheep in uneven ways, thereby leading to differences in mandible morpholo-

gy. Despite these variations, certain mandibular measurements (especially MH1 and ML6) show significant correlations with body parameters. For example, the strongest correlations were observed between the head length and the height of the ascending branch (MH1), and between the thoracic perimeter and the mental foramen length (ML6) (Figure 3).

Regarding the correlations between the mandibular and craniometric parameters, the results indicate that ML6 reflects the linear skull dimensions, while mandibular height (MH1) is more closely associated with cranial widths. These results suggest that the mandibular axes (ML6, MH1, MB1) showing significant correlations with the three main skull dimensions (length, width, and height). This reflects harmonious growth between mandibular and cranial structures, confirming that the mandible and skull may develop in an interdependent manner.

The results indicate that the mandibles of Ouled Djellal females are both larger and more slender than those of other breeds, with adults exhibiting even greater size and slenderness compared to young adults. Across the population, significant correlations were observed between body and mandibular measurements. Additionally, the three axes of the mandible are significantly correlated with skull measurements, reflecting the harmonious growth between the mandible and skull. Most correlations between mandibular, craniometric, and body parameters remain consistent across age groups, while others vary. Significant correlations are more frequent in adults, suggesting that they have reached a stable, mature form in both zootechnical and osteological aspects, whereas young adults exhibit differential growth patterns. The identified correlations highlight the importance of taking into account the age of the specimens when mandibular measurements are used for estimating body and craniometric dimensions. This study paves the way for age-specific predictive models in archaeozoology.

Materials and Methods

This study was conducted on 30 female Ouled Djellal sheep obtained from the slaughterhouses in Aïn Fakroun and Télaghma, northeastern Algeria, between March 2022 and May 2023. All animals appeared healthy and were over two years old. They were divided into two age groups: young adults (YA) aged 2 to 4 years, and adults (A) over 4 years.

Body Measurements

Before slaughter, eight body measurements (Figure 5) were recorded using a tape measure (cm): withers height (WH), scapulo-ischial length (SIL), thoracic perimeter (TP), cannon perimeter (CP), head length (hL), head width (hW), ear length (eL), and ear width (eW). Live weight (LW) was estimated using body weight prediction formulas: LW= 0.635 TP - 23.026 and LW = 0.7536 SIL - 19.2234 [13].

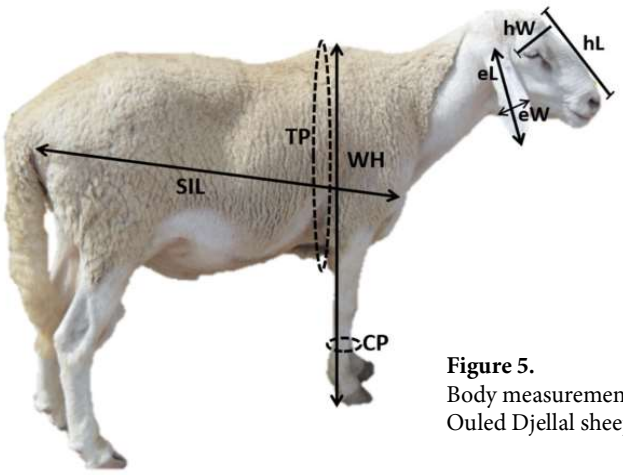

Figure 5.
Body measurements on Ouled Djellal sheep

Specimen Preparation

After slaughter, each head was collected, labeled with identification number, and linked to its corresponding body measurement data. Soft tissues were removed, and the bones were cleaned by boiling for several hours, rinsing in running water, and air-drying. Each skull and mandible (right side) were labeled accordingly. Mandible weight (MW) and skull weight (SW) were recorded in grams using a precision scale.

Osteometric Measurements

Eight mandibular and sixteen cranial measurements were taken in millimeters using a caliper (accuracy ± 0.02 mm), a ruler for linear dimensions (e.g., CL1, CL2), and a thickness compass for specific parameters (e.g., CH6). Measurement protocols followed Ridouh's [14] methodology (Figures 6 and 7, Table 6). Additionally, four indices (RM1, RM2, RC5, and RC7), were selected based on criteria proposed by Guintard [15], then were calculated to provide further morphometric insights.

Statistical Analysis

All statistical analyses were conducted using R (version 4.3.1) with the RStudio interface. Descriptive statistics, including mean (m), minimum (min), and maximum (max) values, were calculated for each age group and the total population (TP). Variability was assessed using the standard deviation (σ) and coefficient of variation (CV% = (σ/m) × 100).

The Wilcoxon-Mann-Whitney test was applied to compare univariate measurements between age groups, with significance set at $p < 0.05$. Pearson correlation coefficients (r) were calculated for each variable pair, interpreted as: 0–0.10 for no correlation, 0.10–0.39 for low correlation, 0.40–0.59 for moderate correlation, 0.60–0.79 for strong correlation, and 0.80–1 for very strong correlation. Additionally, p-values were also used to assess the significance of the correlations. Two-way ANCOVAs was used to evaluate the homogeneity of correlations between young adults and adults.

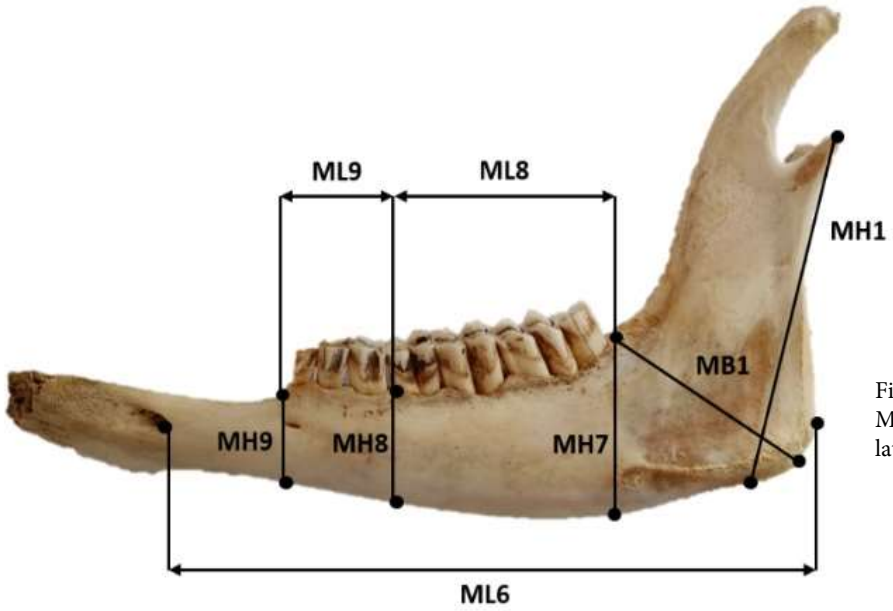

Figure 6.
Measurements of the right mandible in lateral view.

Table 6.
Denomination of mandibular measurements (variable names starting with M) and craniometric measurements (variable name starting with C), and indices (variable name starting with R).

Mandibular Measurements	Denominations	Craniometric Measurements	Denominations
ML6	Mental foramen length	CL1	Total length
ML8	Molar tooth row length	CL2	Condylobasal length
ML9	Premolar tooth row length	CL7	Oblique length of the muzzle
MB1	Width at the mandibular angle	CL10	Median frontal length
MH1	Aboral height of the ascending branch	CL20	Orbit base to jugular process length
MH7	Mandibular height behind M3	CL31	Naso-dental oblique length
MH8	Mandibular height in front of M1	CL34	Temporal fossaLength
MH9	Mandibular height in front of P1	CB2	Greatest breadth of the occipital condyles
RM1	MH7 / ML6 × 100	CB3	Greatest breadth at the bases of the paraoccipital processes
RM2	MB1 / MH1× 100	CB8	Least frontal breadth
		CB10	Least breadth between the orbits
		CB14	Greatest palatal breadth
		CB18	Greatest breadth across the premaxillae
		CB19	Zygomatic breadth
		CH5	Least height of the occipital
		CH6	Splanchnocranial height
		RC5	CB8 / CL1 × 100
		RC7	CH5 / CL1 × 100

M3: Third molar, M1: First molar, P1: First premolar.

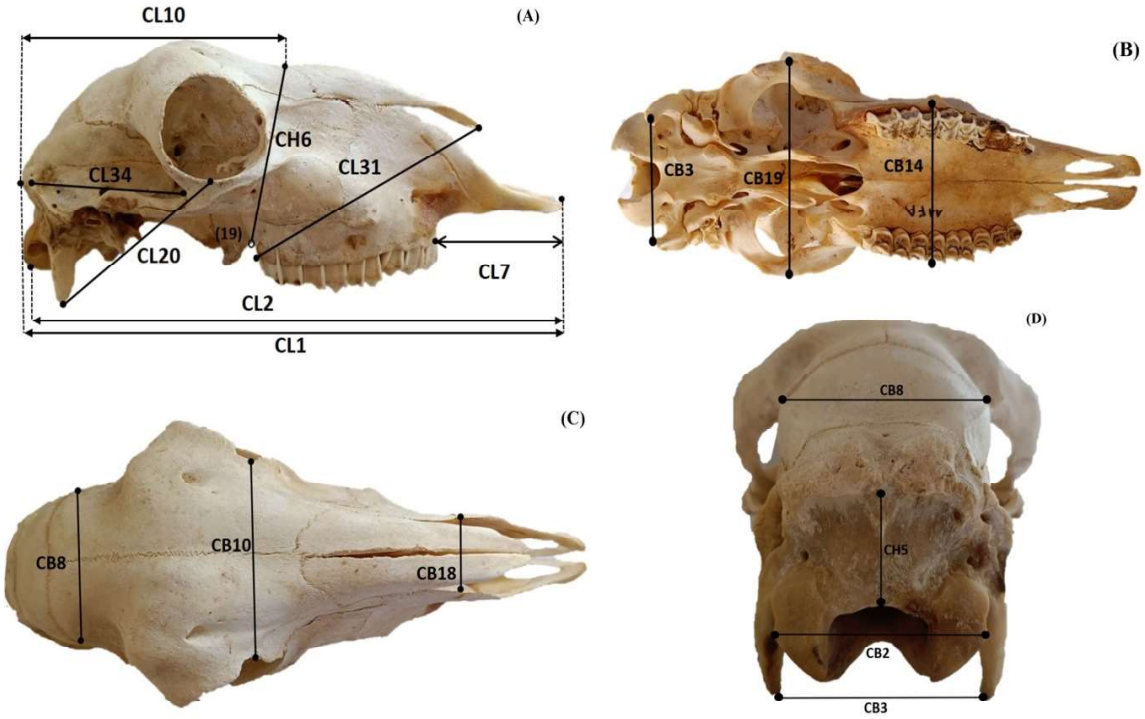

Figure 7.
Skull measurements: (A) lateral view, (B), ventral view (C) dorsal view, (D) caudal view.

Authors' Contributions

MB contributed to the collection of the specimens, methodology, statistical analysis, and writing the first draft. RR contributed to the interpretation of the results, the writing of the discussion and revised the first draft. AED worked on the methodology. FTZ revised the final draft. BB revised the final draft. AE was involved in statistical analysis, writing, review, and editing. CG provided the original idea and revised the final draft. All authors provided critical feedback and helped shape the research, analysis and manuscript.

Acknowledgements

We would like to thank Dr. Abderrahmane Boukerrou for his assistance in sample collection, Dr. Hafida Koutchoukali for her support in specimen preparation, and Pr. El Hacene Brerhi for his invaluable guidance. We also thank the staff of the Ain Fakroun and Teleghma slaughterhouses for their cooperation.

AE work is supported by the European Research Council (ERC) under the European Union's Horizon 2020 research and innovation program (Grant Agreement No. 852573).

Competing Interests

The authors declare that there is no conflict of interest.

Reference

1. Adaouri M. Evaluation des paramétres zootechniques de la nouvelle race ovine en cours de constitution issue d'un croisement génétique alternatif d'amélioration antre Ouled Djellal et D'man [Thèse de Doctorat en Sciences Agronomiques]: Ecole Nationale Supérieure Agronomique, Algérie; 2019.

2. Feliachi K, Kerboua M, Abdelfettah M, Ouakli K, Selheb F, Boudjakji A. Rapport national sur les ressources génétiques animales: Algérie. MADR; 2003.

3. Duval M, Sahnouni M, Parés JM, van Der Made J, Abdessadok S, Harichane Z, et al. The Plio-Pleistocene sequence of Oued Boucherit (Algeria): A unique chronologically-constrained archaeological and palaeontological record in North Africa. Quaternary Science Reviews. 2021;271:107-16. Doi:10.1016/j.quascirev.2021.107116.

4. Geraads D. Pleistocene Carnivora (Mammalia) from Tighennif (Ternifine), Algeria. Geobios. 2016;49(6):445-58. Doi:10.1016/j.geobios.2016.09.001.

5. Merzoug S, Kherbouche F, Sehil N, Chelli R, Hachi S. Faunal analysis of the Neolithic units from the Gueldaman Cave GLD1 (Akbou, Algeria) and the shift in sheep/goat husband-

ry. Quaternary International. 2016;410:43-9. Doi:10.1016/j.quaint.2015.08.076.

6. Ami K. Approche ostéo-morphométrique des têtes de la population ovine autochtone [Thèse de Magister en Médecine Vétérinaire]. Algérie Université des Frères Mentouri Constantine 1; 2014.

7. Guintard C, Tekkouk-Zemmouchi F. Osteo-biometric approach of the Ouled Djellal breed (Ovis aries, L.-Algeria). Revue de Médecine Vétérinaire. 2010;161(11):521-31.

8. Guintard C, Ridouh R, Thorin C, Tekkouk-Zemmouchi F. Etude ostéométrique des métapodes de chèvres (Capra hircus, L., 1758) d'Algérie: cas de la race autochtone Arabia. Revue de Médecine Vétérinaire. 2018;169:221-32.

9. Ridouh R, Tekkouk-Zemmouchi F, Thorin C, Guintard C. Prédiction du sexe à partir d'un échantillon de métacarpes de chèvres (Capra hircus L., 1758) de race Arabia (Algérie): réalisation d'un référentiel pour l'archéozoologie. Revue de Paléobiologie, Genève 2019;38(1):255-65.

10. Babelhadj B, Adamou A, Thorin C, Tekkouk-Zemmouchi F, Benaissa A, Guintard C. Étude ostéo-biométrique comparée des «races» camelines Algériennes Sahraoui et Targui (Camelus dromedarius L., 1758). Revue de Médecine Vétérinaire. 2016;167:77-92.

11. Dib M, Babelhadj B, Benaissa A, Oudini E, Brahimi Z, Tekkouk Zemmouchi F, et al. Osteo-morphometric Approach to the Heads of Dromedaries (Camelus dromedarius, L, 1758): Case of the Algerian Targui Population. Agricultural Science Digest - A Research Journal. 2024;44(2):372-81. Doi:10.18805/ag.DF-590.

12. Ridouh R. Crâniométrie et ostéométrie des métapodes de la chèvre autochtone [Thèse de Doctorat en Sciences Vétérinaire]: Université des Frères Mentouri Constantine 1, Algérie; 2021.

13. Shehu SA, Bello A, Sonfada ML, Suleiman HM, Umar AA, Danmaigoro A, et al. Morphometrical study of the mandiblar bone of female Yankasa sheep (Ovis aries Linne). Journal of Anatomy and Physiological Studies. 2018;2(1):001-6.

14. Özüdoğru Z, Ilgün R, Teke BE. A Morphometric Study on Mandibula of Konya Merino. Uluslararası Tarım ve Yaban Hayatı Bilimleri Dergisi. 2019;5:392-5. Doi:10.24180/ijaws.599005.

15. Yılmaz B. İvesi Koyunlarında (Ovis aries) Mandibula'nın Morfometrik İncelemesi. Harran Üniversitesi Veteriner Fakültesi Dergisi. 2020;9(2):189-93. Doi:10.31196/huvfd.813490.

16. Guintard C, Fouché S. Osteometric study of osseous heads of sheep (Ovis aries, L.). Revue de Médecine Vétérinaire. 2008;159(12):603-17.

17. Karimi I, Hadipour M, Nikbakht P, Motamedi S. The lower jawbone of Mehreban sheep: a descriptive morphometric approach. World's Veterinary Journal. 2011;2:57-60.

18. Demiraslan Y, Gülbaz F, Özcan S, Dayan MO, Akbulut Y. Morphometric analysis of the mandible of Tuj and Morkaraman sheep. Journal of Veterinary Anatomy. 2014;7(2):75-86. Doi;10.21608/jva.2014.44813.

19. Monfared AL. Clinical Anatomy of the Skull of Iranian Native Sheep. Global Veterinaria. 2013;10(3):271-5. Doi:10.5829/idosi.gv.2013.10.3.7253.

20. Jashari T, Duro S, Gündemir O, Szara T, Ilieski V, Mamuti D, et al. Morphology, morphometry and some aspects of clinical anatomy in the skull and mandible of Sharri sheep. Biologia. 2021;77:423 - 33.Doi:10.1007/s11756-021-00955-y.

21. Dalga S, Aydın U, Bayram R. Radiological, Morphological and Morphometric Investigation of Mandible in Norduz Sheep. Dicle Üniversitesi Veteriner Fakültesi Dergisi. 2023;16(2):85-90. Doi:10.47027/duvetfd.1334159.

22. Karimi I, Onar V, Pazvant G, Hadipour MM, Mazaheri Y. The Cranial Morphometric and Morphologic Characteristics of Mehraban Sheep in Western Iran. Global Veterinaria 2011;6(2):111-7.

23. Mohamed R, Driscoll M, Mootoo N. Clinical anatomy of the skull of the Barbados Black Belly sheep in Trinidad. Int J Curr Res Med Sci. 2016;2(8):8-19. Doi:10.4322/jms.112017.

24. Marzban Abbasabadi B, Hajian O, Rahmati S. Investigating the morphometric characteristics of male and female Zell sheep skulls for sexual dimorphism. Anatomical Sciences Journal. 2020;17(1):13-20.

How to cite this article
Boukerrou M,Ridouh R , DjegharAE, Tekkouk - Zemmouchi F, BabelhadjB, Evin A, Guintard C. Osteo-Morphometry in Ouled-Djellal White Arab Sheep: Age-Related Correlations between Mandible, Skull and Body Measurements. Iran J Vet Sci Technol. 2025; 17(3): 8-20.
DOI: https://doi.org/10.22067/ijvst.2025.92718.1491
URL:https://ijvst.um.ac.ir/article_47051.html

Iranian Journal of Veterinary Science and Technology

Received: 2025- Jan- 05
Accepted after revision: 2025- Jun-02
Published online: 2025- Jun- 03

RESEARCH ARTICLE

DOI: 10.22067/ijvst.2025.91424.1454

Peganum harmala extract delayed the lethal effect of viper snake *Echis carinatus* venom in mice

Soheila Shirkhani, Behrooz Fathi

Department of Basic Sciences, Faculty of Veterinary Medicine, Ferdowsi University of Mashhad, Mashhad, Iran.

ABSTRACT

This study investigated the possible antagonistic effects of *Peganum harmala* extract against the lethal toxicity of *Echis. carinatus* venom. A total of 72 adult albino mice were divided into 12 equal groups in 6 experimental protocols. In protocol I (control), Group A only treated with *E. carinatus* venom (10 mg/kg). They died after 80 min averagely. In protocol II, Groups B1 and B2 were treated simultaneously with 15 and 30 mg/kg of *P. harmala*, respectively, and 10 mg/kg venom. Their survival time increased to 232 and 210 min, respectively. In protocol III, groups C1 and C2 were treated with 10 mg/kg venom followed 15 min later by *P. harmala* at 15 and 30 mg/kg respectively. Their time to death was increased to 246 and 220 min respectively. In protocol IV, groups D1 and D2, treated with pre-incubated of venom with 15 and 30 mg/kg of *P. harmala*. Their survival time increased to 211 and 195 min, respectively. In protocol V groups E1 and E2 received only *P. harmala* extract intraperitoneally (15 and 30 mg/kg). In protocol VI, groups F1, F2, and F3 received only *P. harmala* extract (orally) at 15, 30, and 60 mg/kg. All mice in these groups remained alive. *Peganum harmala* extract significantly ($p < 0.05$) increased animal survival time, has an antagonistic effect against lethal action of *Echis carinatus* venom.

Keywords

Snakebite, Echis carinatus, Venom, Peganum harmala, Antivenom, Mice

Number of Figures: 2
Number of Tables: 1
Number of References:: 39
Number of Pages: 8

Abbreviations

PLA2: Phospholipase A2
IV: Intravenously
IP: Intraperitoneal
µl: Microliter
MAO: Monoamine oxidase
WHO: World Health Organization
LD50: Lethal dose 50%
LD100: Lethal dose 100%
FUMH: Ferdowsi University of Mashhad Herbarium
DPPH: 2, 2-diphenyl-1-picrylhydrazyl

Corresponding author: *Behrooz Fathi*
Email: *b-fathi@um.ac.ir*
Tel:+98(91)5976-5651

Introduction

Snakebites are a considerable global public health concern that pose a significant threat to both humans and animals. Approximately 5.4 million individuals are bitten by snakes annually, resulting in up to 138,000 deaths . Therefore, it is essential to promptly diagnose and provide appropriate treatment to minimize potential complications of envenomation [1,2].

Iran, located in West Asia, possesses remarkable biodiversity and a land of 81 snake species, of which 25 are venomous and considered medically significant. Among these, the *Echis. carinatus*, (Figure 1) a member of the Viperidae family, is predominantly found in the southern regions of Iran [3]. *E. carinatus* is infamous for its aggressive behavior and a highly toxic venom, which primarily disrupts blood coagulation and the haemostatic system [4]. Warrell et al. (1977) reported that bites from *E. carinatus* result in a higher mortality rate than those caused by other venomous snake species in Northern Africa and Asia [5]. Between 2002 to 2011, Iran recorded 53,787 snakebite cases and 67 related deaths [6].

Antivenom therapy remains the important mainstay of snakebites treatment. It can effectively neutralize venom toxins and alleviate their adverse effects. However, several limitations are associated with antivenom use. First, antivenoms often exhibit limited specificity and may not be effective against venom variants. Additionally, their administration can trigger allergic reactions in recipients, ranging from mild skin rashes to severe life-threatening anaphylaxis. Furthermore, antivenoms may not always be readily available, especially in remote areas or low-resource countries, due to high production costs. Administering antivenoms can be complex, as they often require careful dosing and monitoring. In some cases, multiple doses may be needed, factors that increase cost and logistical challenges. Moreover, their effectiveness in addressing localized tissue damage induced by venoms is limited and in severe cases, if left untreated, local effects may lead to disability, permanent tissue necrosis, or amputation [7,8,9]. Given these limitations, the development of improved or adjunctive treatments for snakebite envenomation is essential. Therefore, scientists are searching for safer alternative treatment options that are easier to produce, store, transport, purchase, and administer, in order to overcome these barriers.

In regions where snakebite incidents are prevalent and access to medical facilities is limited, plant-based medicine stands as an exceptional reservoir for seeking antivenom. In such regions, herbal remedies may often be the only treatment available [10,11].

It is worth noting that while herbal medicines have their advantages, the efficacy of many of them have not been scientifically investigated, nor have their active components been identified and isolated [13]. In some tribal areas of India, sometimes local populations rely on plant extracts to manage the severe local effects of Daboia russelli russelli (Russell's viper) envenomation, without any scientific validation [14]. However, some plant species have demonstrated scientifically measurable anti-venom properties. For instance, the Withania somnifera (ashwagandha) has been shown to neutralize venom of the speckled cobra [15], and aqueous root extract of Mimosa pudica have inhibited hyaluronidase and protease activities from venoms of Indian snake, *Naja naja*, *Vipera russelli* and *E. carinatus*, in dose dependent manner [16]. These compounds have natural PLA2 inhibitors and interact with the active site of PLA2s, proving their efficacy as anti-inflammatory and antidotes [17].

Figure 1.
Viper snake Echis carinatus, also called saw-scaled viper (prepared by B. Fathi)

It has been reported that Tabernaemontana alternifolia root extracts neutralize enzymatic activities of *E. Carinatus* and Naja naja venom [18]. The compounds such as flavonoids, polyphenols, tannins, sterols, terpenoids, and polysaccharides, found in this plant, neutralize the venom's hydrolytic enzymes, specifically phospholipases, proteases, and hyaluroni-

dase. These compounds effectively interfere with the harmful effects of the venom [13, 19], thereby preventing the release of inflammatory, vasodilatory, and vasoconstrictive mediators that typically occur during envenomation. This, in turn, minimizes damage to local tissue, inflammation, myonecrosis, impairment of vital organs, and modifications in coagulation components [13, 20].

Peganum harmala L, (Syrian Rue) is a perennial plant belonging to the family Zygophyllaceae [21,22]. *P. harmala*, particularly in its seed, contains a variety of phytoconstituents mostly bioactive alkaloids [23], including harmine, harmalol, harmaline, harmol, vasicine, vasicinone, deoxyvasicine, deoxyvasicinone, and several β-carboline [24,25]. These compounds contribute to the *P. harmala*'s broad spectrum of therapeutic beneficial properties such as, antidiabetic, anti-asthmatic, anti-arthritis, antihypertension, anticancer, antimicrobial, anti-inflammatory, antiviral, antidiarrheal, antiemetic, antidepressant, anthelmintic, and antioxidant effects[26]. In Iranian folk medicine, burning *P. harmala* seeds and utilizing the resulting smoke is a common practice for air disinfection.

There been unverified reports suggesting the use of *P. harmala* in certain regions of Iran for relieving bites and stings from various animal sources. However, these claims have yet to be supported by scientific evidence and research. The present study, aimed to investigate the potential of *P. harmala* extract as a treatment for snakebites, marking the first examination of its effectiveness against the lethal effects of *E. carinatus* venom.

Results

Protocol I

In Protocol I, group A served as control group and received an intraperitoneal injection of *E. carinatus* venom at a dose of 10 mg/kg. The mortality rate in this group was 100%, and the average time to death recorded at 80 ± 5 minutes (Figure 2).

Protocol II

In this protocol, mice in groups B1 and B2 were received *P. Harmala* extract at the doses of 15 and 30 mg/kg, respectively, in combination with 10 mg/kg of *E. carinatus* venom administered simultaneously. In this group, the mortality rate was 100%, and the average time to death was 232 minutes in Group B1 and 235 minutes in Group B2. These values were significantly different from the time to death of animals in Group A ($p < 0.01$). (Figure 2) (Table 1).

Protocol III

In this protocol, animals in Groups C1 and C2 received *P. harmala* extract at doses of 15 and 30 mg/kg, respectively, 20 minutes after being injected with 10 mg/kg of *E. carinatus* venom. The average time to death were 246 minutes for Group C1 and 220 minutes for Group C2. These values were significantly different from the time to death of animals in Group A ($p < 0.01$)

Table 1.
Application of different protocols and summary of the experiment results

Protocols	Groups	No of mice	venom mg/kg	P. Harmala mg/kg	Average time to death (min)
I	A	6	10	-	80
II	B1	6	10	15	232
II	B2	6	10	30	235
III	C1	6	10	15	246
III	C2	6	10	30	220
IV	D1	6	10	15	211
IV	D2	6	10	30	195
V	E1	6	-	15	Live
V	E2	6	-	30	Live
VI	F1	6	-	15/Po	Live
VI	F2	6	-	30/Po	Live
VI	F3	6	-	60/Po	Live

Protocols: I, Group A, only received venom at dose of 10 mg/kg (control).
Protocols: II, Groups B1& B2, received venom at 10 mg/kg along with P. harmala at 15 and 30 mg/kg (simultaneously).
Protocols: III, Groups C1 & C2, received venom at 10 mg/kg and P. harmala at 15 and 30 mg/kg respectively, after a 15-minute interval.
Protocols: IV, Groups D1 & D2 received venom at 10 mg/kg along with P. harmala at 15 and 30 mg/kg incubated for 30 min prior to injection. The intraperitoneal (IP) route was used for injection.
Protocols: V Groups E1 & E2 received only P. harmala at 15 and 30 mg/kg orally (IP).
Protocols: VI Groups F1, F2 & F3 received only P. harmala at 15, 30 and 60 mg/kg orally(Po).

(Figure 2) (Table 1).

Protocol IV

In this protocol, groups D1 and D2 received a pre-incubated mixture of *P. harmala* extract at doses of 15 and 30 mg/kg, respectively, with 10 mg/kg of *E. carinatus* venom. The extract and venom were incubated together for 20 min prior to injection. The average time to death was 211 minutes in Group D1 and 195 minutes in Group D2. These values were significantly different from the time to death of animals in group A ($p < 0.01$) (Figure 2) (Table 1).

Protocol V

In this protocol, groups E1 and E2 received only *P. Harmala* extract at doses of 15 and 30 mg/kg, respectively, via intraperitoneal injection. All mice in these groups survived, indicating no observable toxic effects at these dosages.

Protocol VI

In this protocol, groups F1, F2, and F3 received *P. Harmala* extract at doses of 15, 30 and 60 mg/kg, respectively, administered orally. All mice in these groups survived (Table 1). This observation indicates no toxic effects of the extract at the tested concentrations.

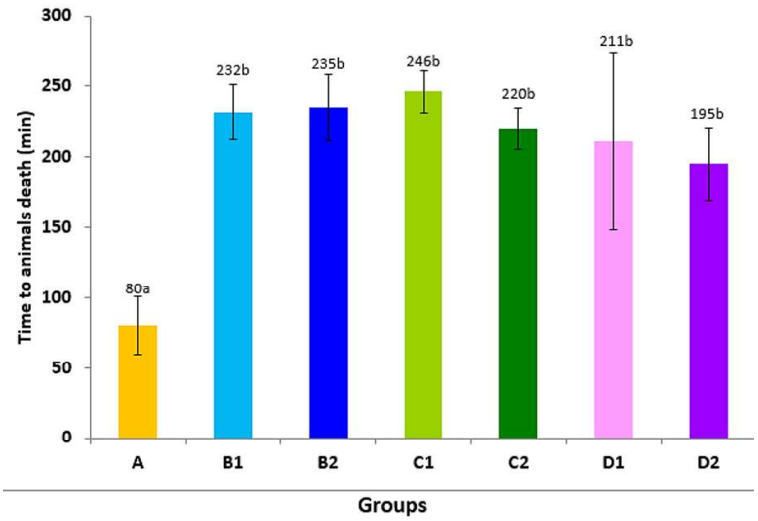

Figure 2.
Display the Mean and standard deviation of the survival time for different treatments groups. Values that are followed by different superscript letters (a, b) indicate a significantly difference at the level of ($p < 0.05$).
Group A, received only venom at 10 mg/kg, Groups B1& B2, received venom at 10 mg/kg along with P. harmala at 15 and 30 mg/kg (simultaneously).
Groups C1 & C2, received venom at 10 mg/kg and P. harmala at 15 and 30 mg/kg respectively, after a 15-minute interval.
Groups D1 & D2 received venom at 10 mg/kg along with P. harmala at 15 and 30 mg/kg incubated for 30 min prior to injection. The intraperitoneal (IP) route was used for injection.

Discussion

To date, there has been no documented scientific research on the interaction between *P. harmala* and animal venom particularly the venom of *E. carinatus*. The findings of this study provide initial evidence that *P. harmala* extract possesses a notable antagonistic effect against the lethal toxicity of *E. carinatus* venom.

Statistical analysis confirmed that simultaneous administering of *P. harmala* extract at doses of 15 and 30 mg/kg with the venom significantly increased the average survival time compared to the control group. Interestingly, this protective effect did not appear to follow a strict dose-dependent pattern. In fact, increasing the dose from 15 to 30 mg/kg resulted in a decrease in average survival time in some groups (C2 and D2). Although *P. harmala* extract did not fully neutralize the lethality of *E. carinatus* venom, it significantly increased the average survival time of the tested animals. The mechanism underlying this protective effect remains unclear. Previous studies on other plant-derived compounds have suggested different mechanisms, that maybe could also potentially apply to *P. harmala* as well.

Importantly, the extract of *P. harmala* did not exhibit any toxic effects on its own at different dosage levels, whether administered through injection or oral administration. This observation supports its potential safety as a therapeutic agent at these concentrations. Nonetheless, it is important to note that *P. harmala* extract can be toxic at higher orally doses [22]. The antagonistic effect of extract when combined with venom, may suggest it's possible interference with the venom's molecular interactions. The exact mechanism is still unknown.

The venom of *E. carinatus* consists of PLA_2, hyaluronidase, and Zn^{2+} metalloprotease, it's known for potent hemorrhagic and procoagulant effects. [4,16]. PLA_2 enzymes are particularly damaging due to their ability to hydrolyze phospholipids in cell membranes, leading to the rupture of erythrocytes and capillaries, and resultant hemorrhage [27]. Beyond bleeding, these enzymes can induce various systemic effects, including cardiotoxicity, myotoxicity, neurotoxicity (both pre or post-synaptic), edema, hemolysis, hypotension, convulsion and platelet aggregation [28].

In addition to PLA_2, the zinc-dependent metalloprotease found in viper venom including that of *E. carinatus*, degrade the endothelial linings of blood vessels, resulting in spontaneous hemorrhage [29]. The synergistic action of metalloprotease

and PLA_2 is responsible for the release of endogenous inflammatory mediators, promotes local edema, and increased free radical formation at the bite site.

It is possible that the hemorrhagic activity of this venom is interfered by the *P. harmala* extract components. These compounds may have antagonistic effects with the metalloprotease and PLA_2 activities or chelate metal ions such as Zn^{2+} or Ca^{2+}; which are essential cofactors for the enzyme's functionality [30,31].

Previous research have been reported with other plant extracts. For example, Andrographis paniculata and Aristolochia indica have demonstrated the ability to block the hemolysis caused by *E. carinatus* venom in agarose-erythrocyte gels [32]. Likewise , Horsfieldia amygdaline is a plant from which PLA_2 inhibitors have also been extracted [33]. Also, it has been reported that Vitis vinifera extracts have shown efficacy in neutralizing venom induced edema [34[. It is plausible that *P. harmala* extract operates through a comparable mode of action, which contains numerous anti-inflammatory and active chemical constituents These include phenolic compounds, amino acids (such as phenylalanine, valine, histidine, and glutamic acid), flavonoids (such as coumarin, tannins), sterols, and toxic alkaloids known as β-carbolines (which include Harmine, Harmaline, Harmol, and Harmalol) [25,24]. These β-carbolines have an affinity for multiple receptor type, such as serotonin, muscarinic, histamine, and benzodiazepine [35]. We can assume that the extract of *P. harmala* extract interferes with interaction between the specific receptors and their counterpart components present in the venom of *E. carinatus* , thereby potentially diminishing the venom's lethal potency.

In addition to receptor- level effects, several studies suggest that the bioactive alkaloids, harmaline and harmine, possess the capability to interfere with various enzymatic activity. Harmaline and harmine are selective inhibitors of monoamine oxidase (MAO), an enzyme responsible for the degrading crucial neurotransmitters, such as serotonin, dopamine, and norepinephrine [36].

Some snake venoms can block acetylcholine release and inhibit the neuromuscular junction [37]. Interestingly, *P. harmala*'s substances has demonstrated the ability to inhibit acetylcholinesterase and butyrylcholinesterase. Inhibiting acetylcholinesterase can lead to the accumulation of acetylcholine, prolonging muscle stimulation and delaying paralysis [38].

Another critical avenue through which snake venom often exerts its toxicity is through the generation of reactive oxygen species (ROS), leading to oxidative stress, inflammation and tissue damage. *P. harmala* has been found to possess strong antioxidant properties, known as 2, 2-diphenyl-1-picrylhydrazyl (DPPH). Its β-carbolines have shown considerable anti-inflammatory and antioxidant properties, which can effectively neutralize ROS. This ability to reduce oxidative stress, inflammation, and pain potentially contributes to its antivenom activity against *E. carinatus* venom" [39].

Conclusion

In conclusion, our study demonstrates that the extract of *Peganum Harmala* effectively extract possesses significant protective effects and can delay the lethal toxicity of *Echis. carinatus* venom. Consequently, it can be considered as an adjunctive therapy to complement standard clinical treatments, particularly in remote areas where immediate access to healthcare facilities and anti-venom is limited.

Materials and Methods

Ethical Considerations

Compliance with ethical guidelines: The proposal and experiments were approved by the Animal Ethical Committee of our Faculty of Veterinary Medicine. (Ethics code IR.UM.REC.1401.171).

Venom

The freeze-dried crude venom of *E. carinatus* was kindly provided by the Razi Vaccine and Serum Research Institute (Karaj, Iran). It was stored at 4°C and freshly prepared by dissolving it in a sterile saline to a final volume of 500 µl prior to administration.

Preparation of Peganum harmala extract

The *P. harmala* plants were harvested from agricultural fields near the city of Sabzevar (36°12'45"N and 57°40'35"E), located in the western region of Razavi Khorasan province in Iran. The species was identified at the Herbarium of Ferdowsi University of Mashhad (13613-FUMH). After drying the plant material in a dark room at 28 ± 4 °C for two weeks, the black seeds were separated and ground into a fine powder. Ethanolic extraction was carried out at Department of Pharmacognosy, Faculty of Pharmacy, Mashhad University. About 100 grams of the powdered seeds were poured into a 500 ml Erlenmeyer flask, and 300 ml of methanol was added until the solvent covered the powder by approximately 2 cm. The mixture was stirred, covered, and kept in a dark location for 48 hours. Then the upper portion of the solution was filtered using Whatman no. 1 filter paper. Additional methanol was added to the sediment portion and stirred for 30 minutes, and this process was repeated multiple times until the upper phase of the solution turned completely colorless. The resulting solution was subjected to a vacuum rotary evaporator (IKARV 10, Germany) set at 45 °C and 60 rpm. . The solvent was gradually evaporated, eventually yielding a viscous extract. The extract was then transferred onto a plate and oven-dried to fully remove residual solvent. Finally, the extract was wrapped in aluminum foil and stored in a refrigerator at 4°C. Initial efforts to dissolve the extract using conventional solvents were unsuccessful. Ultimately, it was found that the most effective method involved dissolving the extract in 2 Normal HC followed by pH adjustment to 7.5 using NaOH , resulting in a stable and fully soluble preparation.

Animals

A total of 72 healthy adult albino mice (8-10 weeks and weighing 35±5 grams) were obtained from the Animal House at Mashhad University of Medical Sciences. The mice were housed in the animal facility at Faculty of Veterinary Medicine, with controlled environmental conditions including a 12:12 light-dark cycle, a temperature of 22±3°C, and a relative humidity of 55±10%. Animals were maintained in standard rodent cages with free access to food and water. All experimental protocols were approved by the Animal Ethics Committee at Ferdowsi University of Mashhad (code: IR.UM.REC.1401.171).

Experimental protocols

The study was designed using six experimental protocols (I-VI) (Table 1). involving 12 equal groups of mice (n = 6 per group): A, B1, B2, C1, C2, D1, D2, E1, E2, F1, F2 and F3.

Protocol I (control): group A received only *E. carinatus* venom at a dose of 10 mg/kg intraperitoneally (IP). Protocol II: groups B1 and B2 were treated with 15 and 30 mg/kg of P. Hermala extract, respectively, simultaneously with 10 mg/kg of venom (IP). Protocol III: group C1 and C2 were treated with 15 and 30 mg/kg of P. Hermala extract, respectively, 20 minutes after receiving venom at 10 mg/kg (IP). Protocol IV: group D1 and D2 received a mixture of venom and P. Hermala extract (15 and 30 mg/kg, respectively), that were pre-incubated at room temperature (26±2°C) for 20 minutes before IP injection. Protocol V: groups E1 and E2 received only P. Hermala extract at doses of 15 mg/kg and 30 mg/kg, respectively, via IP injection. Protocol VI: groups F1 and F2 and F3 received only P. Hermala extract orally at doses of 15, 30 and 60 mg/kg, respectively. The survival time of each animal after the administration of venom, extract or venom-extract combinations was recorded in minutes. These values were statistically compared with the across groups.

Statistical analysis

Data are presented as mean ± SEM. All the results were analyzed using SPSS-19 (SPSS Inc., Chicago, Illinois). One way analysis of variance (ANOVA) was used, followed by a post-hoc analysis using a Tukey test. A p-value of less than 0.05 was considered statistically significant.

Authors' Contributions

FB supervised, design the experiment and wrote the manuscript, revised and corrected it FB. SS performed the experiments, collected data, analyzed and interpreted the results, and prepared the manuscript. All authors read, discussed, commented, and approved the final manuscript.

Acknowledgements

We would like to express our gratitude to Mrs. Monir Taheri for her effort, patience, and dedication during the submission of this article to the IJVST. We also wish to thank Mr. Jalal Moghbel, the technician of the pharmacology lab, for his invaluable assistance. Additionally, we extend our appreciation to Ferdowsi University of Mashhad for their generous financial support. Furthermore, we thank Razi Vaccine and Serum Research Institute, Tehran, Iran, for generously providing the lyophilized crude venom.

Competing Interests

The authors have declared that there is no conflict of interest.

Reference

1. Gutiérrez JM, Calvete JJ, Habib AG, Harrison RA, Williams DJ, Warrell DA. 2017. Snakebite envenoming. Nat Rev Dis Primers, 3: 1-21. Doi:10.1038/nrdp.2017.63.

2. World Health Organization. 2019. Snakebite Envenoming: A Strategy for Prevention and Control. World Health Organization, Geneva.

3. Latifi, M. 2010. The Snakes of Iran. Published by Environment Protection organization, Tehran, 2010. 478 pp. (in Persian, with Latin index).

4. Yamada D, Sekiya F, Morita T. 1996. Isolation and characterization of Carinactivase, a novel prothrombin activator in Echis carinatus venom with a unique catalytic mechanism, J Biol Chem, 271: 5200-5207.

5. Warrell DA, Davidson NM, Greenwood BM, Ormerod LD, Pope HM, et al. 1977. Poisoning by bites of Saw-scaled viper or carpet viper (Echiscarinatus) in Nigeria, Q J Med, 46: 33-62.

6. Dehghani R, Fathi B, Shahi MP, Jazayeri M. 2014. Ten years of snakebites in Iran. Toxicon, 90: 291-298. Doi:10.1016/j.toxicon.2014.08.063.

7. de Silva HA, Ryan NM, de Silva HJ. 2016. Adverse reactions to snake antivenom, and their prevention and treatment. Brit J Clin Pharm, 81:446-452. Doi:10.1111/bcp.12739.

8. Lalloo DG, Theakston RD. 2003. Snake antivenoms. J Toxicol Clin Toxicol, 41: 277-290. Doi: 10.1081/clt-120021113.

9. Habib AG, Brown NI. 2018. The snakebite problem and antivenom crisis from a health-economic perspective. Toxicon. 150: 115-123. Doi: 10.1016/j.toxicon.2018.05.009.

10. Dey A, De JN. 2011. Traditional use of plants against snakebite in Indian subcontinent: a review of the recent literature. Afr J Tradit Complement Altern Med, 9: 153-174. Doi:10.4314/ajtcam.v9i1.20.

11. Shirwaikar A, Rajendran K, Bodla R, Kumar CD. 2004. Neutralization potential of Viper russelli russelli (Russell's viper) venom by ethanol leaf extract of Acalypha indica. J Ethnopharmacol, 94: 267-273. Doi:10.1016/j.jep.2004.05.010.

12. Rahman R, Faiz MA, Selim S, Rahman B, Basher A, Jones A, d'Este C, Hossain M, Islam Z, Ahmed H, Milton AH. 2010. Annual incidence of snake bite in rural bangladesh. PLoS Negl Trop Dis. 10: e860. Doi:10.1371/journal.pntd.0000860.

13. Soares AM, Ticli FK, Marcussi S, Lourenço MV, Januário AH, Sampaio SV, Giglio JR, Lomonte B, Pereira PS. 2005. Medicinal plants with inhibitory properties against snake venoms. Curr Med Chem, 22:2625-2641. Doi:10.2174/092986705774370655.

14. Chandrashekara KT, Nagaraju S, Nandini SU, Basavaiah K, Kemparaju K. 2009. Neutralization of local and systemic toxicity of Daboia russelii venom by Morus albaplant leaf extract. Phytother Res, 23: 1082–1087. Doi:10.1002/ptr.2735.

15. Lizano S, Domont G, Perales J. 2003. Natural phospholipase A (2) myotoxin inhibitor proteins from snakes, mammals and plants. Toxicon, 42: 963-977. Doi:10.1016/j.toxicon.2003.11.007.

16. Girish K, Mohanakumari HP, Nagaraju S, Vishwanath B, Kemparaju K. 2004. Hyaluronidase and protease activities from Indian snake venoms: neutralization by Mimosa pudica root extract. Fitoterapia, 75: 378–380. Doi:10.1016/j.fitote.2004.01.006.

17. Nirmal N, Praba GO, Velmurugan D. 2008. Modeling studies on phospholipase A2-inhibitor complexes. Indian J Biochem Biophys, 45: 256-262.

18. Vineetha MS, Bhavya J1, Sunil SM. 2019. Inhibition of pharmacological and toxic effects of Echis carinatus venom by Tabernaemontana alternifolia root extrac. Indian J Nat Prod Resour, 10: 48-58.

19. Owuor BO, Kisangau DP. 2006. Kenyan medicinal plants used as antivenin: a comparison of plant usage. J Ethnobiol Ethnomed, 2: 1–8. Doi:10.1186/1746-4269-2-7.

20. Sajon SR, Sana S, Rana S. 2017. Anti-venoms for snake bite: a synthetic and traditional drugs review. J Pharmacogn Phytochem, 6: 190–197.

21. Lamchouri F, Settaf A, Cherrah Y, Zemzami M, Lyoussi B, Zaid A, Atif N, Hassar M. 1999. Antitumour principles from Peganum harmala seeds. Therapie, 54: 753–758.

22. Asgarpanah J, Ramezanloo F. 2012. Chemistry, pharmacology and medicinal properties of Peganum harmala L. Afr J Pharm Pharmacol, 6: 1573-1580.

23. Mahmoudian M, Jalipour H, Dardashti PS. 2002. Toxicity of Peganum harmala: Review and a case report. Iran J Pharmacol Ther, 1:1-4.

24. Karasawa MMG, Mohan C. Fruits as prospective reserves of bioactive compounds: A Review. 2018. Nat Prod Bioprospect, 8: 335-346.Doi:10.1007/s13659-018-0186-6.

25. Sharifi-Rad J, Quispe C, Herrera-Bravo J, Semwal P, Painuli S, Özçelik B et al. 2021. Peganum spp. A Comprehensive Review on Bioactivities and Health-Enhancing Effects and Their Potential for the Formulation of Functional Foods and Pharmaceutical Drugs. Oxid Med Cell Longev, 5900422. Doi: 10.1155/2021/5900422.

26. Lamchouri F, Settaf A, Cherrah Y, El Hamidi M, Tligui N, Lyoussi B, et al. 2002. Experimental toxicity of Peganum harmala seeds. Annales Pharmaceutiques Françaises, 60: 123-129.

27. Marcussi S, Sant'Ana CD, Oliveira CZ, Rueda AQ, Menaldo DL, Beleboni RO, Stabeli RG, Giglio JR, Fontes MR, Soares AM. 2007. Snake venom phospholipase A2 inhibitors: medicinal chemistry and therapeutic potential. Curr Top Med Chem, 7: 743-756. Doi:10.2174/156802607780487614.

28. Teixeira C, Cury Y, Moreira V, Picolo G, Chaves F. 2009. Inflammation induced by Bothrops asper venom. Toxicon, 54: 67-76. Doi:10.1016/j.toxicon.2009.03.019.

29. Aird SD. 2002. Ophidian envenomation strategies and the role of purines. Toxicon, 40: 335-393. Doi:10.1016/s0041-0101(01)00232-x.

30. Ushanandini S, Nagaraju S, Harish Kumar K, Vedavathi M, Machiah D K, et al. 2006. The anti-snake venom properties of Tamarindus indica (leguminosae) seed extract, Phytother Res, 20: 851-858. Doi:10.1002/ptr.1951.

31. de Moura VM, da Silva WCR, Raposo JDA, Freitas-de- Sousa LA, Dos-Santos M C, et al. 2016. The inhibitory potential of the condensed-tannin-rich fraction of Plathymenia reticulata Benth. (Fabaceae) against Bothrops atrox envenomation, J Ethnopharmacol, 183: 136-142. Doi:10.1016/j.jep.2016.02.047.

32. Meenatchisundaram S, Prajish G P, Subbraj T and Michael A. 2008. Studies on anti-venom activity of Andrographis paniculata and Aristolochia indica plant extracts against Echis carinatus venom, Internet J Toxicol, 6: 1-7.

33. Miyake A, Yamamoto H, Takebayashi Y, Imai Hm Honda K. 1992. The novel natural product YM-26567-1 [(+)-trans-4-(3-dodecanoyl-2,4,6- trihydroxyphenyl)-7-hydroxy-2-(4-hydroxyphenyl) chroman]: a competitive inhibitor of group II phospholipase A2. Mol Cell Pharmacol, 263; 1302-1307.

34. Mahadeshwaraswamy Y H, Nagaraju S, Girish K S and Kemparaju K. 2008. Local tissue destruction and procoagulation properties of Echis carinatus venom: inhibition by Vitis vinifera seed methanol extract. Phytother Res, 22: 963-969. Doi:10.1002/ptr.2462.

35. Glennon RA, Dukat M, Grella B, Hong S, Costantino L, Teitler M, Smith C, Egan C, Davis K, Mattson MV. 2000. Binding of beta-carbolines and related agents at serotonin (5-HT (2) and 5-HT(1A)), dopamine (D (2)) and benzodiazepine receptors. Drug Alcohol Depend, 60:121-132. Doi:10.1016/s0376-8716(99)00148-9.

36. Herraiz, T. González, DC. Ancín-Azpilicueta, C. Arán, VJ, Guillén, H. 2010. β-Carboline alkaloids in Peganum harmala and inhibition of human monoamine oxidase (MAO), Food Chem Toxicol, 48: 839–845.Doi:10.1016/j.fct.2009.12.019.

37. Harris JB. 2009. Neuromuscular junction (NMJ): a target for natural and environmental toxins in humans. Encyclopedia of Neuroscience. Boston: Elesevier Academic Press, 539–549.

38. Yang Y, Cheng X, Liu W, Chou G, Wang Z, Wang C. 2015. Potent AChE and BChE inhibitors isolated from seeds of Peganum harmala Linn by a bioassay-guided fractionation. J Ethnopharmacol, 68: 279-286. Doi:10.1016/j.jep.2015.03.070.

39. Soliman AM, Abu-El-Zahab HS, Alswiai GA. 2013. Efficacy evaluation of the protein isolated from Peganum harmala seeds as an antioxidant in liver of rats. Asian Pac J Trop Med, 6: 285–295. Doi:10.1016/s1995-7645(13)60058-9.

How to cite this article
Shirkhani S, Fathi B. *Peganum harmala* extract delayed the lethal effect of viper snake *Echis carinatus* venom in mice. Iran J Vet Sci Technol. 2025; 17(3): 21-28.
DOI: https://doi.org/10.22067/ijvst.2025.91424.1454
URL:https://ijvst.um.ac.ir/article_46835.html

Iranian Journal of Veterinary Science and Technology

Received: 2024- Sep- 14
Accepted after revision: 2025- Jun-22
Published online: 2025-Jun- 22

RESEARCH ARTICLE

DOI: 10.22067/ijvst.2025.87643.1370

Changes in the Uropygial (*preen*) gland in Fulani ecotype chicken (*gallus gallus domestica*) a post-hatch study

Alhaji Zubair Jaji[a], Latifah Ozohu Abdulkarim[a], Furo Nathan Ahmadu[b], Esther Solomon Kigir[a], Kenechukwu Tobechukwu Onwuama[a], AbdulGaniu Olawale Ibrahim[a], Shaibu Mohammed Atabo[c], Sulaiman Olawoye Salamia[c], Wanmi Nathaniela[a]

[a] Department of Veterinary Anatomy, Faculty of Veterinary Medicine, University of Ilorin, Nigeria.
[b] Department of Veterinary Medicine, Faculty of Veterinary Medicine, University of Ilorin, Nigeria.
[c] Department of Veterinary Anatomy, Faculty of Veterinary Medicine, Bayero University, Kano, Nigeria.

ABSTRACT

The Uropygial (Preen) gland, located dorsocranially to the pygostyle and rectrices in birds, is a bi-lobed structure responsible for secreting oil for plumage maintenance. This study investigated the morphological and histological features during post-natal development in the Fulani Ecotype chicken (*Gallus gallus domestica*) with the aim of documenting anatomical information that will be useful for further biomedical and embryological studies. A total of 56 Fulani Ecotype chickens were sampled, and studied across four developmental phases, with each phase comprising 7 males and 7 females. For each bird, live body weight, uropygial gland weights and preen oil weights were documented. Morphometric characteristics of the excised gland were documented before extraction and measuring the preen oil. Additionally, uropygial glands from selected birds per phase were excised, and fixed in 10% buffered formalin solution for gross and histological analysis. The gland appeared as early as week 2–3 post-hatch, presenting two pear shaped lobes and a short papilla. Three layers of the secretory cells were recognised at 7-8 months post hatch. The results confirm that uropygial gland of the Fulani ecotype chicken develops early, at week 2-3 post hatch, and that its weight increases with the body weight, reaching full histological development between 7-8 months post hatch.

Keywords

Histology, Morphology, Post Hatch, Uropygial gland

Number of Figures: 8
Number of Tables: 3
Number of References:: 30
Number of Pages: 9

Abbreviations

Not used.

Corresponding author:
Kenechukwu Tobechukwu Onwuama
Email: onwuama.kt@unilorin.edu.ng
Tel:+23(480)3642-5961

Introduction

The Nigerian indigenous chicken is one of the major sources of dietary protein to the Nigerian people. With an estimated population of 180 million birds, Nigeria hosts the second largest chicken population in Africa, following South Africa [1].

Indigenous Nigerian chickens are classified into two main ecotypes based on their geographical distribution: the Fulani Ecotype and the Forest savannah (Yoruba) Ecotypes [3]. The Fulani Ecotypes often regarded as the "heavy ecotypes", is found in the Sahel, guinea savannah parts of Nigeria, cattle Kraals, and Montane regions of the north [4]. Adaptation to environmental conditions, such as rainfall and humidity, is critical for these birds. One adaptive mechanism involves the secretion of oil from the uropygial (preen) gland to waterproof and maintain their feathers [5].

The Uropygial gland is a well-recognized feature of most bird species [6]. Structurally, it is bi-lobed and encapsulated by irregular connective tissue composed of collagen, elastic and reticular fibres [7]. Its secretory tubules comprise four cell layers: a germinative layer (basal), an intermediate layer, a secretory layer and a degenerative layer [8].

The Oleaginous secretion of the preen gland is a combination of extruded cells, ester waxes, fatty acids, fat and secretory granules [9]. Its chemical composition varies both within and across bird species [10]. Beyond maintenance of feather integrity, the gland is also of current interest because it provides source of chemicals used for communication in birds. While its anatomy has been investigated in species such as Kiwi [6], ducks [11] and gulls [12], limited information exists on post-natal developmental changes, particularly in indigenous breeds like the Fulani Ecotype. This study aims to examine the gross morphological and histological development of the uropygial gland in Fulani ecotype chickens to address existing gaps in the literature regarding avian gland development.

Figure 1.
Photographs showing in situ position of the Preen gland (arrow) of the Fulani ecotype chicken as seen at the base of the tail (Week 2-3).

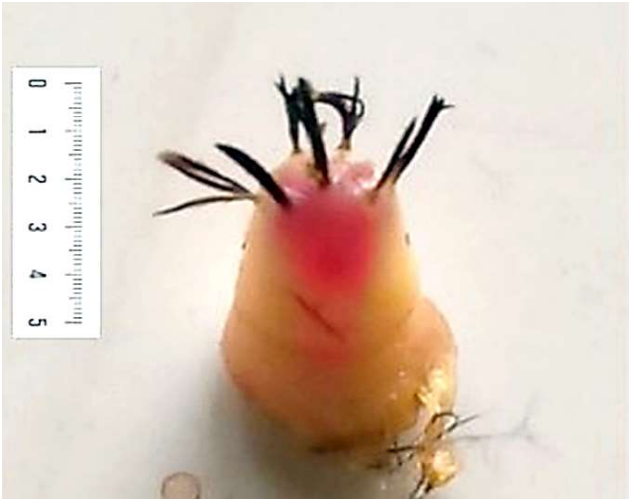

Figure 2.
Photograph of the excised preen gland of the Fulani ecotype chicken with circlet feathers (arrow heads) (Week 2-3).

Result

Gross morphology

The Preen gland of the Fulani ecotype chicken was located at the base of the tail, situated between the fourth caudal vertebra and the pygostyle (Fig. 1). It was made up of two pear shaped lobes and a short, nipple like papilla. Each papilla was surrounded by 5-7 tufts of fine downy circlet feathers (Fig. 2), depicting a type 2 circlet arrangement, as classified by13. The gland was observed as early as week 2 - 3 of age and continued to develop and function throughout the growth of the bird .

Morphometry

The means weight and standard deviations of the preen glands and preen oils (measured in grams) across genders and growth phases were compared to the live body weights of the birds and the significant differences across groups were obtained. The weights showed sig-

nificant differences across the age groups ($p < 0.001$) (Table 1). Age gender related difference in the live body weight, preen glands weight and preen oils quantity were evident starting from the chick stage (Table 2).

A marked statistically significant difference existed between the weights of the preen gland and preen oil in both male and female birds (Table 3). However, there was no significant difference between the gland weights of male and females. Notably, at 18–24 months of age, the weight of the preen oil in males was significantly higher than in females (Table 3).

From age 2-3 months onward, the weights of both the preen gland and its oil increased in weight in both sexes. This growth is likely associated with rising metabolic and hormonal demands, as well as the necessity of maintaining feather hygiene. (Table 3).

Histology

In the early developmental phase (weeks 2–3), the secretory tubules of the Fulani ecotype chicken's preen gland showed minimal secretions in their lumens, and the parenchyma was not fully developed. Cellular stratification was poorly outlined due to widely spread parenchyma tissue. Nonetheless, distinct cellular aggregations or granules, ranging from spherical and oval to ecliptic shapes, were observed throughout the developing preen gland (Fig. 3).

Table 1.
Mean ± Standard Deviation of the Weights of Preen Oil, Preen Gland and Live Birds.

Parameters (Mean ± S.D)	Sex	Postnatal Growth Phases (n = 6 per growth phase)			
		2-3 weeks	2-3 months	7-8 months	18-24 months
Bird Live Weight (g)	Male	33.94 ± 3.09	427.00 ± 63.00 [b]	969.67 ± 111.70 [c]	1090.67 ± 417.21 [c]
	Female	32.35 ± 0.87	229.67 ± 37.82 [a]	931.33 ± 79.86 [c]	1279.67 ± 174.08 [c]
Preen gland Weight (g)	Male	0.10 ± 0.01	0.40 ± 0.08 [b]	0.74 ± 0.18 [c]	0.86 ± 0.25 [c]
	Female	0.04 ± 0.01	0.45 ± 0.02 [c]	0.77 ± 0.02 [c]	0.90 ± 0.07 [c]
Oil weight (g)	Male	0.01 ± 0.01	0.05 ± 0.02	0.15 ± 0.03 [c]	0.43 ± 0.07 [c]
	Female	0.02 ± 0.01	0.07 ± 0.03 [b]	0.09 ± 0.07 [c]	0.12 ± 0.07 [c]

[a] = significant ($p < 0.05$, [b] = very significant ($p < 0.005$), [c] = extremely significant ($p < 0.001$).

Table 2.
Comparisons of the Mean ± Standard Deviation of the Weights of Preen Oil, Preen Gland and Live Birds

Features		2-3 weeks	2-3 months	7-8 months	18-24 months
Male vs female live weights	Male	ns	ns	c	a
Male vs female preen gland weights	Female	ns	b	c	b
Male vs female preen oils weights	Male	ns	ns	c	ns
Weight of gland vs Weight of oil	Female	ns	b	c	b
		ns	ns	b	ns
Relative weight of pineal gland	Male	c	c	c	c
		c	c	c	c
Relative weight of pineal oil	Female	c	c	c	c
		c	c	c	c

ns = not significant at $p = > 0.05$; [a] = significant ($p < 0.05$, [b] = very significant ($p < 0.005$), [c] = extremely significant ($p < 0.001$), Vs= Versus

Table 3.
Relationship between the mean live weight, mean gland weight and mean oil weight of Fulani ecotype chicken during four post-natal growth phases.

Pearson's correlation coefficients (r)			
Correlated parameters	**Male (n=3)**	**Female (n=3)**	**Both sexes (n=6)**
Mean live weights vs mean gland weights	0.9994***	0.9460^{n}	0.9833*
Mean live weights vs mean oil weights	0.8395^{n}	0.2468^{n}	0.8918^{n}

* = Significant correlation ($P < 0.05$) *** = Highly significant correlation ($P < 0.001$) n = Non significant correlation, vs= Versus.

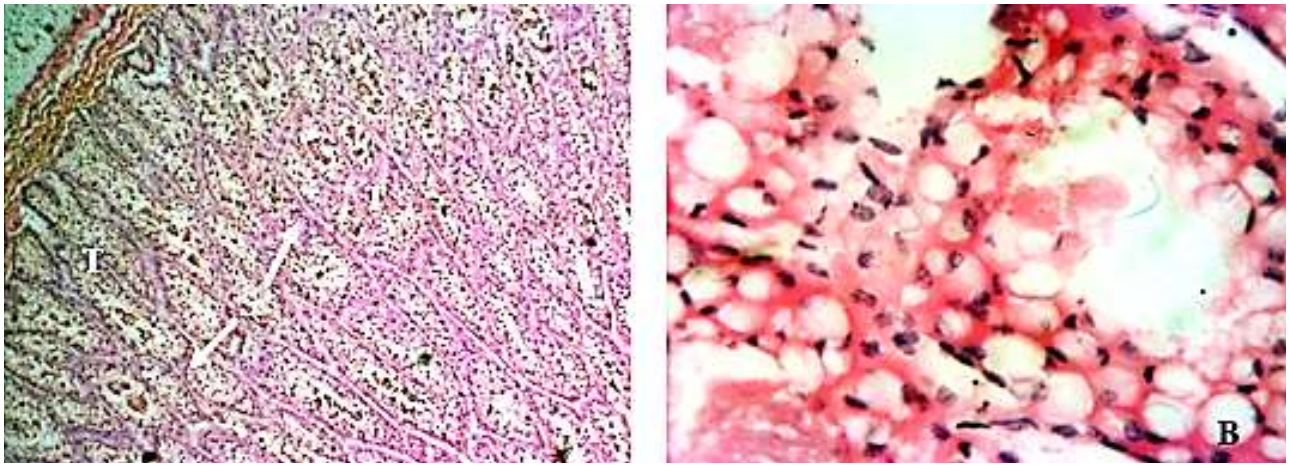

Figure 3.
Micrograph of the Preen gland in a 2–3-week-old chicken. A: Depicts thick connective tissue septae (S) demarcating poorly lumenized developing secretory tubules (T). H&E X 40. B: Depicts poorly arranged glandular cells. H&E X 400.

At 2–3 months, secretory tubules were separated by thick connective tissue septae. The structure was non-classical luminization, and lacked capsule, with few blood vessels and haphazard cellular arrangement (Fig. 4). Subsequent developmental stages were characterized by developed states of the preen gland. The organization, size and the overall parenchyma of the secretory tubules were improved, leading to improvement in preen oil secretion levels. Black spotted bodies were replaced by secretory cells, forming tripartite cellular strata (Fig. 4).

The parenchyma continued to develop at the second developmental phase (4-6 months). At this stage, the secretory tubules were separated by thinner connective tissue septae and exhibited clearly defined lumenes The arrangement of the secretory tubule cells improved significantly (Fig. 5).

By 6-9 months, secretory tubule cells were organized into three distinct layers: basal layer of cuboidal cells adjacent to the basement membrane, an intermediate layer of polyhedral cells, and a secretory layer that had more secretory vacuoles, adjacent to the tubular lumen. As the cells neared the tubular lumen, their cytoplasm vacuolization and size increased, due

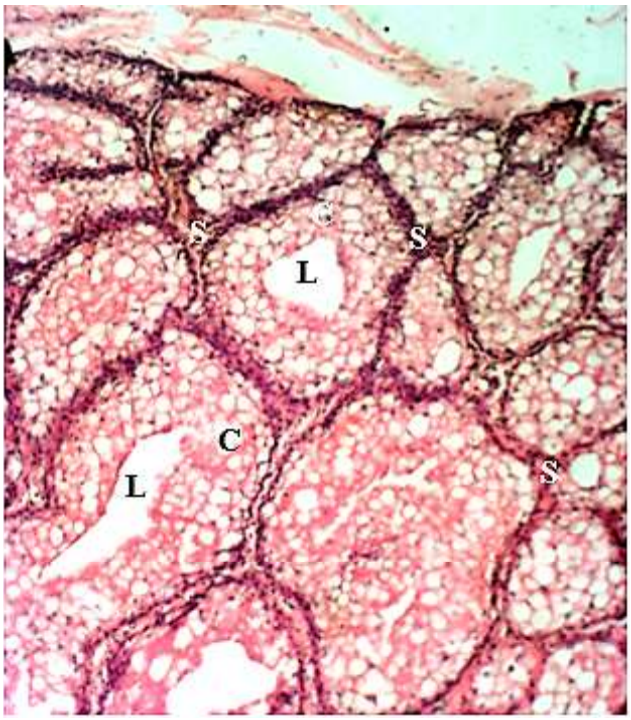

Figure 4.
Micrograph of the Preen gland in a 2-3 month old chicken depicting thin connective tissue septae (S) demarcation of secretory tubules and clearer tubular lumen (L). The cells (C) of the tubules were better arranged. H&E X 100.

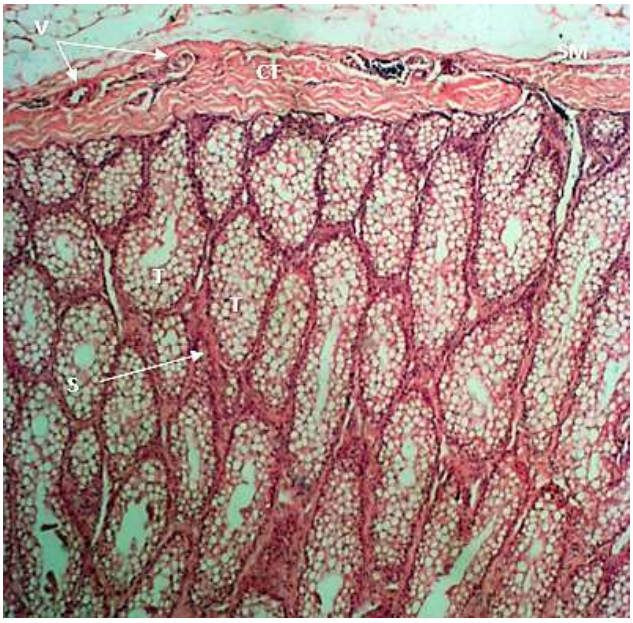

Figure 5.
Micrograph of the Preen gland in a 4-6 month old chicken depicting the dense irregular and elastic connective tissue (CT) and smooth muscle (SM) fibres that make its thick capsule. The capsule is vascularized (V) and septae (S) into the glandular parenchyma to separate the secretory tubules (T). H&E, X 40.

to their increasing secretory content (fig. 6).

At 18 – 24 months post hatch, the gland showed numerous simple, branched tubular secretory units that terminated blindly near the capsule. The entire gland was enclosed in a thick capsule composed of dense irregular, elastic, adipose and smooth muscle tissues. The capsule divided the gland into two separate lobes, was vascularized and innervated, and extended septae into the substance of the parenchyma of each lobe. These septae demarcated secretory tubules, and established a linkage of drainage channels to a central canal, which ultimately opened to the exterior through the papilla (Fig. 7).

Figure 6.
Micrograph of a fully developed Preen gland in a 6- 9 month old chicken depicting layers of i) basal cells (B), ii) intermediate cells (I) and iii) secretory cell (S) of a secretory tubule. The basal cells (cuboid shaped) are next to the basement membrane (BM), H&E X 400.

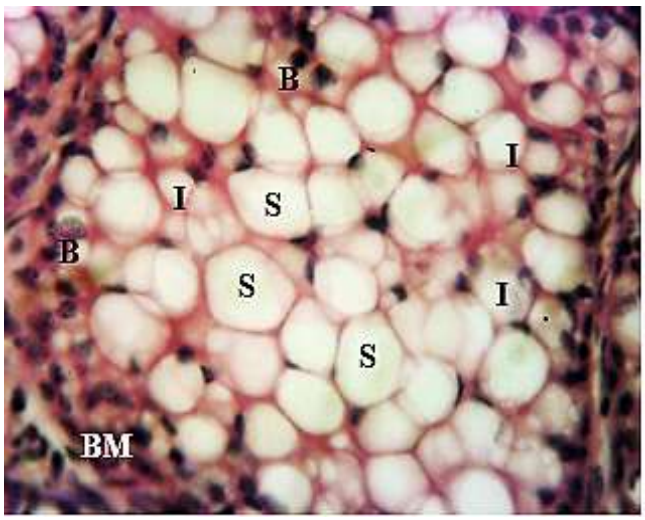

Figure 7.
Micrograph of a fully developed Preen gland in a 6-9 month old chicken depicting layers of i) basal cells (B), ii) intermediate cells (I) and iii) secretory cell (S) of a secretory tubule. The basal cells (cuboid shaped) are next to the basement membrane (BM), H&E X 400.

Discussion

In this study, the uropygial gland of the Fulani ecotype chicken was located between the fourth caudal vertebra and the pygostyle, dorsally positioned above the levator caudalis muscle at the base of the tail. This anatomical positioning aligns with report on uropygial Glands of most birds [14], which describe the gland as being dorsally and medially located within the synsacocaudal region and visible to the naked eye. The Uropygial gland of Fulani ecotype chickens exhibited a bi-lobed, conical flask-like structure, each lobe featuring a single opening, along with short nipple-like Uropygial papilla situated dorsocaudally to the gland. Preen glands have been observed in a variety of configurations, for instance a heart-shaped preen gland with a broad bean-sized base was documented in Ankra putra chickens [15]. However, according to [16] the duck's uropygial gland has different development pattern, suggesting that gland size may not serve as a significant determinant in this species.

The uropygial gland plays a crucial role for preserving feather hygiene and integrity, regardless of feathers shape [18], preening, and dust bathing [19]. These could be one of the main reasons for the uropygial gland's growth at week 2-3, which coincides with the formation of feathers.

According to [20], in chicken, the uropygial papilla is long and thin; in turkey, it is broad and short; in geese, it has two openings; and in musk ducks, it is absent altogether [21]. Additional reports describe the papilla as being slightly above the tail and nipple shape [14]. A connective tissue separates clearly sepa-

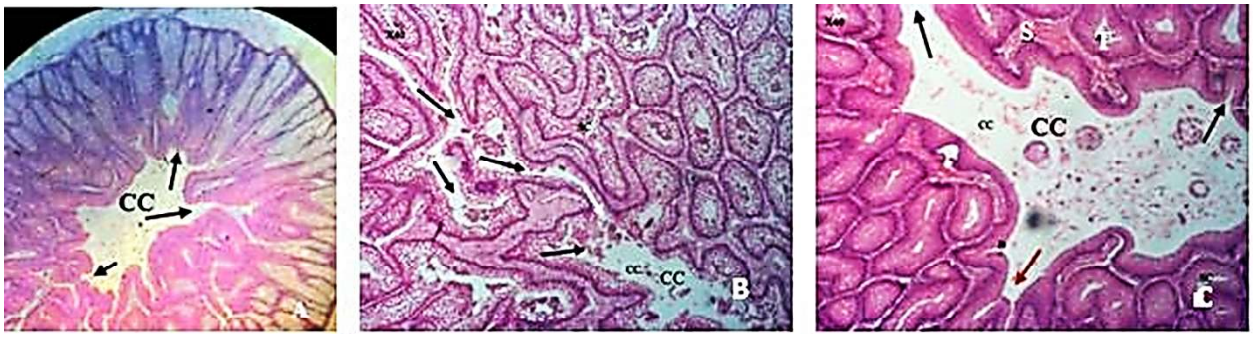

Figure 8.
Micrographs of the parenchyma of the Preen gland in an 18-24-month old chicken. Depicting connective tissue septae (S) demarcating its secretory tubules (T) and linking drainage tributaries (Arrow) to the central canal (CC) H&E X 40.

rates the papilla from the gland lobes [22].

At week 2-3 of age, each papilla is surrounded by 5-7 tufts of fine downy circlet feathers, forming a type 2 circlet arrangement accordance with the classification by Johnston 1988. This arrangement supports previous findings [21,14]. According to [21], the circlets help smear the oily secretion onto the bill.

The live bird weights and their preen gland weights continuously grow, with the exception of the female's preen oil. This is consistent with other observations, like those of [22] on wild rock pigeons (Columbia livia) and [23] on the helmeted guinea fowls, where males generally exhibit higher weights than females of the same species.

Due to its holocrine form, along with its close relationship between the histology of fowl and guinea fowl, the uropygial gland of the Fulani ecotype chicken corresponds with the mammalian sebaceous gland [24]. The preen gland is surrounded by an irregular connective tissue capsule made up of adipocytes and smooth muscles in domestic ducks [25], although this smooth muscle component is reportedly absent in kiwis [26]. Smooth muscle is necessary for contraction, which leads to the opening of primary ducts and the ejection of secretion from the gland; however, there are other supportive systems in existence to compress secretions, therefore the lack of this smooth does not imply a lack of secretion [27].

In this study in order to develop and link its drainage channels to a central canal, which is then drained to the exterior by the papilla, the capsules were vascularized and sent septae into the substance of the parenchyma of each lobe, demarcating secretory tubules. According to [28], the gland is made up of a lot of simple branched tubular secretory units ending blindly close to the capsule. Its holocrine nature is demonstrated by cellular fragmentation in the transitional layers of secretary tubules, as seen in guinea fowls [29].

At 2-3 weeks post hatch, interfollicular septae were poorly visible. This demonstrates that interfollicular septae develops lobules of follicular cells as the chicken grows. The thickness of the interfollicular septae varies between species. The interfollicular septae are narrow in Indian peafowl and thicker in water rails [30].

The glandular zones present in the secretory tubules were separated into a peripherally greater outer zone near the tubular wall, bordered with stratified epithelium, and proportionally a lesser interior zone of larger cells adjacent to the lumen.

Between the formal layer and the bottom layer, which is made up of the tiniest cells that border the basement membrane, is an intermediate zone of relatively smaller cells. This finding is consistent with a prior work by [31]. In this study, the basal layer cells had a low cuboidal shape. They make up the top two layers of the secretory tubules' glandular cells. The cytoplasm of the cells in this layer is highly basophilic and darker than the cytoplasm of other guinea fowl cells, and the nuclei of these cells are spherical and darkly pigmented [7]. The Gallus domestica lack this exhibition.

Conclusion

This study concluded that there is a relationship existing between age of the Fulani ecotype chicken to the weight of the gland and sex. From micromorphological perspectives, the preen gland at week 2- 3 was undeveloped lacking a well-formed capsules, septae and cellular layers. These structures began to fully form from 6-9 months post Hatch. Having concluded with the above statement, it should be noted that limitations to this study may include sample size and environmental factors such as temperature and humidity.

Materials and Methods

Ethical approval

Ethical approval for this study was obtained from the institutional Animal care and Use Committee (IACUC) of University of Ilorin (Reference Number: FVM/UERC/0012021).

Animals

A total of fifty-six (56) Fulani ecotype chickens obtained from local backyard poultry farms in Ilorin metropolis (8.4882° N, 4.5341° E), Ilorin, Kwara state, Nigeria. All micro morphological study was carried out at the Veterinary Gross Anatomy Laboratory, Faculty of Veterinary Medicine, University of Ilorin, Ilorin, Kwara state, Nigeria. The birds were housed in a ventilated facility and provided food and water ad libitum for one week prior to experimentation.

Study design and data collection

The birds were grouped into 4 phases of development with each group having 7 males and 7 females. Thus: the chick phase (2-3-week-old), the young phase (2-3-month-old), the young adult phase (6–9-month-old) and the adult phase (18 – 24 Months). Live body weight (g) of each bird was measured using a Harvard trip weighing balance (Citizen® with 0.1 g – 100 kg range). The in-situ anatomical location of the preen gland was documented in each case. After humane slaughter, the gland were excised, weighed using a Golden-Metler electronic balance (U.S.A., GF-300 Analytical Balance 310 * 0.001g, (A&D Weighing, India), and photographed using a digital camera (Nikkon Coolpix A100). Preen oil was then squeezed and weighed using the same balance.

For histological analysis, preen glands from two birds (one male and one female) per developmental phase were excised, and fixed in 10 % buffered formalin solution for processing onto histological slides. The prepared slides were viewed under the Olympus microscope. Micrographs were captured using the AMscope 500 microscope software (Figure 8).

Statistical analysis

Descriptive statistics (Mean ± SD) were carried out using the Microsoft excel worksheet (Microsoft office 2013 software, Microsoft©). Inferential statistics analyses, including analysis of Variance, were carried out using the GraphPad software (GraphPad prism 5) to compare means across age and gender groups. Pearson's correlation coefficient of Graph pad prism version 5.0 was also used to assess the relationship between live weight, gland weight, and oil weight. A p-values of less than 0.05 was considered statistically significant.

Authors' Contributions

A.Z.A, L.O.A, F.N.O, E.S.K, and K.T.O. conceived and planned the experiments. L.O.A, A.O.I, and S.M.A carried out the experiments. A.Z.A., S.O.S, W.N. and L.O.A. planned and carried out the simulations. L.O.A., K.T.O, A.O.I, E.S.K., and W.N. contributed to sample preparation. A.Z.A., F.N.O., K.T.O., S.O.S., S.M.A and E.S.K. contributed to the interpretation of the results. A.Z.A., and K.T.O took the lead in writing the manuscript. All authors provided critical feedback and helped shape the research, analysis and manuscript.

Acknowledgements

The technical staff in the Departments of Veterinary Anatomy and Pathology, Faculty of Veterinary Medicine, University of Ilorin are highly appreciated.

This research was funded by efforts from individual staff who are authors of this manuscript.

Competing Interests

The authors declare that there is no conflict of interest.

Reference

1. Ajala AO, Ogunjimi SI, Famuwagun OS and Adebimpe AT. 2021. Poultry production in Nigeria: exploring its potentials for rural youth empowerment and entrepreneurship. Nigerian Journal of Animal Production, 48(10):114-123. Doi:10.51791/njap.v48i1.2890.

2. Adeyonu A, Okunola A., Alao M., Oyawoye E and Okonkwo C. 2021. An assessment of broiler value chain in Nigeria. Open Agriculture, 6 (1) 296-307. Doi:10.515/opag-2020-0168.

3. Odubote K. 2015. The Local Chickens Of Nigeria-A Review. https://www.researchgate.net/publication/276058544 (accessed 6.4.2024). Doi:10.13140/RG.2.1.2193.5520.

4. Adeleke MA, Bello KO, Akinyemi IO, Irekhore OT, Ilori BM, Adeyeye OA and Famakinde SA. 2022. Morphological variations of qualitative and quantitative traits of Fulani ecotype chickens in Nigeria. Genetika 54 (1): 43-62. Doi:10.2298/GENSR2201043A.

5. Giraudeau M, Duval C, Guillon N. 2010. Effects of access to preen gland secretions on mallard plumage. Nature weissen schaften, 97(6) 577-581. Doi:10.1007/s00114-010-0673-z.

6. Reynolds SM, Castro I, Alley MR. 2017. Apteryx Spp. (Kiwi) possess an uropygial gland: Anatomy and Pathology. European Journal of Anatomy. 21 (2): 125-139.

7. Ushakumary S, Venkatesan S, Sabiha HB. 2011. Histoloy and histochemistry of the preen gland in guinea fowl. Indian Veterinary Journal, 88(6), 132–134.

8. Harem I, Kocak M, Kozlu T. 2010. Histologic Structure of the Uropygial Gland of the Osprey(Pandion haliaetus). Journal of Zoo Wildlife Medicine, 41(1), 147–150. Doi:10.16.1638/2008-0205.1.

9 Sandilands V, Powell K, Keeling LJ, Savory J. 2004. Preen gland function in layer fowls: Factors affecting preen oil fatty acid composition. British Poultry Science, 45 (1):109-15. Doi:10.1080/00716604100016689 32.

10. Moreno-Rueda G. 2017. Preen oil and bird fitness: a critical review of the evidence. Biological Reviews. Doi:10.1111/

brv.12324.

11. Rajathi S, Ashok N, Kumaravel A, Muthkrishnan S. 2013. Histological Development of papilla of preen gland in Duck. Indian Journal of Veterinary Anatomy, 90 (7): 56-58.

12. Al-khazraji KI. 2017. Histological and Morphological study of the Uropygial gland in Gull (Larus canus). Diyala Journal of Pure Science, 13 (3): 230-239. Doi:10.24237/djPS.1303.308a.

13. Johnston DW. 1988. A morphological atlas of the avian gland. Bulletin of the British Museum of Natural History. Zoology, 54, 199–259.

14. Moller AP, Laursen, K. 2019. Function of the Uropygial gland in eiders (Somateria mollissima). Avian Research 10, 24. Doi:10.1186/s40657-019-0163-8.

15. Jawad HSA, Naji LHBI, Bakar SA. 2015. Partial Ablation of Uropygial Gland Effect on Production Performance of Akar Putra Chicken. International Journal of Poultry Science, 14 (4), 213–221. Doi:10.3923/ijps.2015.213.221.

16. Das LN, Mishra DB, Biswal G. 1962. Comparative anatomy of the domestic duck (Anas bochas). Indian Veterinary Journal, 42: 320-326.

17. Delius JD. 1988. Preening and associated comfort behavior in birds. Annals of New York Academy of Sciences 525: 40–55. Doi:10.1111/j.1749-6632.1988.tb38594.x.

18. Cotgreave P, Clayton DH. 1994. Comparative-analysis of time spent grooming by birds in relation to parasite load. Behaviour, 131 (3-):171–187. Doi:10.1163/156853994X00424.

19. Van LDW, Bokma S. 1987. Short-term feather maintenance as a function of dust-bathing in laying hens. Applied Animal Behaviour Science, 18, 197—204. Doi:10.1016/0168-1591(87)90193-6.

20. Shawkey MD, Pillai SR, Hill GE. 2003. Chemical Warfare Effects of Uropygial Oil on Feather Degrading Bacteria. Avian Biology, 34 (4):345–349.

21. Stettenheim PR. 2000. The integumentary morphology of modern birds – an overview. Am Zoology, 40, 461–477. https://academic.oup.com/icb/article/40/4/461/101379.

22. Wanmi N, Samuel MO, Byanet O. 2016. Morphormetric Study of the Forebrain and Cerebellum of the Wild Rock Pigeon (Columba livia). International journal of Vet. Sci. 5(3): 118-121.

23. Gosomji IJ, Salami SO, Nzalak JO, Kawu MU, Tizhe E.M, Gurumyem YG, Dung EC.2015. Morphological Development of the Gastrointestinal Tract Of Helmeted Guinea Fowl (Numida meleagris) at Pre-Hatch and Post-Hatch. Journal of Vet. Anatomy 8(2)17 – 27. Doi:10.1155/2016/9827956.

24. Sara Q, Cecilia M, Chiara, D, Alexandra MG, Giovanni D. 2006. Adaptive evolution of secretory cell lines in vertebrate skin. Caryologia, 59 (2): 187-206. Doi:10.1080/00087114.2006.10797915.

25. Mobini B, Ziaii A. 2011. Comparative histological study of the preen of broiler and native chicken. Journal of Veterinary Microbiology 6 (2 (20)): 121–128.

26. Rajathi S, Ashok N, Kumaravel A, Muthukrishnan S. 2014. Post hatch micrometrical development of the preen gland in the duck. Indian Veterinary Journal. 91 (7) : 51-53.

27. Sadoon AH. 2011. Histological study of European Starling uropygial gland (Sturnus vulgaris). International Journal of Poultry Science, 10 (8): 662–664. Doi:10.3923/ijps.2011.662.664.

28. Hassanin A, Shoeib M, Massoud D. 2021. Micro and Macroanatomical features of the uropygial gland of duck (Anas platyrrhynchos) and pigeon (Columba livia). Biotechnic and Histochemistry, 96 (93), 213-222. Doi:10.1080/10520295.2020.1782990.

29. Isbilir F, Avci Kupeli Z, Isbilir I, Arican I, Ozyigit O. 2024. Macroscopic and microscopic characteristics of uropygial gland of Budgerigars (Melosittacus undulatus). Turkish Journal of Veterinary Research, 8 (1): 43-51. Doi:10.47748/tjvr.1393777.

30. Sawad AA. 2006. Morphological and histological study of uropygial gland in moorhen (G. gallinula C. choropus). International Journal of Poultry Science, 5 (10): 938–941. Doi:10.3923/ijps.2006.938.941.

How to cite this article
Jaji A, Abdulkarim L, Furo N, Kigir E, Onwuama K, Ibrahim A, Atabo S, Salami S, Wanmi N. Changes in the Uropygial (preen) gland in Fulani ecotype chicken *(gallus gallus domestica)* a post-hatch study. Iran J Vet Sci Technol. 2025; 17(3): 29-37.
DOI: https://doi.org/10.22067/ijvst.2025.87643.1370
URL:https://ijvst.um.ac.ir/article_46924.html

Iranian Journal of Veterinary Science and Technology

Received: 2025- Apr-30
Accepted after revision: 2025- Jun-25
Published online: 2025- Sep- 01

RESEARCH ARTICLE

DOI: 10.22067/ijvst.2025.93101.1504

Preliminary Evaluation of the Therapeutic Effects of Neem Leaf Extract and Ivermectin in West African Dwarf Goats with Clinical Mange

Olubunmi Titilayo Ojoawo , Jelili Akinwole Akinlade, Opeyemi Agbeniyi, Opeyemi Oladipupo Hammed, Rom-Kalilu Fiwasade Adejoke

Department of Animal Production and Health, Faculty of Agricultural Sciences, Ladoke Akintola University of Technology, Nigeria.

ABSTRACT

This study investigates the therapeutic potential of neem (Azadirachta indica) extract as a topical remedy for mange in West African Dwarf (WAD) goats, a breed commonly raised in Southern Nigeria and are affected by mange, which negatively impacts animal welfare and productivity. Twelve mange-infected goats were randomly assigned to three treatment groups: T1 (10 ml ivermectin pour-on), T2 (5 ml neem extract + 5 ml ivermectin), and T3 (10 ml neem extract). Treatments were administered topically over 14 day period. Clinical evaluations included skin scrapings, red blood cell (RBC), white blood cell (WBC) and serum biochemical indices. Phytochemical analysis of the neem extract revealed notable concentrations of alkaloids, saponins, and phenols. Post-treatment observations showed improvement in skin condition across all groups. Notably, T2 goats exhibited significant increases in RBC and WBC counts ($p < 0.05$). Differences in serum biochemical indices, particularly potassium, were also noted. The findings indicate that neem extract, can serve as an effective alternative or adjunct treatment to ivermectin for mange control in WAD goats. Its use may be particularly beneficial in local environments with poor accesibility to conventional drugs, contributing to improve animal health and production outcomes.

Keywords

Neem leaf, Ivermectin, Mange, West African Dwarf goats, Topical, Food security

Number of Figures: 2
Number of Tables: 3
Number of References:: 23
Number of Pages: 9

Abbreviations

WAD: West African Dwarf
RBC: Red Blood cells
WBC: White Blood Cells
DM: Dry Matter
CP: Crude Protein
MCH: mean corpuscular haemoglobin
MCHC: mean corpuscular haemoglobin concentration
RDW-CV: red cell distribution width-coefficient of variation
MCV: mean corpuscular volume
PDW: platelet distribution width

Corresponding author: *Olubunmi Titilayo Ojoawo*
Email: otojoawo47@lautech.edu.ng-
Tel:+23(480)3646-6744

Introduction

Achieving food security, a central objective of the Sustainable Development Goals, is closely tied to the availability of animal-sourced proteins. This underscores the importance of evaluating and implementing effective strategies to enhance animal production systems [1]. However, numerous factors limit optimal animal productivity, including management challenges, limited feed availability, and the prevalence of parasitic infestations and diseases [2].

One of the prevalent parasitic diseases affecting the WAD goats, particularly in Southern Nigeria is mange [3]. Mange is a parasitic skin disease caused by infestation of the epidermis and hair follicles by mites or lice. This condition affects a wide range of mammalian hosts, including companion animals, livestock, and occasionally humans. The condition is characterised by clinical signs such as intense pruritus, restlessness, excessive scratching and rubbing against surfaces, alopecia, fatigue, reduced growth performance, and cutaneous skin lesions. In livestock, mange presents a significant welfare and economic burden, particularly in severe infestations. Economic losses are attributed to reduced weight gain, compromised skin and fleece quality, anaemia, poor body condition, diminished milk and meat yields, and impaired reproductive performance, such as suboptimal lambing and kidding rates [4, 5, 6]. Mange affects animals of all ages and is often more prevalent under poor management conditions. Mange mites are considered among the most detrimental ectoparasites in livestock management. Transmission is primarily through direct contact with infected animals [7]. Although a variety of ectoparasiticidal drugs are commercially available for mange treatment, high costs and limited accessibility make their use difficult, especially among smallholder and subsistence farmers. As a result, despite significant advances in modern veterinary medicine, traditional medicinal practices remain a primary means of disease management in many rural communities [8]. Numerous medicinal plants have been documented to exhibit antiviral, antifungal, antibacterial, analgesic, and antipyretic activities, suggesting their potential as alternative therapeutic agents for ectoparasitic infections [9]. Most medicinal plants are considered safe, cost-effective, and generally free from issues associated with drug resistance and residual toxicity [10]. Neem (Azadirachta indica A. Juss.), is a highly recognized multipurpose plant, with a broad spectrum of biological activities. Phytochemicals derived from medicinal plants have shown significant promise due to their diverse biological effects and potential medicinal applications, making them valuable resources for the development of pharmaceuticals, industrial products, and the integrated management of agricultural pests [11]. Neem, in particular, is often referred to as a panacea for various dermatological conditions [12]. It was reported that crude aqueous extract of neem 20% concentration has been shown to possess acaricidal efficacy comparable to ivermectin, as it did not induce hepatic and renal toxicity, and it has been associated with improved growth performance in rabbits infected with Sarcoptes scabiei var. cuniculi [7]. Given its therapeutic potential, it is worthwhile to evaluate the efficacy of neem leaves in the treatment of mange. This study was therefore, investigates the effectiveness of topical neem leaf extract compared to ivermectin in the treatment of mange in infected WAD goats.

Result

Biochemical Composition of Neem Extract

The biochemical composition of neem extract and ivermectin pour-on is summarized in Table I. The neem extract contained notable levels of alkaloids (0.468%), saponins (0.379%), and phenols (0.189%), with alkaloids being the most abundant bioactive compound. Glycosides (0.185%) and tannins (0.0033%) were present in moderate amounts, while other compounds were found in trace quantities.

Histopathological Changes

Histological analysis of skin samples before treatment (Figures I a, II a, and III a) revealed hyperker-

Table 1.
Biochemical composition of the neem extract

Parameters	Observation Qualitative	Phyto Quantitative (%)
Neem extract		
Alkaloids	+++	0.4680 ± 0.05
Tannin	++	0.0033 ± 0.03
Phlobatannin	+	0.0011 ± 0.04
Saponin	+++	0.3790 ± 0.07
Flavonoids	+	0.0014 ± 0.05
Terpenes	+	0.0080 ± 0.10
Steroids	+	0.0012 ± 0.08
Anthraquinones	+	0.0026 ± 0.05
Phenol	+++	0.1890 ± 0.02
Chalcones	+	0.0006 ± 0.02
Glycosides	++	0.1850 ± 0.02
Cardenolides	+	0.0050 ± 0.01

+++ = PRESENT in an appreciable amount, ++ = PRESENT in a moderate amount, + = PRESENT in a trace amount

atosis and atrophy, indicative of extensive damage caused by mange infection. After treatment (Figures I b, II b, and III b), the epidermis of the treated WAD goat skins appeared normal with moderate cellular infiltration. Notably, animals treated with neem extract exhibited minimal cellular infiltration compared to the other groups .

Haematological changes

Table II presents the haematological indices of the WAD goats before and after topical treatment with neem extract and ivermectin. Prior to treatment, significant differences were observed in RBC count, haemoglobin concentration, MCH, MCHC, platelet count, RDW-CV, and PDW among experimental groups ($p < 0.05$). However, WBC count, haematocrit, and MCV showed no significant differences ($p > 0.05$). Post-treatment, significant increases were observed in WBC, RBC, MCV, MCH, MCHC levels across all experimental groups after treatment ($p < 0.05$). However, haemoglobin and haematocrit levels did not change significantly ($p > 0.05$). A notable rise in PDW and the percentage of large platelets was observed in groups T1 and T2.

In particular, animals treated with a combination of 5 ml neem extract and 5 ml ivermectin (T2) demonstrated significant changes ($p < 0.05$) in RBC count, haemoglobin concentration, haematocrit, RDW-CV, PDW, and MPV. However, no significant differences were found in WBC, MCV, MCH, MCHC, platelet count, or PLCR among treatment groups ($p > 0.05$). Goats treated with either 10 ml ivermectin (T1) or 10 ml neem extract (T3) showed no significant differences between each other ($p > 0.05$).

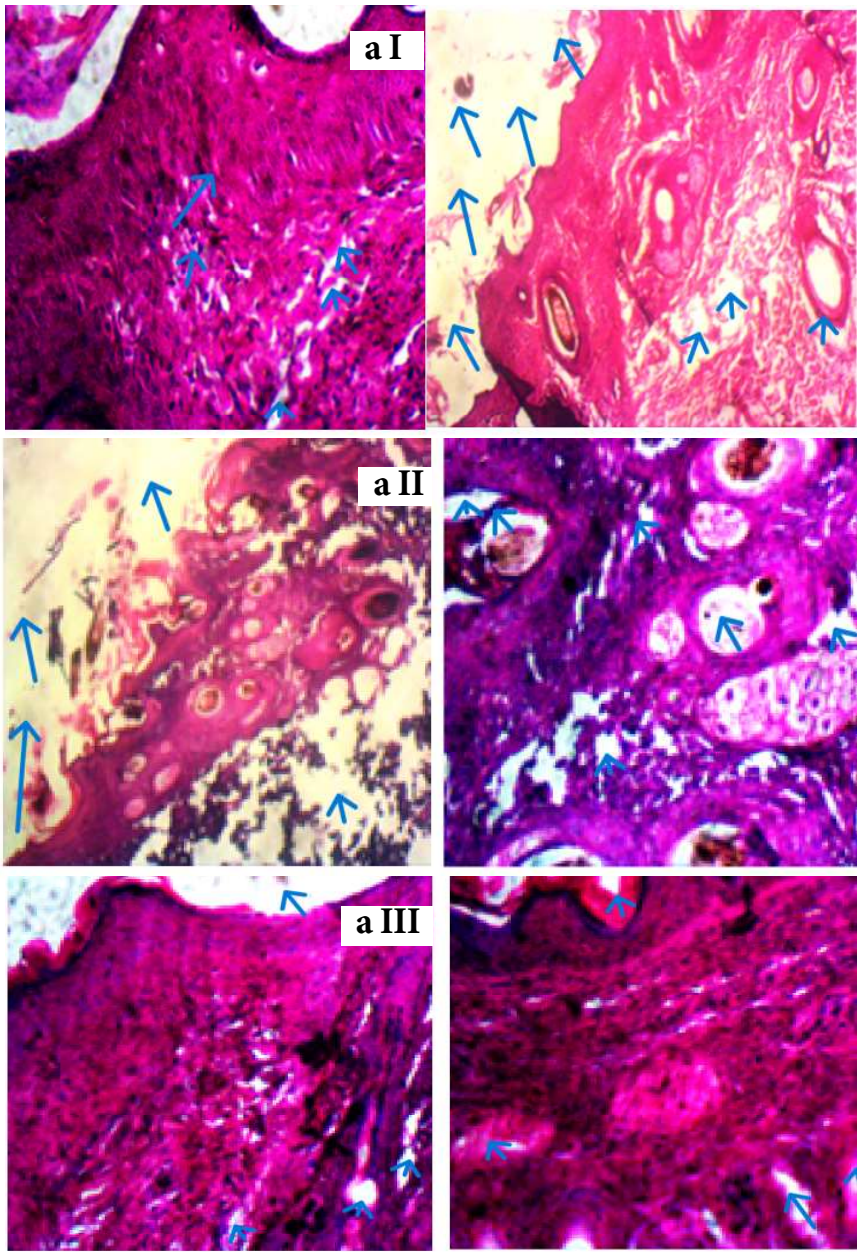

Figure a.
I: The extent of tissue damage as a result of mange infection is evident in the image. The two representative image samples from animals in the treatment revealed hyperkeratosis (thickening of the skin), scabs and inflammation, symptoms of untreated mange. II: The two representative image samples from animals in the treatment revealed scabs, hyperkeratosis (thickening of the skin), inflammation, and alopecia, which are symptoms of untreated mange. III: The two representative image samples from animals in the treatment revealed atrophy of the epidermis, hyperkeratosis (thickening of the skin), scabs, inflammation, and alopecia, which are symptoms of untreated mange.

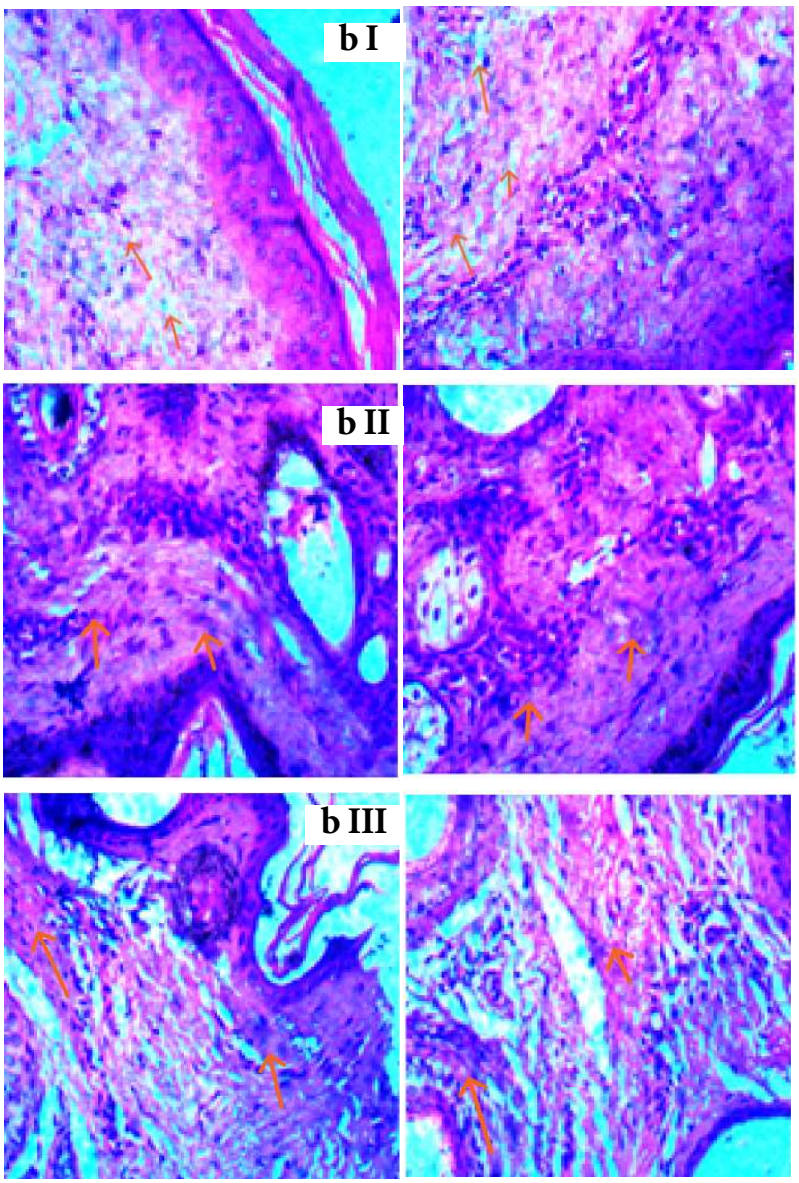

Figure b.
I: After the treatment of the mange infected West African dwarf goats with Ivermectin (T1), the histopathological analysis revealed that the epidermis is normal but there is moderate cellular infiltrate in the dermis. II: After the treatment of the mange infected WAD goats with Ivermectin and neem leaf extract (T2), the histopathological analysis revealed that the epidermis is normal but there is moderate cellular infiltrate and hyperplasia of peri-follicular. III: After the treatment of the mange infected WAD goats with neem leaf extract (T3), the histopathological analysis revealed that the epidermis is normal with a few cellular infiltrates in the dermis.

Serum Biochemical Indices

Table III presents the serum biochemical parameters and mineral levels of the WAD goats pre and post topical treatment with neem extract and ivermectin. For most measured indices, no significant differences were observe ($p > 0.05$). However, potassium levels showed a significant change after treatment ($p < 0.05$).

Discussion

The biochemical analysis of neem extract revealed significant concentrations of alkaloids (0.468%), saponins (0.379%), and phenols (0.189%). These bioactive compounds are known to possess antiparasitic properties, which likely contributed to the neem extract's effectiveness against mange [12]. Specifically, biochemical constituents such as saponin and azadirachtin, may increase the healing rate, and thus the animal can increase its feed intake. Saponin is one of the major constituents of neem that is responsible for the treatment of skin diseases. Alkaloids and saponins were responsible for the positive effect of the neem leaf extract on the mange-infected WAD goats. Saponins are reported to have antibiotic, antifungal and antiviral activities [13].

Neem has been traditionally used as an herbal remedy for various parasitic infestations, with studies showing that its active constituents can exert acaricidal, antibacterial, and antifungal activities [14 and 7]. In the current study, moderate amounts of glycosides (0.185%) and tannins (0.0033%) in neem extract suggest their potential role in enhancing the therapeutic properties, as both tannins and saponins are known for their antimicrobial and anti-inflammatory effects [14]. The ivermectin pour-on, with its active ingredient at 5 mg/ml, aligns with standard concentrations used for treating mange in livestock and was included as a conventional treatment for comparison.

Histopathological examination of skin samples

Table 2.
Haematological Indices of the West African Dwarf Goats Before and After Mange Topical Treatment with Neem Extract and Ivermectin

Parameter		T1(10ml iver-mectin)	T2(5ml iver-mectin+5ml neem extract	T3(10ml neem extract)	SEM
White blood Cell Count	Before	6.85^{y}	9.90y	8.73^{x}	0.65
(* 103µL)	After	18.00^{x}	17.13^{x}	19.83^{y}	0.88
	SEM*	0.85	1.85	3.13	
Red blood Cell Count	Before	1.71b^{y}	3.12^{ax}	1.39^{bx}	0.26
(*106 µL)	After	12.02^{bx}	14.03^{ay}	12.37^{by}	0.33
	SEM*	0.39	0.53	0.30	
Haemoglobin	Before	5.20^{b}	8.90^{a}	4.5b	0.64
g/dL	After	6.48^{b}	11.58^{a}	7.10^{b}	0.82
	SEM*	0.62	1.12	0.61	
Haematocrit	Before	14.05	20.38	14.77	1.64
(%)	After	23.58^{ab}	33.40^{a}	21.13^{b}	2.36
	SEM*	3.07	4.78	1.94	
	Before	10.77^{y}	10.79^{y}	10.15^{y}	0.16
MCV (fl)	After	17.13^{x}	18.00^{x}	17.17^{x}	0.29
	SEM*	0.25	0.70	0.62	
MCH	Before	3.22^{aby}	2.45b^{y}	3.53^{ay}	0.20
(Pg)	After	7.28^{x}	7.70x	7.13^{x}	0.16
	SEM*	0.03	0.07	0.32	
MCHC	Before	28.10^{b}	23.28^{cy}	32.53^{a}	1.33
(%)	After	32.08	31.48^{x}	31.40	0.94
	SEM*	3.67	1.17	2.22	
Platelet count	Before	134.33^{by}	188.65^{ay}	124.48^{by}	9.95
(* 103µL)	After	290.47^{x}	320.27^{x}	311.87^{x}	8.23
	SEM*	17.43	9.46	18.93	
	Before	20.35^{a}	21.85^{a}	18.17^{b}	0.55
RDW-CV	After	18.64^{b}	22.18^{a}	19.17^{b}	0.57
	SEM*	0.76	0.88	0.68	
	Before	10.35^{by}	11.95^{ay}	10.46^{b}	0.25
PDW	After	13.05^{bx}	16.85^{ax}	12.60^{b}	0.75
	SEM*	0.67	1.10	0.90	
	Before	66.25^{a}	69.40^{a}	56.90^{b}	2.10
PLCR	After	59.85	69.78	62.71	2.10
	SEM*	4.38	2.88	2.27	
	Before	14.10 ^{ab}	14.78^{a}	13.23^{b}	0.24
MPV	After	13.63^{b}	15.25^{a}	14.07^{ab}	0.29
	SEM*	-0.58	0.42	0.24	

abc- means with different superscripts in the same row are significantly different ($p < 0.05$); xy= means with different superscripts in the same sub –column are significantly different (t<0.05); SEM= standard error of mean among the treatments; SEM*= standard error of mean for the values before and after the treatment.

Table 3.
Serum Biochemical Indices and minerals of the West African Dwarf goats before and after mange topical treatment with Neem extract and Ivermectin

Parameter		T1(10ml ivermectin)	T2(5ml ivermectin+5ml neem extract	T3(10ml neem extract)	SEM
Total protein	Before	4.30	3.64^{y}	4.44	0.25
	After	5.21	5.50^{x}	4.92	0.18
	SEM*	0.56	0.53	0.46	
Albumin (g/dl)	Before	1.64^{y}	1.65^{y}	1.61y	0.05
	After	3.09^{x}	3.39^{x}	3.16x	0.17
	SEM*	0.27	0.24	0.46	
Globulin (g/dl)	Before	2.66	1.98	2.83	0.25
	After	2.11	2.11	1.77	0.11
	SEM*	0.34	0.56	0.31	
Aspartate Aminotransferase (u/l)	Before	188.03	192.49	187.46^{x}	13.78
	After	168.08	190.42	152.80^{y}	8.47
	SEM*	16.57	48.23	9.69	
Alanine Aminotransferase (u/l)	Before	46.64^{x}	50.21	46.45^{x}	4.43
	After	16.43^{y}	20.75	19.97^{y}	1.07
	SEM*	3.36	3.44	3.00	
Alkaline Phosphatase (u/l)	Before	53.63^{y}	45.41y	56.17^{y}	5.44
	After	123.05^{x}	137.00^{x}	163.67^{x}	8.99
	SEM*	13.13	19.24	29.54	
Albumin-globulin Ratio	Before	0.65^{y}	1.24	0.58y	0.22
	After	1.50^{x}	1.66	1.88x	0.16
	SEM*	0.06	0.58	0.05	
Minerals Sodium (Mmol/l)	Before	105.02	106.34	105.47	0.46
	After	148.33	139.89	130.70	7.79
	SEM*	16.29	11.24	14.38	
Potassium (Mmol/l)	Before	1.99	2.30	2.43	0.17
	After	3.33^{a}	2.25^{b}	2.73^{ab}	0.20
	SEM*	0.35	0.77	0.46	
Phosphorus (100mg/ml)	Before	1.88	2.06	1.75	0.08
	After	1.80	2.03	2.05	0.07
	SEM*	0.24	0.28	0.46	

abc- means with different superscripts in the same row are significantly different ($p < 0.05$); xy= means with different superscripts in the same sub –column are significantly different (t < 0.05); SEM= standard error of mean among the treatments; SEM*= standard error of mean for the values before and after the treatment.

pre and post treatment confirmed considerable dermal healing, especially in the neem treated group (Figure III b). Before treatment, all animals (Figures I a, II a and III a) showed signs of hyperkeratosis (a skin condition that occurs when the skin becomes thicker than usual in some places [15]) and epidermal atrophy, both characteristic lesions of mange infestation [7]. After treatment, the skins of the neem-treated goats showed a normalized epidermis with minimal cellular infiltration (Figure III b), suggesting that neem extract not only alleviated the clinical symptoms of mange but also promoted skin recovery. These findings align with previous research indicating the skin-healing and anti-inflammatory properties of

neem, which contribute to its effectiveness in treating skin conditions [7].

Haematological parameters further provided insights into the systemic effects of the treatments. The significant differences in the haematological parameters and the low values before the treatment, with the exception of WBC, haematocrit and MCV implies that the severity of the mange infection varies among the animals. Following treatments, significant increases were observed in WBC count; RBC count, MCV, MCH, and MCHC. These changes suggest a possible improvement in immune function and RBC production, likely in response to the reduction in parasitic load [9]. The increased WBC values remained within the recommended range for WAD goats (6.8-20.1×103µ/l, reported by [16]). Interestingly, no significant changes were observed in haemoglobin or haematocrit, indicating that these parameters may be less sensitive to the effects of the treatments in the short term. Moreover, increases in PDW and PLCR, particularly in groups T1 and T2, can suggest a heighten thrombopoietic response to infection and subsequent treatment [9].

The values for post-treatment of albumin levels (3.09-3.16g/dl) fell within the normal physiological range for goats (2.7-3.9g/dl, reported by [17]) as the normal range of albumin for goats. Albumin is quantitatively the most important plasma protein synthesized by the liver, and it indicates its health status. Total protein levels (4.90-5.60 g/dl) was lower than that reported by [18] (5.5-9.0g/dl) but remained consistent with reported by [19] (6.0–7.0 g/dL). Abnormally low protein levels indicate anaemia. Lower total protein before treatment likely resulted from the activities of the parasitic microorganisms, thus interfering with the normal absorption of nutrients [20]. This confirms the activities of the mites that feed on the blood of the host animal. The significant increase in total protein post-treatment supports the neem extract biochemicals probably disrupted mites' activity.

Serum biochemical analyses showed no significant changes across most parameters, except for potassium, which increased significantly post-treatment. Potassium is essential for maintaining cellular functions. Its increased levels post treatment may reflect improved cellular health and metabolic function [21]. The absence of significant changes in other biochemical markers suggests that the treatments did not induce major metabolic disruptions or deficiencies, further highlighting the safety of neem extract and ivermectin as topical treatments for mange.

In conclusion, neem extract proved to be a promising alternative or complementary treatment for mange in WAD goats, offering improvements in blood profile and skin recovery similar to ivermectin. Neem's bioactive compounds, such as alkaloids and saponins, may contribute to its acaricidal and growth-promoting effects. These effects mirror those of ivermectin, making neem a viable alternative or adjunct treatment. Given its efficacy, affordability, and safety, neem extract represents a valuable tool for managing mange in small ruminant production systems, particularly in resource-limited settings.

Materials and Methods

Experimental site and location

The study was carried out at the Small Ruminant Unit of the Ladoke Akintola University of Technology Teaching and Research Farm, located in Ogbomoso, Oyo State, Nigeria. All procedures adhered to ethical guidelines for the care and use of animals in research and were approved by the Committee on Research Ethics, Faculty of Agricultural Sciences, Ladoke Akintola University of Technology.

Preparation of the test ingredient

Fresh neem (Azadirachta indica) leaves, weighing approximately 5 kg, were harvested from trees within the farm premises. The leaves were allowed to slightly wilted before being homogenized with 10 litres of clean water. The resulting mixture was allowed to macerate overnight in a dark, enclosed environment to minimize photodegradation and prevent fermentation. The mixture was then filtered using a muslin cloth to obtain a clear extract, which was stored in a clean, airtight plastic container until use. Ivermectin, used as the conventional treatment, was sourced from a certified veterinary pharmacy. The formulation consisted of a mixture of 22,23-dihydroavermectin B1a (≥90%) and 22,23-dihydroavermectin B1b (≤10%), with the active ingredient concentration at 5 mg/ml in a pour-on form.

Experimental animals, housing and management

Twelve WAD goats, with an average body weight of 10.22 kg and diagnosed with mange, were sourced from local ruminant farmers. Upon arrival, the experimental pen was thoroughly cleaned and disinfected. Wood shavings were used as bedding material. The goats were quarantined for two weeks and followed by a subsequent two-week acclimatization period before the trial began. During the acclimatization phase, the goats were fed a basal diet of Megathyrsus maximus, and supplemented with concentrate feed (20% Brewers dry grain, 41% cassava peel, 35% wheat offal, 2% salt, 1% bone meal and 0.5% premix). Salt lick were provided, and goats had free access to water ad libitum.

After the acclimatization period, animals were weighed amd balanced by body weight, then randomly assigned into three treatment groups; with each animal individually tagged for identification. The treatment groups were: Treatment 1 (T1), which received 10 ml of ivermectin pour-on; Treatment 2 (T2), which received a combination of 5 ml of neem extract and 5 ml of ivermectin pour-on; and Treatment 3 (T3), which received 10 ml of neem extract. All treatments were applied topically along the dorsal midline using a improvised syringe, once daily for two weeks to ensure elimination of the causal organisms.

Data collection

A comprehensive physical examination was performed to

diagnose mange infection. Skin scrapings were collected using sterile surgical blades and immediately preserved in 10% neutral-buffered formalin for histopathological analysis. Blood samples (10 ml) were drawn from the jugular vein of each animal at both the beginning and end of the trial. For haematological analysis, approximately 5 ml of blood was drawn into sample tubes containing Ethylene Diamine Tetraacetic Acid to prevent coagulation. Serum biochemical indices were assessed using 5 ml sample collected in plain tubes. All samples were immediately sealed and gently inverted for one minute to mix, and were transported to the laboratory in an ice-packed containers to maintain sample integrity. Blood analyses were conducted using a Haema-autoanalyser B1110 5 plus (Prestige Diagnostics Ltd, United Kingdom).

Laboratory Procedure and Chemical Analysis

The neem extract was evaluated for the presence of alkaloids, tannins, phlobatannins, saponins, flavonoids, terpenes, and steroids. Standard phytochemical screening procedures were followed, as reported by [22].

Experimental design: The study used a Completely Randomized Design for the experiment.

Statistical analysis: Data were analyzed using a one-way analysis of variance (ANOVA) using the SAS software package [23]. In cases where ANOVA revealed significant differences among treatment means, Duncan's Multiple Range Test (DMRT) was used to determine which means differed significantly. Statistical significance was set at $p < 0.05$.

Authors' Contributions

OT conceived and planned the experiments. OT,O, OO and FA carried out the experiments. JA, OT, O, OO and FA contributed to sample preparationand the interpretation of the results. OT took the lead in writing the manuscript while JA proof read it. OT, JA, O, OO, FA provided critical feedback and helped shape the research, analysis and manuscript.

Acknowledgements

We would like to thank the students, field assistants, and authors are appreciated for their teamwork, collaborative efforts, and financial contributions. Funding assistance was not received during the research.

Competing Interests

The authors declare that there is no conflict of interest.

Reference

1. Oosting S, van der Lee J, Verdegem M. Farmed animal production in tropical circular food systems. Food Security. 2022; 14 :273–292. Doi:10.1007/s12571-021-01205-4

2. Bamaiyi PH. Factors Militating Against Animal Production in Nigeria. Intl. J. of Livestock Res. 2013; 3(2) ISSN 2277-1964 www.ijlr.org

3. Anyaogu D, Chukwudi C, Onuorah P, Shoyinka V. Diagnosis of mange in the West African Dwarf and Red Sokoto goats. Intl. J. of Inf. Diseases. 2018; 603 :73(314) Doi:10.1016/j.ijid.2018.04.4128

4. Fthenakis GC, Papadopoulos E, Himonas C, Leontides L, Kritas S, and Papatsas J. Efficacy of moxidectin against sarcoptic mange and the effects on milk yield of ewes and growth of lambs, Vet. Paras. 2000; 87: 207-216.

5. Taylor MA, Coop RL, Wall RL. Veterinary Parasitology. 3rd Edition, Blackwell Publishing, Oxford, 717, 2007.

6. Murshed M, Al-Quiraishy S, Mares MM. Survey of mange mite infesting sheep in Riyadh region, Saudi Arabia. Saudi J. of Bio. Sci. 2022; 29(1):595-600

7. Seddiek SA, Khater HF, El-Shorbagy MM, Ali MM. Effect of neem extract and ivermectin on mite (Sarcoptes scabiei) in experimentally infected rabbits. Proceeding of the 7th Int. Sci. Conf., Mansoura, 28-30 August, 2012.

8. Yuan H, Ma Q, Ye L, Piao G. The traditional medicine and modern medicine from natural products. McPhee D. J. (Ed.) Molecules. May; 2016; 21(5): 559. Doi: 10.3390/molecules21050559

9. Aladesanmi AJ, Iwalewa EO, Adebanjo AC, Akinkunmi EO, Taiwo BJ, Olorunmola FO, Lamikanra A. Antimicrobial and antioxidant activities of some Nigerian medicinal plants. Afr. J. of Trad. Comple. Alter. Med. 2006; 4(2):173-84. Doi:10.4314/ajtcam.v4i2.31206.

10. Tipu MA, Akhtar MS, Anjum MI, Raja ML. New dimension of medicinal plants as animal feed. Pak. Vet. J.; 2006 ;26(3).10-15

11. Hashmat I, Azad H, Ahmed A. Neem (Azadirachta indica A. Juss) –A nature's drug store: an overview. Intl. Res. J. of Bio. Sci. 2012; 1(6): 76-9.

12. Gopinath H, Karthikeyan L. Neem in dermatology: Shedding Light on the traditional panacea. Ind. J. of Derma. 2021; 66 (6): 706. Doi: 10.4103/ijd.ijd_562_21

13. Soetan KO, Oyekunle MA, Aiyelaagbe OO, Fafunso MA. Evaluation of the antimicrobial activity of saponins extract of Sorghum bicolor L. moench. Afr. J. of Biotech. 2006; 5(23): 2405-2407.

14. Mulla MS. Neem in pest management. Bioresource Technology, 2009; 100(19), 5252-5256.

15. Nall R. What you should know about hyperkeratosis. Medically reviewed by Cynthia Cobb. 2018 Accessed on August 23, 2023.

16. Okpara O, Obakanurhe O, Irikefe-Ekeke EP, Inweh D. Evaluation of Growth, Blood Parameters and Carcass Quality in WAFD Goats Fed Graded Amount of Concentrate Diets. Advances in Animal and Veterinary Sciences. 2025; 13. Doi:10.17582/ journal.aavs/ 2025/13.5.934.942.

17. Okpanachi U, Okpanachi GAC, Kaye J, Agu CI, Odah EO. Haematological profile and serum biochemistry of West African dwarf goats fed sun-dried yellow cashew pulp-based diets. J. of Appl. Sci. 2019; 19: (4): 319-324

18. Merck Veterinary Manual (MVM). Haematological reference ranges. Merck veterinary manual.2012. Retrieved from http://www.merck manuals.com.

19. Mohammed SA, Razzaque MA, Omar AE, Albert S, Al-Gallaf WM. Biochemical and haematological profile of different breeds of goat maintained under intensive production system. Afri. J. of Biotech. 2016 ;15(24):1253-1257. Doi: 10.5897/ AAJB2016.15362.

20. Ikwunze K, Jiwuba LC, Okoye LE, Amaduruonye W, Ilo SU, Okah U, Ahamefule FO. Haematology and serum biochemistry of West African Dwarf goats fed Pleurotus tuber-regium treated cassava root sievate based diets. Res. Sq. 2022. doi: Doi:10.21203/rs.3.rs-1324593/v1.

21. Barton MD Management of antimicrobial resistance in veterinary medicine. Microbial Drug Resistance. 2009; 15(1): 27-34.

22. Statistical Analysis System. Users guide for Windows. Analysis System Institute Inc. North Carolina, USA., 2003.

23. Ushie OA., Aikhoje EF, Aasegh TJ, Ibrahim AI, Bako B and Ettah AO. Estimation of total alkaloids, saponins flavonoid, tannins and phenols in Thaumatococcus danielli leaves. World Journal of Pharmaceutical and Medical research. 2022;8(4): 242-246.

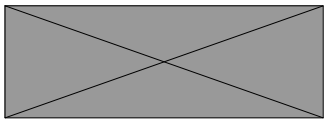

How to cite this article
Ojoawo O, Akinlade J, Furo Agbeniyi O, Hammed O, Rom-Kalilu F. Preliminary Evaluation of the Therapeutic Effects of Neem Leaf Extract and Ivermectin in West African Dwarf Goats with Clinical Mange. Iran J Vet Sci Technol. 2025; 17(3): 38-46.
DOI: https://doi.org/10.22067/ijvst.2025.93101.1504
URL:https://ijvst.um.ac.ir/article_46923.html

Iranian Journal of Veterinary Science and Technology

2024- Oct- 02
2025- Jun-19
2025-Jun-20

Received: 2024- Oct- 02
Accepted after revision: 2025- Jun-19
Published online: 2025-Jun-20

RESEARCH ARTICLE

DOI: 10.22067/ijvst.2025.89892.1422

Radioanatomical Study of the Rose-Ringed Parakeet (*Psittacula Krameri*) Head Based on the Findings of Computed Tomography Scanning

Siamak Alizadeh[a], Mohammadreza Hosseinchi[b], Raman Esmaeilnejad[c]

[a] Department of Clinical Sciences, Faculty of Veterinary Medicine, Nag.C., Islamic Azad University, Naghadeh, Iran.
[b] Department of Basic Sciences, Faculty of veterinary medicine, Ur.C., Islamic Azad University, Urmia, Iran.
[c] Doctor of Veterinary Medicine, Faculty of Veterinary Medicine, Ur.C., Islamic Azad University, Urmia, Iran.

ABSTRACT

Computed tomography (CT) is one of the most practical and accurate diagnostic imaging methods for evaluating the bird's head. This study aimed to present the normal anatomical data of Rose-ringed parakeet (Psittacula krameri) head using the CT imaging. In this research, the features of this bird's head were investigated in terms of bones, joints, muscles, sinuses, and other constituent tissues. A retrospective cross-sectional study was conducted on of six adult Rose-ringed parakeet carcasses (3 males and 3 females), aged 1–5 years and weighted between 115–125 g. Following preparing the CT images, the heads underwent gross anatomical studies. Based on the results, reconstructed CT images allowed clear identification of most structures, including the parietal, mandible, occiput, maxillary, preimaxillary, palatine, pterygoid, quadrate, and temporal bones, epithelial membranes, external ear canal and bony labyrinth, ossicles, entoglossal bones, different parts of the infraorbital sinus, brain hemispheres, and various parts of the eyeball and nasal conchae. The results related to the CT evaluation and anatomical examination of the Rose-ringed parakeet's head demonstrated a high correlation. The results of this research provide a valuable reference and can be employ for identifying anatomical features, examining different species of the parakeets, teaching veterinary anatomy, interpreting CT images, and supporting clinical examinations and treatment in this type of parrots.

Keywords

Computed tomography, Head, Radioanatomical, Rose-ringed parakeet (Psittacula krameri)

Abbreviations

CT: Computed Tomography

Number of Figures: 5
Number of Tables: 0
Number of References:: 47
Number of Pages: 14

Corresponding author: *Siamak Alizadeh*
Email: *Si.Alizadeh@iau.ac.ir*
Tel:+98(91)4189-1709

Introduction

Rose-ringed parakeet (Psittacula krameri), is a member of the green parrots (Psittaculidae) family [1]. This parrot is also known as Halsbandsittich (German), Perruche à collier (French), or Cotorra de Kramer (Spanish) [2]. It is similar in appearance to the Alexandrine parakeet (Psittacula eupatria), and it is smaller than the king parrot (Alisterus scapularis), plus lacks the red spots on the edges of its wings [3]. Typically, this parakeet measures approximately 40 cm in body length with a wingspan ranging between 15–17.5 cm. Its weight averages between 115 and 130 g, with males generally being slightly larger than females. In captivity, the species has a life expectancy of 20–30 years, with some individuals living beyond 40 years. The head is normally large and make up about 15–20% of the bird's total body weight [4]. The eyes constitute the bulk of the skull and are placed inside a sclerotic pupil (Figure 1). In some parrot species, the lower part of the eye is surrounded by a unique bony arch or suborbital arch [5]. The rostrum is connected with the skull bone by a joint, which gives the rostrum the ability to move upwards. Furthermore, parrot's tongue is more active and agile due to the entoglossal bones inside the mouth [6]. The mandible and maxilla are placed inside the upper and lower elements of the beak [7]. Inside the upper jaw, nasal cavity, stretched longitudinally aligned turbinates, or conchae. Among the diagnostic imaging techniques, conchae can merely be detected with CT [8]. Parrots also have distinctive facial sinuses, including the primary sinus chamber and the infraorbital sinus, which surround the ventral part of the eyeball and extend to areas around the eyes and ears through a series of canals. Some of these canals, along with the cervicocephalic air sac, extend to the central concha, the lower jaw, and the posterior parts of the neck. Except for the rostral part of the infraorbital sinus, these sinuses can be examined only through CT or magnetic resonance imaging (MRI) [9]. Anatomically, parrots lack the prefrontal, postfrontal, temporal, and postparietal skull bones. Their palatal bones are small and light. These birds lack teeth and have a relatively large and ossified brain chamber, which leads to weight loss and facilitate flight [10, 11]. Domesticated parrots are vulnerable to head injuries, particularly from collisions with window or landing an inappropriate places, which leads to traumatic injuries. In such cases, various imaging techniques can be beneficial in diagnoses. Among these, CT is one of the most accurate and practical diagnostic imaging methods for evaluating head diseases in birds. Previous studies have demonstrated CT's value in avian cranial anatomy. Veladiano et al. (2016) examined the natural anatomy of the heads of blue-and-yellow macaws (Ara ararauna), African gray (Psittacus erithacus), and monks (Myiopsitta monachus) by CT, labeled different parts of their heads on CT images, and finally introduced the obtained findings as an atlas of the natural head anatomy of these parrots [12]. Faillace et al. (2021) applied CT to investigate the anatomical features of the head of the blue-fronted Amazon parrot (Amazona aestiva), and found anatomical variations in some of these features, such as the size and position of the nasal conchae, the infraorbital sinus chamber, the nasopharyngeal duct, and the paraglossum, compared to other parrot species, which can be used in anatomy analysis [13]. Their findings also emphasized the difficulty of examining the inner ear and its related structures and the paratympanic sinus using normal CT images. Thurber et al. (2015) evaluated the differential diagnosis of parrots' neurolog-

Figure 1.
Rose-ringed parakeet (Psittacula krameri)

ical symptoms caused by hydrocephalus syndrome. They concluded that CT is a suitable screening tool for diagnosing hydrocephalus in this type of sick bird [14]. Similarly, Jones et al. (2019) used potassium iodide contrast medium and CT imaging to investigate the radioanatomical characteristics of the rock dove (common pigeon) especially in the head. They found that CT scanning can be utilized as a preferred method for examining different body tissues of this type of bird, and the images obtained with this method will be a valuable source for clinical applications and educational and research purposes [15]. Using CT, Duymus et al. (2013) compared the head anatomy of white, brown, and wild Japanese quails in terms of the head and brain volume, parietooccipital air space volume, and calvarial bone volume and indicated that the head of white quails had the lowest volume values, likely due to genetic differences [16]. Other studies further support and showed the value of CT in the diagnosis of complications and disorders of the head of parrot. Hébert (2019) confirmed Rostroparasphenopalatal luxation in a red-crowned parakeet (Cyanoramphus novaezelandiae) using CT, and the bird completely recovered after therapeutic measures [17]. Krautwald-Junghanns et al. (1998) compared radiology and CT scan techniques in the diagnosis of head diseases in sick parrots and reported the superiority of the CT method in the diagnosis of complications such as bone fractures and identification of hypercalcification or hypocalcification and carcinoma in this area [18]. The investigation of the tomographic features of the head of the Rose-ringed parakeet can be beneficial in identifying anatomical features and evaluating its pathological cases. However, a precise examination of details related to the normal anatomy (morphology and morphometry) of the different parts of this bird's head is necessary. Currently, radioanatomical studies of the head of the Rose-ringed parakeet are rare, and there are no detailed reports in this respect. Accordingly, this study aimed to investigate the normal anatomy of the Rose-ringed parakeet's head by CT using three-dimensional (3D) modeling.

Result

Reconstructed CT images revealed that most structures of the head of the Rose-ringed parakeet (Psittacula krameri) were identifiable. In the 3D images, the parrot's head appeared rounded and compact. The jugal arch and the palatine bone were fused in the remaining parts of the skull, except for the cranial facial bones. Even small bones of the head, such as ear bones and entoglossal bones inside the mouth, could also be evaluated in these CT images. Using the lung window filter, it was possible to observe the bony trabecular in the head. This setting also enabled evaluation of the parietal and temporal bones, nasal conchae, epithelial membranes, the external ear canal, and bony labyrinth. Further, with covering tissues, different parts of the infraorbital sinus could be observed using this filter. Furthermore, different soft tissue windows were adjusted to allow for the identification of brain hemispheres, the cerebellum, optic nerve, pupil muscles, and eye lenses (Figures 2-3). Based on the findings, the columella ossicle, its external cartilage, and the cochlea were not detectable on CT. The eyeballs of all parrots were complete and bony and located on the skull's lateral side (Figure 2i). The mandible appeared bony and lacked a distinct symphysis (Figures 2b and 3a), while the rostrum was keratinous, large, and ventrally curved. The operculum was observed on the dorsal base of the nostrils. Bones such as occipital, maxillary, premaxillary, mandible, palatine, pterygoid, and quadrate were pneumonized and had air bubbles. The nasal cavities were divided by a septum, which thickened slightly from the rostral to the caudal side. Its caudal third was cartilaginous, while the middle third and the rostral were bony. The ectethmoid, mesethmoid, maxillary, and preimaxillary bones were involved in the formation of the nasal cavity, and the nasal cavity comprised three parts: olfactory, respiratory, and vestibular. Each nasal cavity had a single duct with caudal, middle, and rostral cartilaginous conchae. The rostral concha C-shaped and located in the vestibular part of the nasal cavity decreased in thickness from the rostral to the caudal direction and contained a basal lamella along the lateral nasal cavity wall. The middle concha was in the form of long ducts that originated from a basal lamella and was located in the upper respiratory tract of the nasal cavity. This lamella also splits into a sinusoidal and a spiral lamella. The spiral lamella extended to the entrance of the nasopharyngeal canal. The caudal concha, smaller and hollow, was located at the nasal cavity's rear. The nasal and oral cavities were connected through the nasopharyngeal canal (Figures 3c and 4h), which connected the maxilla-palatal process and the palatine bone's choanal part from the rostro-lateral and caudal sides. The caudal part of this duct linked with the interorbital septum (Figures 3e and 4f). The oral cavity included the palatal, mandible, premaxillary, and maxillary bones, along with associated muscles and tongue. These bones, along with the pterygoid, contributed to pharynx formation (Figures 4c-d). The choana was located in the dorsal part of the pharynx and oral cavity and connected the oral cavity to the nasal cavity (Figure 2g). The tongue was strong and large, and could be identified in the CT images, located in the middle third and caudal of

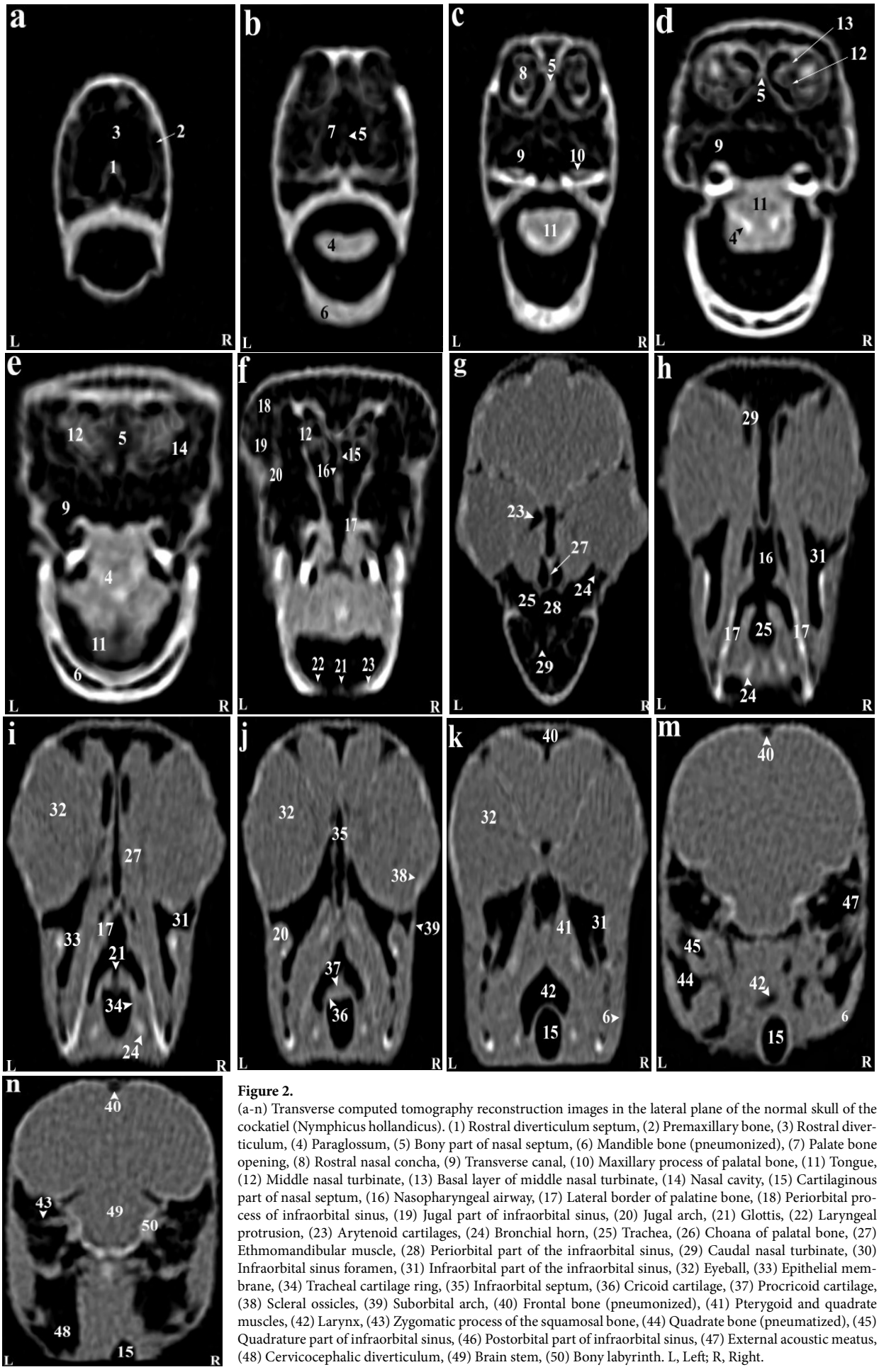

Figure 2.
(a-n) Transverse computed tomography reconstruction images in the lateral plane of the normal skull of the cockatiel (Nymphicus hollandicus). (1) Rostral diverticulum septum, (2) Premaxillary bone, (3) Rostral diverticulum, (4) Paraglossum, (5) Bony part of nasal septum, (6) Mandible bone (pneumonized), (7) Palate bone opening, (8) Rostral nasal concha, (9) Transverse canal, (10) Maxillary process of palatal bone, (11) Tongue, (12) Middle nasal turbinate, (13) Basal layer of middle nasal turbinate, (14) Nasal cavity, (15) Cartilaginous part of nasal septum, (16) Nasopharyngeal airway, (17) Lateral border of palatine bone, (18) Periorbital process of infraorbital sinus, (19) Jugal part of infraorbital sinus, (20) Jugal arch, (21) Glottis, (22) Laryngeal protrusion, (23) Arytenoid cartilages, (24) Bronchial horn, (25) Trachea, (26) Choana of palatal bone, (27) Ethmomandibular muscle, (28) Periorbital part of the infraorbital sinus, (29) Caudal nasal turbinate, (30) Infraorbital sinus foramen, (31) Infraorbital part of the infraorbital sinus, (32) Eyeball, (33) Epithelial membrane, (34) Tracheal cartilage ring, (35) Infraorbital septum, (36) Cricoid cartilage, (37) Procricoid cartilage, (38) Scleral ossicles, (39) Suborbital arch, (40) Frontal bone (pneumonized), (41) Pterygoid and quadrate muscles, (42) Larynx, (43) Zygomatic process of the squamosal bone, (44) Quadrate bone (pneumatized), (45) Quadrature part of infraorbital sinus, (46) Postorbital part of infraorbital sinus, (47) External acoustic meatus, (48) Cervicocephalic diverticulum, (49) Brain stem, (50) Bony labyrinth. L, Left; R, Right.

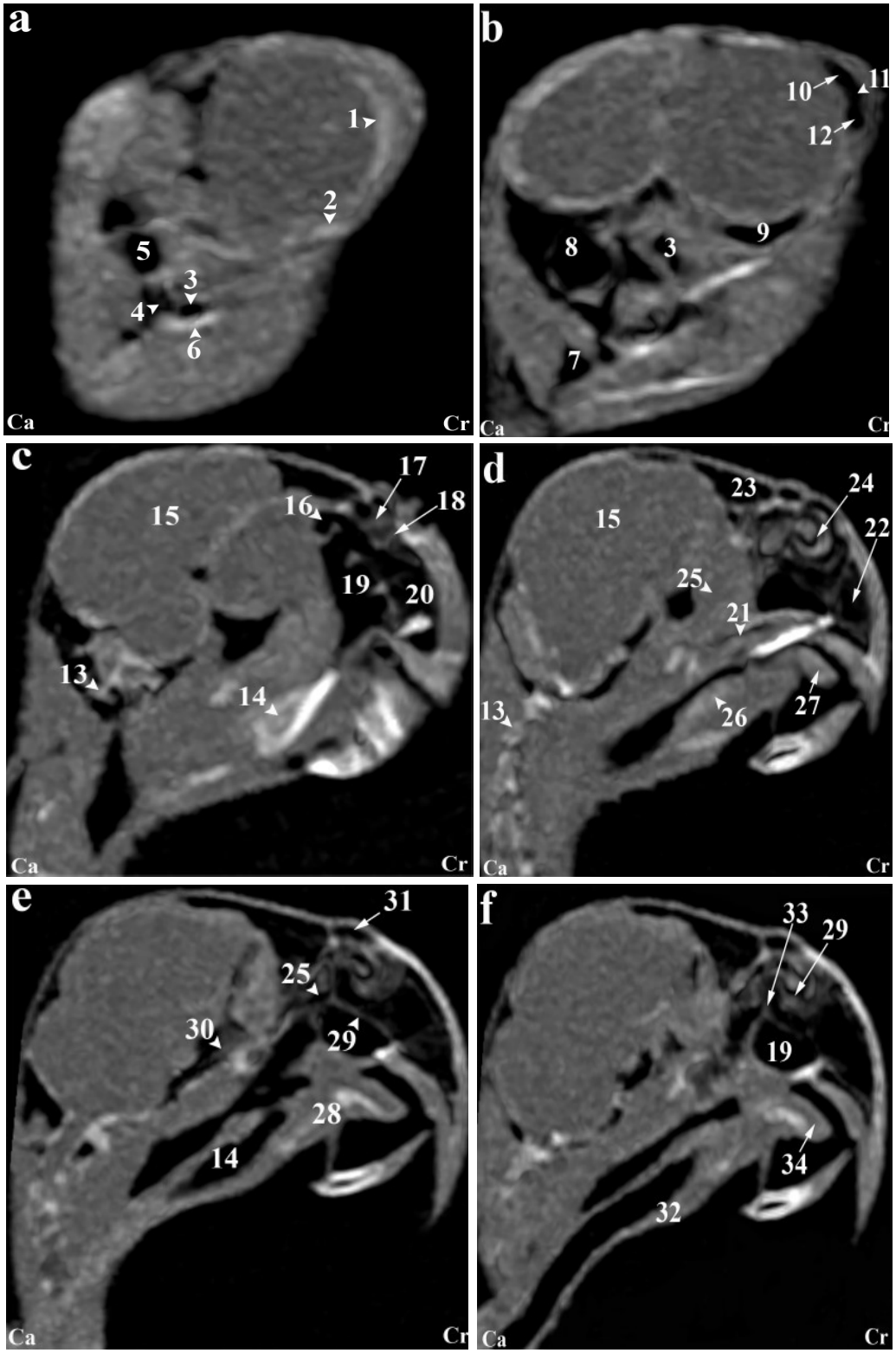

Figure 3.
(a-f) Sagittal computed tomography reconstruction images (lateromedial plane) of the normal skull of the cockatiel (Nymphicus hollandicus). (1) Scleral bones, (2) Suborbital arch, (3) Postorbital part of the infraorbital sinus, (4) Quadrate bone (pneumonized), (5) External ear foramen, (6) Mandible bone, (7) Cervicocephalic diverticulum, (8) Occipital bones (pneumonized), (9) Infraorbital part of infraorbital sinus, (10) Periorbital process, (11) Epithelial membrane, (12) Jugal portion of infraorbital sinus, (13) Cervical vertebrae, (14) Trachea, (15) Encephalon of the brain, (16) Caudal nasal turbinate, (17) Middle nasal turbinate, (18) Rostral nasal turbinate, (19) Transverse canal, (20) Premaxillary bone (pneumonized), (21) Palate bone (pneumonized), (22) Rostral diverticulum, (23) Frontal bone (pneumonized), (24) Nasal cavity, (25) Nasopharyngeal airway, (26) Larynx, (27) Paraglossum, (28) Basihyal, (29) Bony part of nasal septum, (30) Infraorbital septum, (31) Nostril, (32) Tracheal rings, (33) Cartilaginous part of nasal septum, (34) Tongue. Ca, Caudal; Cr, Cranial.

the inferior part of the oral cavity (Figures 2c-d). The oral cavity had a hyobranchial apparatus. The tongue's base was in close contact with the paraglossum and the cranial part of the basihyal. Bishyal processes and uhorial bones were detectable in the trachea's larynx and cranial part. The branchial horn (caudal part of the hyobranchial apparatus) was located in the inner part of mandible's ramus, or tracheal cranial part. Its caudal third was associated with mandible masseter muscles. The larynx consisted of a ring-shaped cricoid cartilage and two pyramid-shaped arytenoid cartilages. The results of the current study demonstrated that the procricoid cartilage was located within the middle part of the cricoid cartilage and formed the larynx 's dorsocaudal part (Figures 2b-j). The glottis was centrally placed in the larynx and surrounded by arytenoid cartilages. While laryngeal mounds (Mons laryngealis) were visible in CT cross-sectional. The place where the cricoid joins the tracheal cartilages also appeared ring-shaped in these images (Figures 2f and 4f).

The entire pupil cavity was filled with an oval eyeball bordered externally by the frontal bone and suborbital arch. A bony trabecular septum separated the pupils. All parrots under study had a complete bony eyeball (Figures 2j and 4h). In the obtained CT images, the eye lens was not clearly detectable, and the cranial chamber (aqueous) and the caudal (vitreous) were not distinguishable. The retina was unrecognizable. Eyeball muscles, lacrimal glands, and the third eyelid (nictitating membrane) had similar attenuation values and were indistinguishable. Scleral bones appeared as two indistinct lines on cross-sections images and as circular or round in sagittal images (Figures 2j, 3a, and 4h).

The parakeet's encephalon could be evaluated in the CT images (Figures 3c and 4i). Although, brain hemispheres such as the telencephalon and diencephalon, along with the brainstem and cerebellum, were well identified and could be distinguished from each other in cadavers, they shared similar attenuation in CT, making them difficult to differentiate. The findings revealed that the external acoustic meatus and the external opening of the ear were recognizable in CT images (Figures 2m and 4c), but the tympanic membrane was not visible in either CT images or carcasses examinations. Hence, different parts of the middle ear were not distinguishable. Nonetheless, the presence of low-resolution lines in the distal third of the external acoustic meatus can demonstrate parts of the middle ear such as infraorbital (columella) and extracolumella cartilage. The bony labyrinth of the inner ear was clearly visible in both in the cadaver samples and CT images.

Based on our findings, the paratympanic sinus could not be identified in CT images. Muscles of the head were only faintly visible hyperattenuated lines. Larger muscles, such as quadrate, pterygoid, and ethmomandibular, were somewhat distinguishable, although the jaw adductor muscle despite its size, was poorly detectable in CT images (Figures 2g and 4c). The infraorbital sinus was surrounded by skull bones and covering and muscular tissues and was found as a large triangular cavity that covered a large part of the head. The premaxillary bone was located in the rostral part of this sinus, with palatine and pterygoid bones located in its inner part. Further, the quadrate, jugal arch, and mandible were located in the lateral part. This sinus included the rostral diverticulum, transverse canal, postorbital, preorbital, infraorbital, quadrate bones, cervicocephalic diverticulum, and mandibular recess. The rostral diverticulum and the transverse canal were single, and the remaining parts were in pairs. Except for the periorbital parts, the transverse canal, and the rostral diverticulum, the remaining parts of the suborbital sinus were covered by the masticatory muscle (Figures 2-4). The rostral diverticulum, extending along the premaxillary bone, was divided into two parts by a thin bony septum, which gradually thinned from rostral to the caudal direction, and eventually disappeared in the middle parts of the diverticulum. The transverse canal was a short and horizontal passage. The maxillary process of the palatine bone and the upper jaw-palatine process (maxillopalatine) of the maxilla, were located in this canal's ventral and distal parts, respectively. This canal connected the periorbital region and rostral diverticulum (Figures 2a, 3d, and 4h). The nasopharyngeal duct divided the periorbital region into left and right parts. The jugal portion was connected dorsally to the periorbital region, ventrally to the choanal part of the palatine bone, and laterally to the jugal arch. A relatively thin epithelial layer separated the periorbital and the jugal portion. These subdivisions were connected in the caudal part, near the infraorbital part of the infraorbital sinus. The infraorbital part, the largest part, covered a large area of the ventral surface of this sinus and extended to the eyeball. It connected to the palatine bone and interorbital septum from the medial part and to the suborbital and jugal arches from the lateral part. The infraorbital and postorbital parts were directly connected. The infraorbital and postorbital parts were the largest parts of the infraorbital sinus, respectively. The postorbital part was located in the pterygoid's lateral part, the zygomatic process's internal part, and the jugal bow's posterior part, which was connected with the musculature. The masseter, pterygoid, quadrate, and temporal muscles were located in the postorbital area. The caudoventral part of postorbital was connected to the quadrate por-

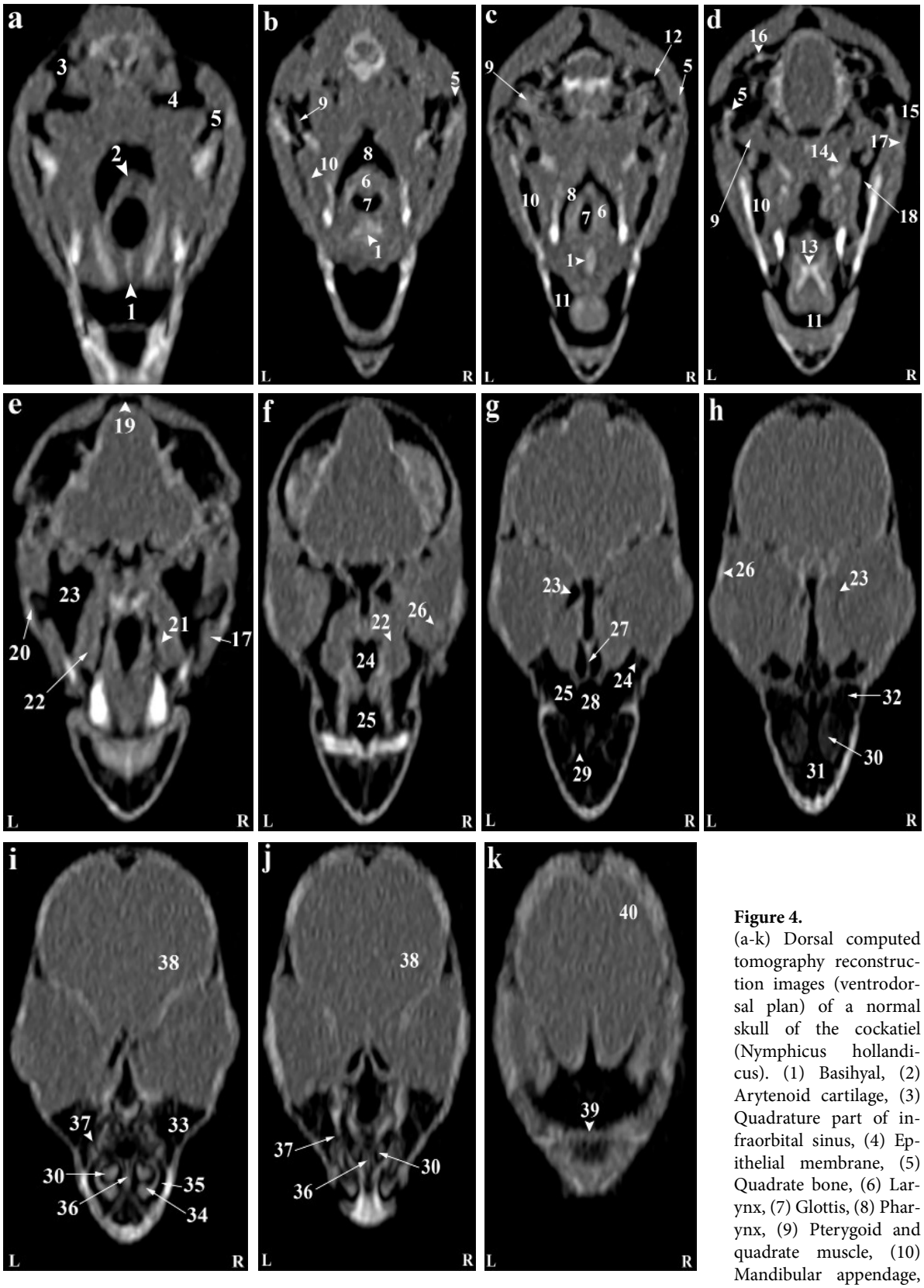

Figure 4.
(a-k) Dorsal computed tomography reconstruction images (ventrodorsal plan) of a normal skull of the cockatiel (Nymphicus hollandicus). (1) Basihyal, (2) Arytenoid cartilage, (3) Quadrature part of infraorbital sinus, (4) Epithelial membrane, (5) Quadrate bone, (6) Larynx, (7) Glottis, (8) Pharynx, (9) Pterygoid and quadrate muscle, (10) Mandibular appendage, (11) Oral cavity, (12) External acoustic meatus, (13) Paraglossum, (14) Pterygoid bone, (15) External ear foramen, (16) Bony labyrinth, (17) Jugal arch, (18) Postorbital part of infraorbital sinus, (19) Occipital bones (pneumonized), (20) Suborbital arch, (21) Palate bone, (22) Ethmomandibular muscle, (23) Infraorbital part of the infraorbital sinus, (24) Nasopharyngeal canal, (26) Scleral ossicles, (27) Infraorbital septum, (28) Cartilaginous part of the nasal septum, (29) Palate foramen, (30) Middle nasal turbinate, (31) Rostral diverticulum, (32) Cranial foramen of eyeball, (33) Preorbital part of the infraorbital sinus, (34) Rostral nasal turbinate, (35) Nasal cavity, (36) Bony part of nasal sinus, (37) Infraorbital sinus foramen, (38) Encephalon, (39) Craniofacial flexion, (40) Frontal bone. L, Left; R, Right.

tion. The smallest part of the infraorbital sinus was related to a quadrate part, which was laterally connected to the quadrate bone. The mandibular recess and cervicocephalic diverticulum were linked to the postorbital part. The mandibular recess was visible in the inner and rostral parts of the mandibular ramus. In fact, this recess was located in the inner part of the postorbital and the ventral part of the infraorbital canal. Lastly, the cervicocephalic diverticulum was detectable and extended to the cervical region (Figures 2n and 3b).

Discussion

In this study, we aimed to investigate the normal anatomy of the Rose-ringed parakeet (Psittacula krameri) head using computed tomography (CT). Based on our results, reconstructed CT images successfully allowed the identification of most skeletal and soft tissue structures of the head, including parietal, temporal, and maxillary bones, ossicles, nasal conchae, infraorbital sinus subdivisions, encephalon, and ocular components. The CT findings showed a high correlation with gross anatomical observations, demonstrating that CT is a practical and accurate method for describing the radioanatomical features of this parrot's head.

The CT and gross anatomy results in this study revealed that the skull of the Rose-ringed parakeet (Psittacula krameri) shares similarities with other parrot species, with no observable difference between the skulls of male and female individuals. CT diagnostic method enabled the anatomical description of the skull, aligning with the reports of some researchers in this field [19, 20]. Despite the small size of the parakeet's head, high quality images were obtained, allowing for clear identification of bones and tissues of the head, such as the jugal arch, palatine bone, ear ossicles, and antoglossum bones inside the mouth and different parts of the infraorbital sinus. Of course, the quality of these images was significantly influenced by the type of CT scanner used (Toshiba Multi-slice CT scanner Asteion Premium 4, Model: TSX-021B, Japan). In this research, the bony trabeculae of the head of the Rose-ringed parakeet were observed by using a suitable window (WW: 2336 HU; WL: 368 HU), the study successfully visualized parietal and temporal bones, nasal conchae, epithelial membranes, external acoustic meatus, and bony labyrinth. Performing head CT in sagittal, transverse, and dorsal planes, were obtained allowing detailed assessment of individual anatomical components, particularly the infraorbital sinus. Scanning the head in different planes solved the problem of superimposition of the images of different tissues, and each of the tissues was individually and specifically evaluated accordingly. These observations are supported by Cubo and Casinos (2000), thay examined the bones of different bird species and reported that some bird bones contain air bubbles [21]. In this study, some of the skull bones, such as the occipital, maxillary, preimaxillary, mandible, palatine, pterygoid, and quadrate bones, are trabecular and pneumonized and have air bubbles. However, Veladiano (2018) investigated the head CT of different birds and described the role of the pneumatic foramen, suborbital and paratympanic sinuses [22], which contradicts our findings. In our scans, the pneumatic foramen was undetectable, and the origin of bone pneumatization could not be evaluated. Furthermore, the paratympanic sinus was not visible , probably due to the fusion with middle ear tissues.

In this study, the tympanic membrane and different parts of the middle ear were also not visible in the CT images. However, the presence of low-resolution lines within the distal third of the external acoustic meatus can demonstrate parts of the middle ear, such as columella and extracolumella cartilage. These results are consistent with Wild's study (2015) [23].

According to our CT images, the tympanic membrane and different parts of the middle ear were not visible. These results are in agreement with Wild's study (2015), which reported that the cochlea, tympanic membrane, extracolumella cartilage, and columella of parrots are extremely small and therefore cannot be observed in CT images. It has been reported that the cochlea, tympanic membrane, extracolumella cartilage, and columella of parrots are extremely small and thus cannot be observed in CT images. Nonetheless, it is suggested that other diagnostic imaging methods, such as micro-CT and MRI, be used to evaluate these parts.

Our findings regarding nasal cavity conchae align with studies reporting three conchae per cavity in birds [24, 25]. The results of the current study revealed that in Rose-ringed parakeet, each nasal cavity, contained of a single meatus with caudal, middle, and rostral cartilaginous conchae. Other species, like the Congo gray parrot (Psittacus erithacus) [26], the budgerigar (Melopsittacus undulates) [27], and the brown-eared nightingale (Hysipetes amaurotis) [28], have been reported to possess only two conchae, while some like petrel (Pagodroma sp.) have more than three [29]. In our study , the middle and caudal turbinates had the largest and smallest sizes, respectively, consistent with the results of other parrot studies done by Hanafy (2021) and Al-Rubaie and Kadhim (2023) [25, 30]. In the skull of the Rose-ringed parakeet, similar to other parrots, the middle concha resembled a long duct,

which is located in the upper respiratory airway and originates from a basal lamella, which itself is divided into a sinus lamella and a spiral lamella. Moreover, the caudal concha is small and hollow and is placed in the caudal nasal cavity. Contradictory findings were reported by Faillace et al. (2021), who examined the CT results of the nasal conchae of the blue-fronted Amazon parrot (Amazona aestiva), described the middle concha as a narrow linear structure inside the rostral concha [13]. They further found that in this type of parrot, the caudal concha can have different sizes, so that the size of this concha is large in some of these birds, while it is extremely small in others. In a study, Madkour (2019) suggested the presence of bone tissue in addition to cartilaginous tissue within nasal conchae of some bird species [31]. Madkour's report does not match the result of our study, according to our observations, the structure of the nasal conchae of the Rose-ringed parakeet was purely cartilaginous, and this finding was confirmed by the attenuation of the CT images of the head. Van Zeeland (2018) investigated the upper respiratory tracts of parrots and reported that the nasopharynx contains adenoids and lymphoid tissues and connects the nasal cavities and the throat [32]. The Van Zeeland's study is somewhat in line with our gross anatomy results. The nasal and oral cavities were linked through the nasopharyngeal duct in the Rose-ringed parakeet. Based on CT images, the nasopharyngeal duct was rostrolaterally and caudally connected to the maxilla-palatal process of the maxillary bone and the choanal part of the palatine bone, respectively. The caudal part of the nasopharyngeal duct was linked to the interorbital septum. Unfortunately, we found no valid literature on the nasopharyngeal CT characteristics of birds and because of that we couldn't compare our results on that with other studies.

The Rose-ringed parakeet oral cavity had a hyobranchial apparatus, with its caudal part located in the inner part of the mandible's ramus, in other words, cranial part of trachea. These findings conform to the results of other studies performed on parrots. According to our observations, the tongue's base was in close contact with the paraglossum and the cranial part of basihyal.

Our results also demonstrated that the pupil of the Rose-ringed parakeet is completely bony. In the gross anatomy studies, it was possible to determine the anterior and caudal chambers, lens, and optic nerve of this bird's eye, which matches the reports of most researchers, and it seems that the eye anatomy of this type of parrot does not particularly differ from that of other birds [33]. However, unlike the gross anatomical evaluations, the lens was not clearly visible, and it was impossible to distinguish the ocular chambers in the obtained CT images. The retina, eyeballs' muscles, lacrimal glands, and third eyelid (nictitating membrane) were indistinguishable and therefore could not be separated from each other. The researchers of this study could not find written and specific reports about CT scans of birds' eyes and compare them with the results of our study. However, according to the findings of our study, we recommend the use of diagnostic imaging methods such as ultrasonography, micro-CT, MRI, and other specialized eye evaluation methods for examining the internal tissues of the eye.

In the CT images, while, the masticatory muscle could be identified due to their large size, other head muscles, including eyeball's muscles, and even nerve vessels showed highly close attenuation, and it was difficult to distinguish between them; thus, they did not undergo separate analyses. Different radiation factors were employed to increase the clarity and contrast of these tissues, but no suitable answer was obtained in this regard.

Based on anatomical examination of the budgerigar and Casco (African grey parrot), Smallwood (2014) reported that the cricoid cartilage of the larynx of these birds is wide and has a rostral process [34]. In another study, Silva et al. (2020) found that the cricoid cartilage of the larynx of the cockatiel is smooth and small and has two rostral and lateral processes [35], which contradicts our findings. In contrast to the findings of both Smallwood (2014) and Silva et al. (2020), our study showed that in the Rose-ringed parakeet, the larynx consisted of an annular cricoid cartilage and two pyramidal arytenoid cartilages, with a smooth and thin cricoid cartilage lacking processes. Additionally, a procricoid cartilage was present in the middle part of the cricoid, forming the dorsocaudal portion of the larynx.. In the Rose-ringed parakeet, the larynx consisted of an annular cricoid cartilage and two pyramidal arytenoid cartilages. The cricoid cartilage was smooth and thin and had no processes. In the middle part of the cricoid cartilage, there was the procricoid cartilage, which formed the dorsocaudal part of the larynx.

Although several studies, have examined the anatomy of the infraorbital sinus in some poultry such as hens, turkeys, and geese [36], there is no detailed and comprehensive report about the anatomy and CT features of the infraorbital sinus in parrots. Our research showed that in the Rose-ringed parakeet, the infraorbital sinus was surrounded by skull bones and covering and muscular tissues, and in the CT images, it was detected as a large triangular cavity that covered a large part of the head. The premaxillary bone was located in the rostral part, the palatine and pterygoid bones were located in its inner part, and the quadrate bone, jugal arch, and mandible bones were

located in the lateral part of this sinus. Grist (2006) conducted an anatomical study on domestic chickens and found that there were fewer infraorbital sinus chambers in the head of this type of bird [37], though he did not named and characterize these chambers. Eventually, it was indicated that this sinus is shorter in other birds and is limited by the infraorbital part. According to our observations, this sinus included the rostral diverticulum, transverse canal, postorbital, preorbital, infraorbital, and quadrate parts, cervicocephalic diverticulum, and mandibular recess in the Rose-ringed parakeet. The head and neck of this type of parrot were widely pneumatized with this sinus. No specific homologies were inferred in this regard since the analogy of the infraorbital sinus and phylogenetic evaluations between the Rose-ringed parakeet and other parrots was impossible.

Massari et al. (2020) performed CT on the head of a macaw and reported that the infraorbital, periorbital, and rostral diverticulum of the infraorbital sinus can be easily detected, which is mainly due to the large chambers of this sinus and the absence of covering muscles in this region [38]. It was further indicated that the postorbital, quadrate, and mandibular recess parts were not detectable because they were small and superimposed by the masticatory muscle. These findings somewhat corroborate the results of our study. Based on our findings in the Rose-ringed parakeet, except for the periorbital, transverse canal, and rostral diverticulum, the remaining parts of the suborbital sinus were covered by the masticatory muscle.

In some studies, the existence of a paratracheal recess was reported in Amazon and Cockatoo [39], as well as Anodorhynchus and Ararauna macaws [40], but we found no such structures in the Rose-ringed parakeets; therefore, this feature can be mentioned in the comparative anatomy of this type of parrot.

The skull of the Rose-ringed parakeet was relatively small, and the limit distance of its constituent bones was visible. The periorbital sinus was located in the anterorbital fenestra, and the zygomatic process of the squamosal bone surrounded the postorbital sinus. CT images showed head muscles as hyper-attenuated lines and not very clear. However, relatively larger muscles such as quadrate, pterygoid, and ethmomandibular were somehow distinguishable. The jaw adductor muscle, although large, it could not be detected in the CT images, and its boundaries was determined based on the topography of the bones in that region.

Finally, the columella ossicle, its external cartilage, and cochlea were not recognizable in CT images likely due to their small size. Hence, it is recommended that other diagnostic imaging methods such as micro-CT or MRI be utilized in cases where it is intended to evaluate these structures.

Overall, this study demonstrates that the skull of the Rose-ringed parakeet is not that much different from that of other parrots. The only morphological differences were related to some parts of the nasal cavity, infraorbital sinus, and, to some extent, the hyobranchial apparatus and nasopharyngeal duct.

In conclusion, the CT scan is one of the most effective and non-invasive diagnostic imaging methods to describe and dissect most of the hard and soft tissues of the Rose-ringed parakeet's head. The results of this study demonstrated its utility on examining the infraorbital sinus and the turbinates, or conchae, of nasal cavities. The investigation of the tomographic features of the Rose-ringed parakeet's head can be useful in identifying anatomical features and evaluating its pathological cases. The results of this research can be utilized as a standard reference and atlas for identifying anatomical characteristics, examining various species of Rose-ringed parakeets, teaching anatomy, and interpreting CT scan images. Moreover, these findings can be used for clinical examinations and aid in treatment of this type of parrot.

Materials and Methods

Ethical consideration

This work involved the use of procedures that did not differ from established internationally recognized high standards (best practice) of veterinary clinical care for the individual animals. The study was approved by the Ethical Committee of Islamic Azad University, Urmia, under registration code Ir.iau.urmia.rec.1403.038

Study design and Specimens

The current retrospective cross-sectional study was conducted using carcasses of six adult Rose-ringed parakeets (Psittacula krameri) (3 males and 3 females) with an average age range of 1–5 years and an average weight between 115–125 g. These birds were well-nourished during their lifetime. The carcasses were collected from a private Rose-ringed parakeet breeding facility in Tehran and stored at -20°C until use. The parrots, which previously died for various reasons, were used in this study, and the cause of their deaths was unrelated to this study. Maturity of the specimens was confirmed by factors such as assessing neck ring coloration, the amount of scales on the feet, the condition of the feathers, and the beak color. Sex of the specimens was also determined following a necropsy of the carcass [41, 42].

Computed tomography (CT) studies

For CT imaging, each parrot was placed on the scanner table in a sternal recumbent position, with the head oriented forward and the mandible aligned perpendicular to the gantry. Scanning was performed in the sagittal, transverse, and dorsal planes with a thickness and interval of 1 mm. A helical scanner (Toshiba Multislice CT Scanner Asteion Premium 4, Model: TSX-021B, Japan) was employed for CT. In addition, appropriate windows were selected to examine soft and bone tissues. The technical factors of the CT scanner included gantry rotation time (400 ms), slice thickness (1 mm), reconstruction distance (0.5–1 mm), pitch ratio

(1), kVp (120), mAs (10), physical detector collimation (32 × 0.6 mm), final section collimation (64 × 0.6 mm), resolution (512 × 512 pixels), and resolution range (0.92 × 0.92), Kernel (10 H), and increment (0.5 mm) [13, 43]. Imaging was performed based on the above-mentioned factors, and the obtained images were saved in DICOM format [44].

Three-dimensional reconstruction

DICOM images were imported to a computer system equipped with 3D modeling software (Onis CT software, Multi-Modality Workplace: VE 2.5A) and displayed using bone window settings (window width: UH 4500 and window level: UH750), consistent with previous research [45]. Further analyses was performed using 3D slicer software [46]. Based on our observations, this technique allowed the use of lung (WW: 2336 HU; WL: 368 HU) and bone (WW: 950; WL: 390) windows, thus providing high-resolution images of the tissues and structures that constitute the head region of the parrots.

Anatomical studies

Following CT imaging, each frozen parrots head was transversely sectioned using an electric band saw at 5 mm intervals, from the rostral part of the rhamphotheca to the anterior end of the neck. Each slice was rinsed with water and cleaned with a soft brush and photographed. Visible textures and structures were identified and labeled on these photographs. Further, CT images were matched with these photos and labeled accordingly. Nomina Anatomica Veterinaria guidelines was used as the obtained scientific term [47] (Figure 5).

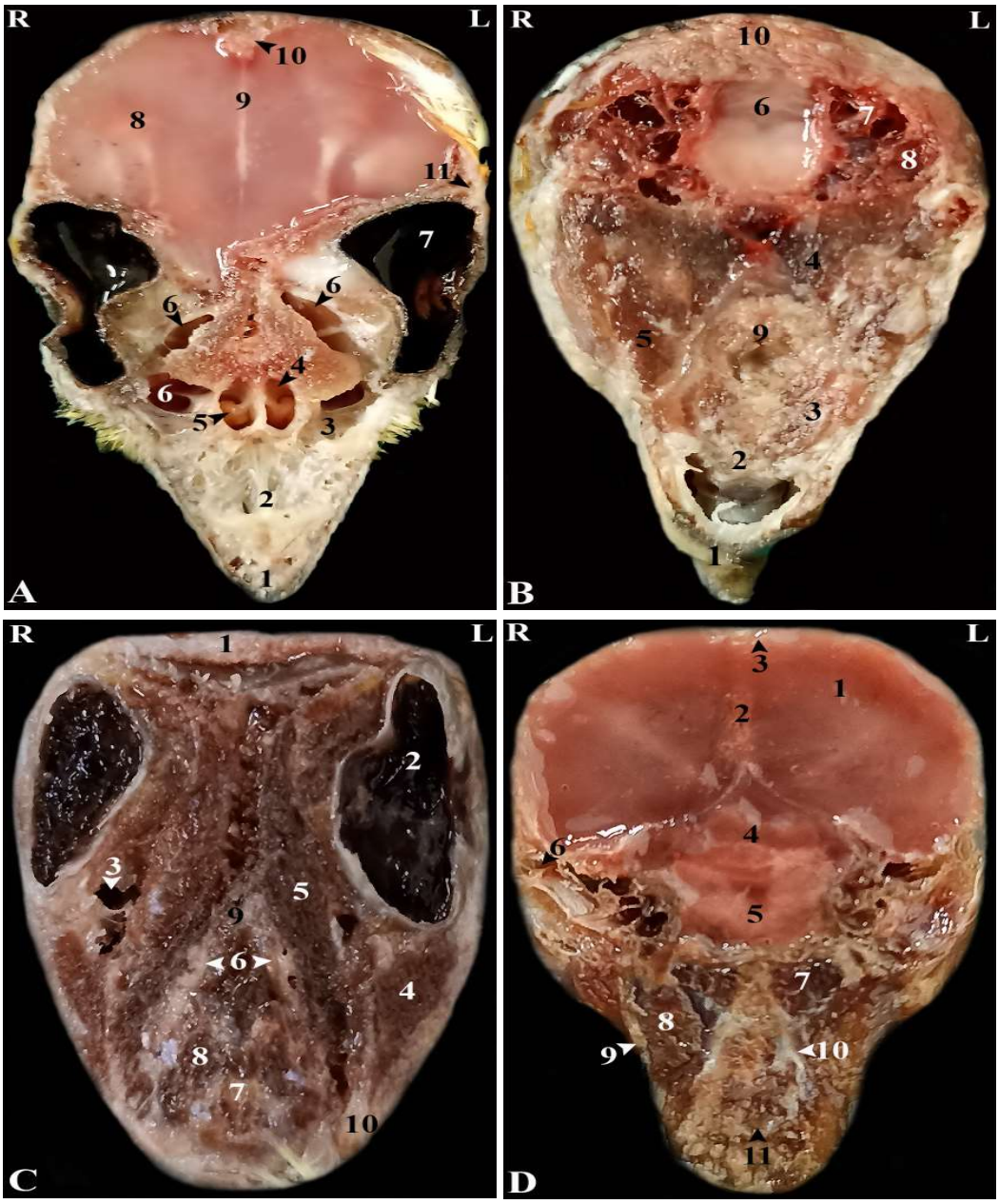

Figure 5.
Representative photographs of anatomic cross sections of the adult cockatiel (Nymphicus hollandicus) head. A (level of the Eye) and B (level of the external acoustic meatus) in the dorsal plane and C (level of the rostral border of the orbital fossa) and D (level of the external acoustic meatus) in the transverse plane. A: (1) Rhamphoteca, (2) Premaxilla bone, (3) Maxilla bone, (4) Left nasal cavity, (5) Caudal nasal concha, (6) Infraorbital sinus, (7) Eye, (8) Brain hemispheres, (9) Falx cerebri, (10) Occipital bone, (11) Temporal bone. B: (1) Rhamphoteca, (2) Premaxilla bone, (3) Palatine bone, (4) Ethmomandibularis muscle, (5) Pterygoideus muscle, (6) Cerebellum, (7) Bony labyrinth, (8) External acoustic meatus, (9) Caudal nasal concha, (10) Occipital bone. C: (1) Fronto-parietal bone, (2) Eye, (3) Infraoebital sinus, (4) Pterygoideus muscle, (5) Ethmomandibularis muscle, (6) Hard Palate, (7) Eye, (8) Caudal nasal concha, (9) Lingual process of hyoid bone, (10) tongue, (11) Choanal cleft, (12) Mandible. D: (1) Cerebrum, (2) Falx cerebri, (3) Occipital bone, (4) Brain stem, (5) Chiasma optic, (6) External acoustic meatus, (7) Ethmomandibularis muscle, (8) Pterygoideus muscle, (9) Mandible, (10) Hard palate, (11) Lingual process of hyoid bone. R, Right; L, Left.

Authors' Contributions

Conceived and designed the experiments: SA, MRH. Performed the experiments: MRH. Analyzed the data: SA, MRH, RE. Research space and equipment: SA, MRH. Contributed reagents/materials/analysis tools: SA. wrote the paper: SA, MRH.

Acknowledgements

The authors thank the Vice Chancellor for Research of Islamic Azad University of Urmia for financial supports (Protocol Code: 3/ 29801).

Competing Interests

The authors declare that there is no conflict of interest.

Reference

1. Abed SA, Salim MA, Alsaffah SM. First record of Alexandrine Parakeet psittacula eupatria (Psittaculidae, psittaciformes)(Linnaeus 1766) in Iraq. Indian Journal of Ecology. 2020;47(3):887-8.

2. Braun M. Die Bestandssituation des Halsbandsittichs Psittacula krameri in der Rhein-Neckar-Region (Baden-Württemberg, Rheinland-Pfalz, Hessen), 1962-2008, im Kontext der gesamteuropäischen Verbreitung. Vogelwelt. 2009;130:77-89.

3. Şahin D, Arslangündoğdu Z. Breeding status and nest characteristics of roseriged (Psittacula krameri) and alexandrine parakeets (Psittacula eupatria) in Istanbul's city park. Applied Ecology & Environmental Research. 2019;17(2). Doi: 10.15666/aeer/1702_24612471.

4. Mentil L, Monti P, Fraticelli F, Carpaneto GM. A morphometric sexing approach for the Ring-necked Parakeet Psittacula krameri in Italy. Ringing & Migration. 2018;33(2):64-7. Doi: 10.1080/03078698.2018.1631609.

5. Henley E. A bird's eye view of breakdown in parrot–caregiver relations. Companion Animal. 2018;23(2):104-8. Doi: 10.12968/coan.2018.23.2.104.

6. Benedict L, Charles A, Brockington A, Dahlin CR. A survey of vocal mimicry in companion parrots. Scientific Reports. 2022;12(1):20271. Doi: 10.1038/s41598-022-24335-x.

7. Forouzan P, Cohen PR. Parrot Beak nail: case report and review of parrot beak nail dystrophy. Cureus. 2021;13(6). Doi: 10.7759/cureus.15974.

8. Langlois I, Barrs VR, Dufresne PJ. Corrigendum to 'Rhinitis due to Aspergillus pseudoviridinutans in an orange-winged Amazon parrot (Amazona amazonica)'[Med. Mycol. Case Rep. 30 (2020) 46–50]. Medical Mycology Case Reports. 2021;33(4):38-55 Doi: 10.1016/j.mmcr.2020.11.001.

9. Faux CM, Logsdon ML. Infraorbital sinusitis. Comparative Veterinary Anatomy: Elsevier; 2022;11(2):1264-70.

10. Hollwarth AJ, Esmans MC, Herrmann A, Dutton TA. Heterotopic Ossification Bone Formation in the Frontal Bones of an African Grey Parrot (Psittacus erithacus). Journal of Avian Medicine and Surgery. 2023;36(4):388-93. Doi: 10.1647/22-00002.

11. Carril J, Tambussi CP, Degrange FJ, Benitez Saldivar MJ, Picasso MBJ. Comparative brain morphology of Neotropical parrots (Aves, Psittaciformes) inferred from virtual 3D endocasts. Journal of anatomy. 2016;229(2):239-51. Doi: 10.1111/joa.12325.

12. Veladiano IA. Tomographic imaging in companion avian species. 2018;13(2):655-666.

13. Faillace ACL, Vieira KRA, Santana MIS. Computed tomographic and gross anatomy of the head of the blue-fronted Amazon parrot (Amazona aestiva). Anatomia, Histologia, Embryologia. 2021;50(1):192-205. Doi: 10.1111/ahe.12618.

14. Thurber MI, Mans C, Fazio C, Waller K, Rylander H, Pinkerton ME. Antemortem diagnosis of hydrocephalus in two Congo African grey parrots (Psittacus erithacus erithacus) by means of computed tomography. Journal of the American Veterinary Medical Association. 2015;246(7):770-6. Doi: 10.2460/javma.246.7.770.

15. Jones ME, Button DJ, Barrett PM, Porro LB. Digital dissection of the head of the rock dove (Columba livia) using contrast-enhanced computed tomography. Zoological letters. 2019;5:1-31. Doi: 10.1186/s40851-019-0129-z.

16. Duymus M, Demiraslan Y, Akbulut Y, Orman G, Ozcan S. The statistical analysis of some volumetric measurements in the japanese quails' head with different feather color: a computed tomography study. Kafkas Universitesi Veteriner Fakultesi Dergisi. 2013;19(4): 681-6. Doi: 10.9775/kvfd.2013.8650.

17. Hébert JA. Closed Reduction of a Rostroparasphenopalatal Luxation in a Red-crowned Parakeet (Cyanoramphus novaezelandiae). Journal of avian medicine and surgery. 2019;33(3):285-8. Doi: 1082-6742-33.3.285.

18. Krautwald-Junghanns M-E, Kostka VM, Dörsch B. Comparative studies on the diagnostic value of conventional radiography and computed tomography in evaluating the heads of psittacine and raptorial birds. Journal of Avian Medicine and Surgery. 1998;149-57.

19. Sabat D, Millan S, Suchismita Sethy P, Marathe S, Sahoo H, Mishra M, editors. Elemental analysis of various feathers of Indian Rose Ringed Parakeet Psittacula krameri. Acta Biology. 2017;14(3):47-66. Doi: 10.1007/978-3-319-46601-9_5.

20. Iwaniuk AN, Dean KM, Nelson JE. Interspecific allometry of the brain and brain regions in parrots (Psittaciformes): comparisons with other birds and primates. Brain Behav Evol. 2004;65(1):40-59. Doi: 10.1159/000081110.

21. Cubo J, Casinos A. Incidence and mechanical significance of pneumatization in the long bones of birds. Zoological Journal of the Linnean Society. 2000;130(4):499-510. Doi: 10.1111/j.1096-3642.2000.tb02198.x

22. Veladiano IA, Banzato T, Bellini L, Montani A, Catania S, Zotti A. Computed tomographic anatomy of the heads of blue-and-gold macaws (Ara ararauna), African grey parrots (Psittacus erithacus), and monk parakeets (Myiopsitta monachus). American journal of veterinary research. 2016;77(12):1346-56. Doi: 10.2460/ajvr.77.12.1346

23. Wild JM. The avian somatosensory system: a comparative view. Sturkie's Avian physiology. Elsevier. 2015;11(1):55-69. DOI: 10.1016/B978-0-12-407160-5.00005-1

24. Langlois I, Barrs VR, Dufresne PJ. Rhinitis due to Aspergillus pseudoviridinutans in an orange-winged Amazon parrot (Amazona amazonica). Medical mycology case reports. 2020;30:46-50. Doi: 10.1016/j.mmcr.2020.11.001.

25. Hanafy BG. Structural adaption of the nasal conchae of Eurasian common moorhen (Gallinula chloropus chloropus, Linnaeus, 1758)—Histomorphological study. Microsc Res Tech. 2021;84(9):2195-202. Doi: 10.1002/jemt.23778.

26. Pohlmeyer K, Kummerfeld N. Morphologie der Nasenhöhle und der nasen Nebenhöhlen sowie ihre klinische Bedeutung bei Grosspapageien. Kleintierpraxis. 1989;34:127-33.

27. Orosz S. Clinical respiratory anatomy. CABI Digital Library. 2016;247-53.

28. Yokosuka M, Hagiwara A, Saito TR, Aoyama M, Ichikawa M, Sugita S. Morphological and histochemical study of the nasal cavity and fused olfactory bulb of the brown-eared bulbul, Hysipetes amaurotis. Zoological science. 2009;26(10):713-21. Doi: 10.2108/zsj.26.713.

29. Piro A, Acosta Hospitaleche C. Skull anatomy of Wilson's storm-petrel Oceanites oceanicus (Hydrobatidae, Procellariiformes). Polar Biology. 2019;42(8):1501-10. Doi: 10.1007/s00300-019-02536-x.

30. Al-Rubaie NI and Kadhim, K. Anatomical Comparison of the Nasal Cavity in Adult Male and Female Cockatiel (Nymphicus Hollandicus). Acta Biology. 2023;94(3): 2023719.

31. Madkour F. Anatomical descriptions of the nasal cavity of the Aquatic and Non-aquatic birds. SVU-International Journal of Veterinary Sciences. 2019;2(2):101-10. Doi: 10.21608/svu.2019.14982.

32. Van Zeeland Y. Upper respiratory tract disease. BSAVA Manual of Avian Practice: BSAVA Library; 2018;299-316. Doi: 10.22233/9781910443323.20.

33. Moore BA, Oriá AP, Montiani-Ferreira F. Ophthalmology of psittaciformes: parrots and relatives. Wild and Exotic Animal Ophthalmology: Volume 1: Invertebrates, Fishes, Amphibians, Reptiles, and Birds. Springer. 2022; 3(12):349-91. Doi: 10.1007/978-3-030-71302-7_17.

34. Smallwood JE. A Guided Tour of Avian Anatomy. Millennium Pring Group. 2014;155-167.

35. Silva IA, Vieira LC, Mancini VRM, Faillace ACL, Santana MIS. Radiographic anatomy of the cockatiel (Nymphicus hollandicus) axial and appendicular skeleton. Anatomia, histologia, embryologia. 2020;49(2):184-95. Doi: 10.1111/ahe.12510.

36. Casteleyn C, Cornillie P, Van Cruchten S, Van den Broeck W, Van Ginneken C, Simoens P. Anatomy of the upper respiratory tract in domestic birds, with emphasis on vocalization. Anatomia, histologia, embryologia. 2018;47(2):100-9. Doi: 10.1111/ahe.12336.

37. Grist A. Poultry inspection: anatomy, physiology and disease conditions. CABI Digital Library. 2006;276-292.

38. Massari CHdAL, Silva AF, Magalhães HIR, Silva DRS, Sasahara THdC, Miglino MA. Anatomía Comparada de los Picos de Guacamayo Azul y Amarillo (Ara ararauna) y de Tucán Toco (Ramphastos toco). International Journal of Morphology. 2020;38(6):1591-6. Doi: 10.4067/S0717-95022020000601591.

39. Carril J, Tambussi CP, Rasskin-Gutman D. The network ontogeny of the parrot: Altriciality, dynamic skeletal assemblages, and the avian body plan. Evolutionary Biology. 2021;48:41-53. Doi: 10.1007/s11692-020-09522-w.

40. Monção-Silva RM, Ofri R, Raposo ACS, Libório FA, Estrela-Lima A, Oriá AP. Ophthalmic parameters of Blue-and-yellow Macaws (Ara ararauna) and Lear's Macaws (Anodorhynchus leari). Avian Biology Research. 2016;9(4):240-9. Doi: 10.3184/175815516X14725499175746.

41. Webb TJ, Gaston KJ. Geographic range size and evolutionary age in birds. Proc R Soc Lond B Biol Sci. 2000;267(1455):1843-50. Doi: 10.1098/rspb.2000.1219.

42. Vučićević M, Stevanović J, Šekler M, Resanović R, Stanimirović Z. Historical overview of methods for sex determination in birds. Veterinarski glasnik. 2016; 11(2):145-57. Doi: 10.2298/VETGL1604145V.

43. Ma S, Wang L, Liu Z, Luo X, Zhou Z, Xie J, et al. "One stone, two birds": engineering 2-D ultrathin heterostructure nanosheet BiNS@ NaLnF 4 for dual-modal computed tomography/magnetic resonance imaging guided, photonic synergetic theranostics. Nanoscale. 2021;13(1):185-94. Doi: 10.1039/d0nr07590f.

44. Brühschwein A, Klever J, Wilkinson T, Meyer-Lindenberg A. DICOM standard conformance in veterinary medicine in Germany: A survey of imaging studies in referral cases. Journal of Digital Imaging. 2018;31:13-8. Doi: 10.1007/s10278-017-9998-x.

45. Wilhite R, Wölfel I. 3D Printing for veterinary anatomy: An overview. Anatomia, histologia, embryologia. 2019;48(6):609-20. Doi: 10.1111/ahe.12502.

46. Šljivic M, Pavlovic A, Kraišnik M, Ilić J, editors. Comparing the accuracy of 3D slicer software in printed enduse parts.

IOP conference series: materials science and engineering. IOP Publishing. 2019;12(1):100-119. Doi: 10.1088/1757-899X/659/1/012082.

47. Constantinescu GM, Constantinescu IA. The updated international veterinary anatomical and embryological nomenclatures. Journal of Veterinary Science and Animal Husbandry. 2013;1(2):1-3. Doi: 10.15744/2348-9790.1.e201.

How to cite this article
Alizadeh S, Hosseinchi MR, Esmaeilnejad R. Radioanatomical Study of the Rose-Ringed Parakeet (Psittacula Krameri) Head Based on the Findings of Computed Tomography Scanning. Iran J Vet Sci Technol. 2025; 17(3): 47-60.
DOI: https://doi.org/10.22067/ijvst.2025.89892.1422
URL:https://ijvst.um.ac.ir/article_47076.html

Iranian Journal of Veterinary Science and Technology

Received: 2024- Sep-28
Accepted after revision: 2025- Jul-16
Published online: 2025- Jul-17

RESEARCH ARTICLE

DOI: 10.22067/ijvst.2025.89499.1412

Low agreement between serological and molecular tests for the diagnosis of cattle brucellosis

Mehran Ghaemi[a], Mohammad Sadegh Golvajouei[b]

[a] Department of Pathobiology, Faculty of Veterinary Medicine, Ferdowsi University of Mashhad, Iran.
[b] Department of Pathobiology, School of Veterinary Medicine, Shiraz University, Iran.

ABSTRACT

Bovine brucellosis, caused mainly by *Brucella abortus,* is an important cows disease that has created a wide-spread public health problem in humans. Diagnosis primarily relies on serological testing; however, these assays lack sensitivity and, more importantly, specificity. In this study, we tried to compare the performance of serological tests routinely applied in Iran with antigen detection tests. Also, we examined *Brucella* species circulating in cows of Fars province, Iran. In addition, the infection rate of *Yersinia entrocolitica* O9 strain as a probable interfering agent in *Brucella* spp. serological tests were evaluated. Supramammary lymph nodes were sampled from 98 *Brucella* spp. reactor cows of Fars province, Iran, analyzed by bacterial culture and molecular tests, including conventional, multiplex, and real-time PCR. *Brucella* spp. was isolated from 5.1% of cultured samples, while conventional and real-time PCR detected in 15 (15.3%) and 21 (21.4%) samples, respectively. All positive samples were identified as *B. abortus*. Notably, 78.6% of seropositive cows tested Brucella spp. negative by both molecular tests and culture at the time of slaughtering, which showed a high false-positive rate of serological testing. As *Y. enterocolitica* O9 was not detected in any lymph node samples, it could be concluded that immunological cross-reaction with this bacterium was not the reason for the few real-time PCR-positive results among *Brucella* reactor cows. In conclusion, real-time PCR provides valuable information about the Brucella species circulating in the slaughtered cows of each region.

Keywords

Brucella abortus, Yersinia entrocolitica, real-time PCR, serological test

Number of Figures: 4
Number of Tables: 1
Number of References:: 24
Number of Pages: 8

Abbreviations

RBT: Rose Bengal Agglutination Test
STAT: Standard Tube Agglutination Test
ELISA: Enzyme-Linked Immunosorbent Assay
FPA: the fluorescence polarization assay
CFT: Complement Fixation Test
WOAH: World Organization of Animal Health
2ME: 2-Mercapto-Ethanol
PCR: Polymerase Chain Reaction
B.: *Brucella*
Spp: Species

Corresponding author: *Mehran Ghaemi*
Email: m.ghaemi@um.ac.ir
Tel:+98(51)3880-5631

Introduction

Bovine brucellosis is most commonly caused by *B. abortus*, less regularly by *B. melitensis,* and rarely by *B. suis,* all zoonosis pathogens of the genus *Brucella* [1]. Transmission to humans occurs primarily through contact with infected reproductive secretions or consumption of infected dairy products [2]. In cattle, *Brucella* organisms tend to localize in the supra-mammary lymph nodes and mammary glands from which they may be shed into milk [3].

The disease must be eradicated from animals to control brucellosis in the human, and this is largely pursued through national tests and slaughter programs in the endemic areas. To identify *Brucella* spp. For infected cows, different methods are available, but because of the limitations of each test, the exact diagnosis of brucellosis in cows is still challenging. Antigen detection tests, such as bacterial culture and PCR, identify the presence of *Brucella* spp. directly. Although bacterial culture is considered the diagnostic gold standard, it is less sensitive, time-consuming, and labor-intensive, and imposes a serious biohazard on laboratory personnel [4, 5]. Antibody detection or serological assays including the Rose Bengal Agglutination Test (RBT), Standard Tube Agglutination Test (STAT), Enzyme-Linked Immunosorbent Assay (ELISA), fluorescence polarization assay (FPA), and Complement Fixation Test (CFT) can be used as screening tests in the control program of brucellosis [4]. However, these tests are hindered by cross-reactivity between *Brucella* species and other Gram-negative bacteria, such as Yersinia enterocolitica O9, Escherichia coli O157, Francisella tularensis, Salmonella urbana, Vibrio cholera, and stenotrophomonas maltophilia [6]. The structural similarity of smooth lipopolysaccharide O-chain between *Brucella* spp. and these bacteria, underlies this problem. For example, Muñoz and colleagues (2005) reported that up to 15% of cattle herds in brucellosis-free regions produced false-positive results in serological tests due to cross-reaction with Yersinia enterocolitica O9 [7]. Consequently, a single serological test is not sufficiently reliable for screening individual animals [4]. To improve accuracy, at least two antigen and/or antibody detection tests are required to confirm the cattle brucellosis [8]. According to diagnostic regime recommended by the World Organization of Animal Health (WOAH), serological tests are applied in Iran to diagnose positive reactor cows. Serum samples from semi-industrialized and industrialized dairy farms are first screened by RBT, with positive sera are tested using STAT, including Wright's test, and 2-Mercapto-Ethanol (2ME) tests. Animals identified as positive reactors are then slaughtered with biohazard precautions. Because the test results drive the slaughter decisions, the sensitivity and the specificity of these tests are critical. So, paying more attention to the test strategies used to identify *Brucella* spp. in farm animals is an important neglected issue.

In the present study, we tried to evaluate the agreement between serological tests and antigen detection tests for diagnosing bovine brucellosis. Specifically, we evaluated how many serologically positive reactor cows could also be confirmed by bacterial culture, conventional PCR, and real-time PCR. An additional objective was to identify the *Brucella* species infecting cows of Fars province, Iran. Consequently, the presence of Yersinia entrocolitica O9 strain in the lymph nodes of cows was determined to be a probable cause of false-positive results in the brucellosis serological tests.

Result

Out of 98 lymph node samples collected from positive reactor cows, conventional PCR detected *Brucella* genus in 15 samples (15.3%) (Figure 1).

The Bruce-ladder multiplex PCR, designed for *Brucella spp* **absence in most positive reactor cows**

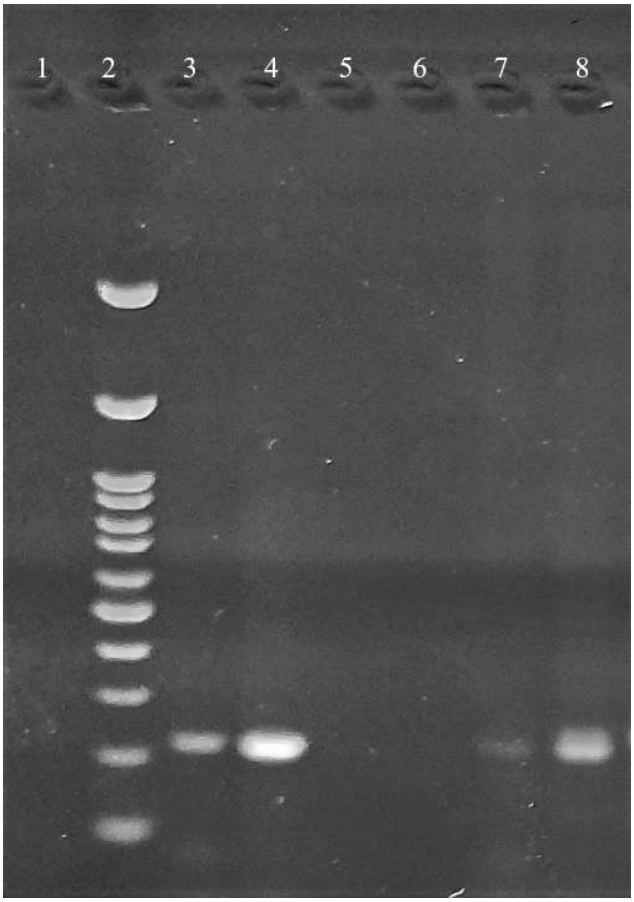

Figure 1.
The gel picture of conventional PCR for Brucella spp. detection. A 223 bp band is obvious in the positive PCR products. Lane 2 shows a 100 bp DNA ladder. Lanes 3 and 4 have different concentrations of positive controls, and lane 1 has no template controls (NTC). Other lanes show samples. An Aliquot of *B. abortus* IRIBA vaccine (Razi, Iran) was used as the positive control.

specie level identification of *Brucella*, did not produce any PCR band from DNA extracted from lymph node tissues. However, when applied to DNA extracted from cultured *Brucella* isolates, the Bruce-ladder PCR was successfully differentiated the species of Brucella isolates (Figure 2).

Real-time PCR analysis identified 21 *Brucella* spp. positive samples (21.4%) out of 98 lymph nodes tested. Melting peak analysis and sequencing of PCR products confirmed all positive samples were *B. abortus* (Figure 3). No statistically significant relationship was observed between real-time PCR-positive samples and the level of 2ME *Brucella* titer.

Brucella spp. was isolated from only 5 samples (5.1%) in bacterial culture, all of which were identified as *B. abortus* using Bruce ladder multiplex PCR.

Given that only 21.4% of positive reactor cows were confirmed positive by real-time PCR, further investigation was conducted to explore the probable reason. As Y. entrocolitica O9 strain was one of the bacteria that might cause serological cross-reactions with *B. abortus* (CSFPH 2018), the prevalence of this strain was evaluated in the lymph node samples. Although 20 lymph node samples tested positive for Y. entrocolitica, none were identified as an O9 serotype.

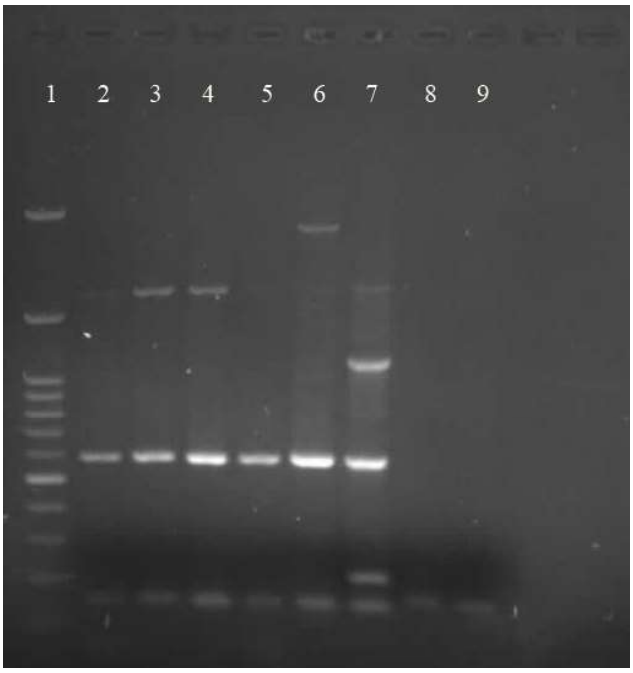

Figure 2.
The gel picture of the Bruce ladder.
Lane 1 was a 100 bp DNA ladder. Lanes 2 to 5 were *B. abortus* from cultured bacterial colonies indicated by 152, 587, and 1682 bp bands. Lane 6 was *B. abortus* IRIBA strain positive control, which was similar to the RB51 strain, showing 152, 587, and 2524 bp bands on the gel, and lane 7 was B. melitensis Rev1 strain positive control, confirmed by 152, 218, 587, 1071, and 1682 bp bands. As 450 and 794 bp bands of the original Bruce ladder did not apply to B. melitensis and *B. abortus* identification, their primers were not used in Bruce ladder PCR.

Discussion

The study demonstrated that among 98 lymph node samples collected from positive reactor cows, *Brucella* spp. was detected only in 15 (15.3%) and 21 (21.4%) samples by conventional PCR and real-time PCR, respectively. In a similar study, O'Leary and colleagues (2006) applied conventional and real-time PCR to different samples from serologically *Brucella* spp. positive cows, slaughtered under Ireland's eradication program. They reported *B. abortus* detected in 3 (14.2%) and 4 (19%) out of 21 supra-mammary lymph nodes samples using conventional and real-time PCR, respectively [9], which these results are consistent to our findings. Also, in another study, Tiwari and colleagues (2014) reported that from 132 STAT-positive

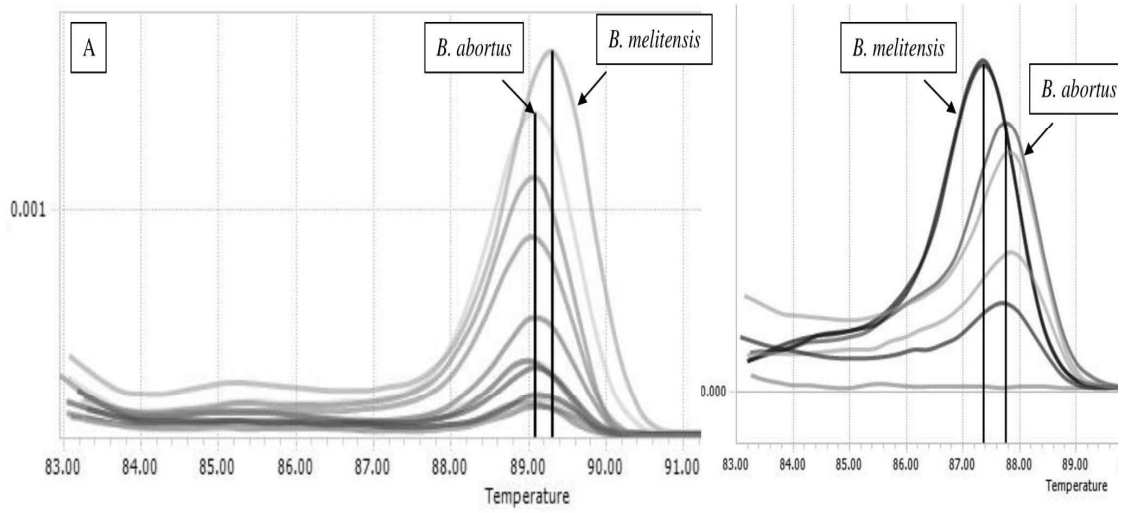

Figure 3.
A) Melting peak analysis of *B. abortus* specific (A) and B. melitensis specific (B) real-time PCR.
The indicator lines show the melting peaks of *B. abortus* IRIBA strain and B. melitensis Rev1 strain positive controls. The graphs show that all of the samples have melting peaks similar to that of *B. abortus* (A) and none of them were located under B. melitensis melting peak (B).

serum samples, only 14 sera (10.6%) were positive by real-time PCR with B4-B5 primers, the same primers used in our conventional PCR assay [10]. A probable reason for the low percentage of PCR-positive results in Tiwari`s study may be partly explained by the type of biological sample, as both our and O'Leary`s studies were conducted on the lymph nodes, whereas Tiwari's was based on serum.

O'Leary and colleagues (2006) also compared *Brucella* spp. detection rate by conventional and real-time PCR across different sample types, including milk, blood, and lymph node. They sampled from both supramammary and retropharyngeal lymph nodes and concluded that the supramammary lymph node is the most reliable tissue for PCR detection of *Brucella* spp. [9]. Their conclusion served as the basis for selecting the sample tissue, and the supramammary lymph nodes were sampled in this research. Nevertheless, according to the tropism of *Brecella* spp. [11], other organs rich in phagocytes, such as the spleen, and organs of the genital system (such as the uterus), could also be suitable sample types for *Brucella* spp. detection.

The real-time PCR result of this study showed that 78.6% of reactor cows were *Brucella* spp. negative at the time of slaughtering. Given that the supramammary lymph node is considered one of the best reservoirs for *Brucella* detection in cows [9], these results suggest that a substantial proportion of reactor cows may be free of infection and are therefore unlikely to shed *Brucella* spp. in milk. These cases were those that *Brucella* spp. bacteria do not remain as an active infection in them. However, their antibody is still detectable by serological tests or individuals never infected with *Brucella* spp. but exposed to other bacteria that immunologically cross-react with *Brucella* spp. Several organisms are known to cause serological cross-reactions with *Brucella,* including Yersinia enterocolitica O9 strain, Escherichia coli O157, Francisella tularensis, Salmonella urbana, Vibrio cholera, and stenotrophomonas maltophilia [6]. As Y. enterocolitica O9 strain was not detected in any lymph node samples, it could be concluded that immunological cross-reaction with this bacterium was not the reason for the few real-time PCR-positive results among *Brucella* reactor cows.

In this study, the sensitivity of conventional and real-time PCR tests was more than that of *Brucella* spp. culture. This observation has been inconsistently reported in the literature. In some studies, PCR sensitivity has been reported more than that of *Brucella* spp. culture method [12, 13]. Hamdy and Amin (2002) compared the sensitivity of PCR and culture methods on bovine milk samples and reported that the PCR sensitivity was greater than that of *Brucella* spp. Culture [13]. whereas in in another study, they reported culture method to outperform PCR [14]. Also, some researchers reported similar results [9]. This study uses Farrell's medium, the most widely used *Brucella* spp. A selective medium was used for the culture prepared by adding six antibiotics to a basal medium. Because some strains of *B. abortus* and B. melitensis may be inhibited by nalidixic acid and bacitracin, two antibiotics in the supplement, the use of this medium may reduce the culture method sensitivity and explain the fewer positive samples of bacterial culture than those of PCR methods.

Molecular characterization in this study identified *B. abortus* as the predominant species infecting cattle in Fars province, Iran. This finding was by multiplex and real-time PCR, and further confirmed by sequencing. Human brucellosis caused by B. melitensis is more severe than the disease caused by *B. abortus* [14], and in terms of public health, B. melitensis is considered a more important zoonosis pathogen. Similar to this study, there are many reports that only isolated *B. abortus* from cow samples from Turkey [15], Pakistan [16], Ireland [9], and Uganda [17], but also there are some studies that isolated B. melitensis in addition to *B. abortus* from cows [18]. The most similar study to ours was performed by Sharifiyazdi et al. (2010), who isolated 17 *Brucella* spp. from 95 positive reactor cows in the same province; of which only one was *B. melitensis,* and the others were *B. abortus* [19]. By comparing these results, it could be concluded that the *Brucella* species infecting cows of this region have not changed from 14 years ago, and cows in Fars province are not the source of human B. melitensis infections.

Finally, it could be concluded that the current serological test combination was conducted in Iran according to WOAH to diagnose the *Brucella* spp. antigen detection tests do not confirm infected cows. We have to know that the lack of specificity in the test regime could waste many healthy cows, limiting the government's potential to widen the brucellosis eradication program to all of the farm animal population, including non-industrialized native cows and sheep. Although real-time PCR is not currently feasible as a routine diagnostic tool directly on serum sample, this test could provide valuable information about the *Brucella* species circulating in the slaughtered cows of each region.

Materials and Methods

Cattle Herds and Sampling

Serum sampling was performed on semi-industrialized and industrialized dairy farms across all regions of Fars province, Iran, under the national brucellosis control program. All cows were lactating Holstein or crossbreeds, raised in the intensive farms. They

had been vaccinated against brucellosis following to the Iranian Veterinary Organization (IVO) guidelines [20] using a vaccine (RVSRI, Iran) containing the IRIBA strain of *B. abortus*. Infected cows were diagnosed using serological assays, including RBT, Wright's agglutination tests, 2-ME agglutination tests, performed in IVO laboratories according to the WOAH guidelines [4]. RBT was applied as the initial screening test, with RBT-Positive sera further evaluated by Wright's agglutination tests and 2-ME agglutination tests. Interpretation of results took into account cow age, vaccination history, and the prior brucellosis condition of the sampled farm. The positive RBT cows would be divided into positive reactors (≥ 4/80 Wright and 4/40 2-ME titers), doubtful, and negative (≤ 1/20 in both tests) cases. Brucellosis cases were retested 3 to 4 weeks later to confirm their status [20].

In this study, supramammary lymph nodes were sampled from 98 serologically *Brucella* spp. positive cows from 20 farms in Fars province, Iran. Lymph nodes were obtained after slaughtering under the national brucellosis control program. Samples were transferred to the laboratory in cool boxes and stored at -20 °C until use.

Bacterial culture

One of the supramammary lymph nodes was transferred to the laboratory of the Department of Brucellosis, Razi Vaccine and Serum Research Institute (RVSRI), Iran, the only nationally authorized laboratory for *Brucella* spp. culture from animal samples. Samples were cultured on *Brucella*-specific agar enhanced with 7% defibrinated sheep blood and *Brucella* supplement (Oxoid, UK). The supplement contained the following quantities of antibiotics for 1 liter of agar: polymyxin B sulfate (5000 IU); bacitracin (25,000 IU); natamycin (50 mg); nalidixic acid (5 mg); nystatin (100,000 IU); vancomycin (20 mg). Plates were incubated at 37°C in 10% CO2 for 21 days. Colonies were identified as *Brucella* spp. based on morphology, serology, and conventional biochemical assays (catalase, oxidase, and urease tests).

DNA extraction

The second supramammary lymph node was used for DNA extraction. Firstly, an emulsion was prepared using a pestle and mortar from 100 µg ground section of each lymph node. Nucleic acid was extracted using a bacterial DNA isolation kit (Denazist Asia, Iran) from emulsion samples according to the manufacturer`s instructions. Some of the extracted DNA was electrophoresed on a 1% agarose gel to check the integrity and purity and the quantity of extracted DNA were determine using a Nanodrop (Bioteck, USA) .

Conventional PCR of Brucella spp.

To detect the *Brucella* genus, a PCR test was conducted in all DNA samples using the following primers: B4: `5-TGGCTCGGTTGCCAATATCAA-`3 and B5: `5-CGCGCTTGCCTTTCAGGTCTG-`3 [21]. A total volume of 25 µl consisted of 1 µl b4 primer (10µM), 1 µl b5 primer (10µM), 12.5 µl Red master mix (Ampliqon, Denmark), 5.5 µl molecular grade water, and 5 µl template DNA. A thermal cycler (BioIntelectica, Canada) was used to run the following PCR program: 5 min at 95 °C as initial denaturation, and 35 cycles of 95 °C 1 min, 63 °C 30 sec, and 72 °C 1 min, followed by 72 °C 10 min.

Multiplex PCR of Brucella spp.

Species-level identification of *Brucella* was performed using the Bruce ladder multiplex PCR. This assay combines eight primer pairs in a single PCR reaction, and *Brucella* species are identified based on each sample's different PCR bands (ladder) [22]. As the bands created by two primer pairs known as BMEI0535f-BMEI0536r and BMEI1436f- BMEI1435r were similar in *B. abortus* and B. melitensis species (expected *Brucella* species in cow), they were not incorporated in a master mix of multiplex PCR, leaving six primer pairs, as shown in the Table 1.

The thermal program consisted of 95 °C 15 min, 35 cycles of 95 °C 35 sec, 63 °C 45 sec, 72 °C 1 min, and finally 72 °C 10 min. 0.62 µl of each forward and 0.62 µl of each reverse primer (10 µM), 12.5 µl of Tempase master mix (Ampliqon, Denmark), and 2.5 µl of DNA sample were mixed (25 µl total volume).

Real-time PCR of Brucella spp.

Two individual Real-time PCR were performed to identify two species of *Brucella* (*B. abortus* and B. melitensis) in all DNA samples using a high-resolution melting (HRM) program. Each real-time PCR differentiates one species from others by comparing the melting peak of an unknown PCR product versus that of a certified positive PCR product. These tests were designed based on a single nucleotide difference in the glk gene of *B. abortus* and the int-hyp gene of *B. melitensis,* with the nucleotide sequence of other species, which causes a slight difference in melting peaks. Real-time PCR primer pairs specific for *B. abortus* and those specific for B. melitensis were named Boa and Bmel, respectively. Their sequences were:

Boa For: `5-GACCTCTTCGCCACCTATCTGG-`3
Boa Rev: `5- CCTTGTGCGGGGCCTTGTCCT-`3
Bmel For:`5- GAGCGATCTTTACACCCTTGT-`3
Bmel Rev:`5- GGACGGTGTAATAAACCCATTGG-`3 [23].

A common thermal program was run by the Light Cycler 96® instrument (Roche, Germany) as follows: initial denaturation of 95 °C for 10 min, then 95 °C for 10 sec and 60 °C for 50 sec repeated 40 cycles followed by HRM program from 65 °C to 95 °C by 0.2 °C /step ramp rate. Some real-time PCR products were sequenced to ensure the substitution of one nucleotide in the glk gene of *B. abortus*.

PCR tests for the detection of Yersinia entrocolitica O9 strain

Two PCR tests were set up to evaluate the Yersinia entrocolitica strain O9 infected cows. Firstly, a PCR test for the detection of all strains of Yersinia entrocolitica was conducted, and then another PCR test was performed on the positive samples of the first PCR to detect specifically the O9 strain. In the first PCR, 227Fmod: (`5-GTCTGGGCTTTGCTGGTC-`3), and YER2: (`5-ATCTTGGTTATCGCCATTCG-`3) primer pair targeting ompF gene, and in the second PCR, perF: (`5-GACGGGGGCAAAAGTAGT-`3), and perR: (`5-CTATTGGGAACACCTCTGGA-`3) primer pair [24] targeting perosamine synthetase gene were used.

In both PCRs, the same master mix components (unless primers), and a common thermal program were applied. For 20 µl total volume of each Y. entrocolitica PCR test, 1 µl of each related primer (10µM) was added to 10 µl Red master mix (Ampliqon, Denmark), 5 µl PCR grade water and 3 µl extracted DNA. Following thermal program: firstly, 95 °C 5 min as initial denaturation, followed by 40 cycles of 95 °C 20 sec, 60 °C 30 sec, 72 °C 30 sec, and finally, 72 °C 7 min as the final extension was applied to PCR microtubes.

To visualize the bands, the PCR products of conventional and multiplex PCR were electrophoresed in 1.5% agarose gels stained with RedSafe (Intron Biotechnology, Korea). The gel pictures were caught by a gel documentation system.

Statistical analysis

Chi-square ($\chi 2$) tests were used to compare the amount of serological 2ME titer and the presence of *B. abortus* in the lymph node samples.

Figure 4 represents a graphical abstract of the materials and methods section.

Table 1.
Names, sequences, amplicon sizes, and target genes of primer pairs used for multiplex PCR, known as Bruce-ladder.

Primer name	Sequence (`5–`3)	Amplicon size (bp)	Target
BMEI0998f	ATC CTA TTG CCC CGA TAA GG	1,682	Glycosyltransferase, gene wboA
BMEI0997r	GCT TCG CAT TTT CAC TGT AGC		
BMEII0843f	TTT ACA CAG GCA ATC CAG CA	1,071	Outer membrane protein, gene omp31
BMEII0844r	GCG TCC AGT TGT TGT TGA TG		
BMEII0428f	GCC GCT ATT ATG TGG ACT GG	587	Erythritol catabolism, gene eryC (Derythrulose- 1- phosphate dehydrogenase)
BMEII0428r	AAT GAC TTC ACG GTC GTT CG		
BR0953f	GGA ACA CTA CGC CAC CTT GT	1,071	ABC transporter binding protein
BR0953r	GAT GGA GCA AAC GCT GAA G		
BMEI0752f	CAG GCA AAC CCT CAG AAG C	218	Ribosomal protein S12, gene rpsL
BMEI0752r	GAT GTG GTA ACG CAC ACC AA		
BMEII0987f	CGC AGA CAG TGA CCA TCA AA	152	Transcriptional regulator, CRP family
BMEII0987r	GTA TTC AGC CCC CGT TAC CT		

As BMEI0535f-BMEI0536r and BMEI1436f- BMEI1435r did not apply to *B. melitensis* and *B. abortus* identification, these two pairs were deleted from the original Bruce-ladder primers.

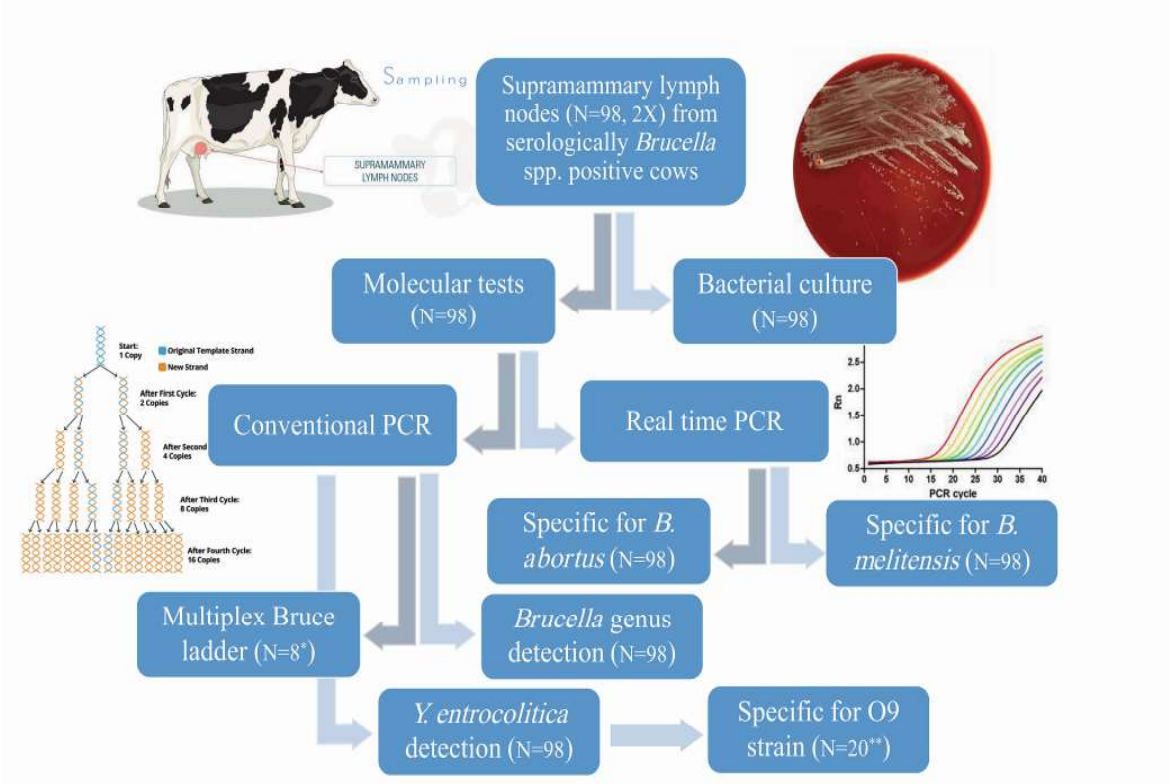

Figure 4.
Graphical abstract.
The diagram shows the sampling and the type of experiments conducted in this study.

Authors' Contributions

All authors contributed to the study conception and design. M.Gh. and M.S.G. performed material preparation, data collection, and analysis. M.Gh. wrote the first draft of the manuscript, and all authors commented on previous versions of the manuscript. All authors read and approved the final manuscript.

Acknowledgements

This study was funded by the Fars province veterinary administration (grant number: 15398-162096).

Competing Interests

The author declares that there is no conflict of interest.

Reference

1. Chisi SL, Marageni Y, Naidoo P, Zulu G, Akol GW, Van Heerden H. An evaluation of serological tests in the diagnosis of bovine brucellosis in naturally infected cattle in KwaZulu-Natal province in South Africa. Journal of the South African Veterinary Association. 2017 Feb 28;88. Doi:10.4102/jsava.v88i0.1381.

2. Alamian S, Esmaelizad M, Zahraei T, Etemadi A, Mohammadi M, Afshar D, et al. A Novel PCR Assay for Detecting Brucella abortus and Brucella melitensis. Osong Public Health and Research Perspectives. 2017 Feb 28;8(1):65–70. Doi:10.24171/j.phrp.2017.8.1.09.

3. Poester FP, Samartino LE, Santos RL. Pathogenesis and pathobiology of brucellosis in livestock. Revue Scientifique et Technique de l'OIE. 2013 Apr 1;32(1):105–15.Doi:org/10.20506/rst.32.1.2193.

4. WOAH (World organization for animal health). Brucellosis (Brucella abortus, B. melitensis and B. suis). Manual of Diagnostic Tests and Vaccines for Terrestrial Animals, 13th edition. 2024. Chapter 3.1.4.

5. Yu WL, Nielsen K. Review of Detection of Brucella sp. by Polymerase Chain Reaction. Croatian Medical Journal. 2010 Aug;51(4):306–13. Doi:10.3325/cmj.2010.51.306.

6. CSFPH (The center for food safety and public health) Brucellosis: Brucella abortus factsheet, 2018 available from: http://www.cfsph.iastate.edu/DiseaseInfo/factsheets.htm.

7. Muñoz P, Marin C, Monreal D, González D, Garin-Bastuji B, Díaz RF, et al. Efficacy of several serological tests and antigens for diagnosis of bovine brucellosis in the presence of false-positive serological results due to Yersinia enterocolitica O:9. Clinical and diagnostic laboratory immunology. 2005 Jan 1;12(1):141–51. Doi:10.1128/CDLI.12.1.141-151.2005.

8. Nielsen K, Gall D, Bermudez R, Renteria T, Moreno F, Corral A, et al. Field trial of the brucellosis fluorescence polarization assay. Journal of Immunoassay and Immunochemistry. 2002 Aug 29;23(3):307–16. Doi:10.1081/IAS-120013030.

9. O'Leary S, Sheahan M, Sweeney T. Brucella abortus detection by PCR assay in blood, milk and lymph tissue of serologically positive cows. Research in Veterinary Science. 2006 Oct;81(2):170–6. Doi:10.1016/j.rvsc.2005.12.001.

10. Tiwari A, Pal V, Afley P, Sharma DK, Bhatnagar CS, Bhardwaj B, et al. Real-time PCR carried out on DNA extracted from serum or blood sample is not a good method for surveillance of bovine brucellosis. Tropical Animal Health and Production. 2014 Sep 4;46(8):1519–22. Doi:10.1007/s11250-014-0664-8.

11. Carvalho TPD, Silva LAD, Castanheira TLL,Souza TDD, Paixão TAD, Lazaro-Anton L, Tsolis RM, Santos RL. Cell and Tissue Tropism of Brucella spp.. Infection and Immunity. 2023 91:e00062-23.Doi: 10.1128/iai.00062-23.

12. Leal-Klevezas DS, Martinez-Vazquez IO, Lopez-Merino A, Martinez-Soriano JP. Single-step PCR for detection of Brucella spp. from blood and milk of infected animals. Journal of Clinical Microbiology. 1995; 33(12):3087-3090.

13. Hamdy MER, Amin AS. Detection of Brucella Species in the Milk of Infected Cattle, Sheep, Goats and Camels by PCR. The Veterinary Journal. 2002 May;163(3):299–305. Doi:10.1053/tvjl.2001.0681.

14. Amin AS, Hamdy MER, Ibrahim AK. Detection of Brucella melitensis in semen using the polymerase chain reaction assay. Veterinary Microbiology. 2001 Oct;83(1):37–44. Doi:10.1016/s0378-1135(01)00401-1.

15. Kaynak-Onurdag F, Okten S, Sen B. Screening Brucella spp. in bovine raw milk by real-time quantitative PCR and conventional methods in a pilot region of vaccination, Edirne, Turkey. Journal of Dairy Science. 2016 May;99(5):3351–7. Doi:10.3168/jds.2015-10637.

16. Ali S, Ali Q, Melzer F, Khan I, Akhter S, Neubauer H, et al. Isolation and identification of bovine Brucella isolates from Pakistan by biochemical tests and PCR. Tropical Animal Health and Production. 2013 Jul 19;46(1):73–8. Doi:10.1007/s11250-013-0448-6.

17. Hoffman T, Rock K, Denis Rwabiita Mugizi, Shaman Muradrasoli, Lindahl-Rajala E, Erume J, et al. Molecular detection and characterization of Brucella species in raw informally marketed milk from Uganda. Infection ecology & epidemiology. 2016 Jan 1;6(1):32442–2. Doi:10.3402/iee.v6.32442.

18. Dadar M, Alamian S, Behrozikhah AM, Yazdani F, Kalantari A, Etemadi A, et al. Molecular identification of Brucella species and biovars associated with animal and human infection in Iran. Veterinary Research Forum. 2019;10(4):315–21. Doi:10.30466/vrf.2018.89680.2171.

19. Sharifiyazdi H, Haghkhah M, Behroozikhah AM, Nematgor-

sis. 2010 Mar 1;48(3):697–702. Doi:10.1128/JCM.02021-09.

23. Stenkova AM, Isaeva MP, Rasskazov VA. Development of a multiplex PCR for detection of the Yersinia genus with identification of pathogenic species (Y. pestis, Y. pseudotuberculosis, Y. enterocolitica). Molecular Genetics, Microbiology and Virology. 2008;3:18-23.

24. Lübeck PS, Mikael Skurnik, Ahrens P, Hoorfar J. A Multiplex PCR-Detection Assay for Yersinia enterocolitica Serotype O:9 and Brucella spp. Based on the Perosamine Synthetase Gene. Advances in experimental medicine and biology. 2004 Jan 1;451–4. Doi:10.1007/0-306-48416-1_89.

How to cite this article
Ghaemi M, Golvajouei MS. Low agreement between serological and molecular tests for the diagnosis of cattle brucellosis. Iran J Vet Sci Technol. 2025; 17(3): 61-68.
DOI: https://doi.org/10.22067/ijvst.2025.89499.1412
URL:https://ijvst.um.ac.ir/article_47219.html

Iranian Journal of Veterinary Science and Technology

Received: 2025- Feb-20
Accepted after revision: 2025- Jun-08
Published online: 2025-Jun-10

Case Report

DOI: 10.22067/ijvst.2025.92011.1470

Oral Squamous Cell Carcinoma in a Budyonny horse: A case report

Seyed Mahdi Ghamsari[a], Omid Azari[a], Fariborz Moayer[b], Ali Rostaei[a], Seyedeh Houra Mortazavi[c]

[a] Department of Surgery and Radiology, Faculty of Veterinary Medicine, University of Tehran, Tehran, Iran.
[b] Department of Pathobiology, Faculty of Veterinary Medicine, Islamic Azad University, Karaj Branch, Karaj, Iran
[c] Student of Veterinary Medicine, Faculty of Veterinary Medicine, University of Tehran, Tehran, Iran.

ABSTRACT

Squamous cell carcinoma (SCC) is a cancerous growth originating from the stratified squamous epithelium and is the most frequently diagnosed oral tumor in horses. This case report describes the clinical, imaging, and histopathological characteristics of gingival SCC in a 23-year-old Budyonny gelding with a history of multiple unsuccessful treatments, including a prior tumor excision attempt. The horse presented with a large, space-occupying soft tissue mass associated with excessive drooling, and lateral tongue protrusion. Laboratory findings were consistent with cancer-related anemia, while diagnostic imaging demonstrated extensive mandibular bone lysis consistent with the tumor's aggressive nature. Histopathology confirmed grade III gingival SCC, characterized by keratin pearl formation and a high mitotic index. Due to the poor prognosis, high treatment costs, and advanced stage of disease, the owner declined further therapeutic intervention. The horse succumbed to the disease and died 6 months after presentation. This case emphasizes the challenges of managing advanced gingival SCC in equines and underscores the importance of early detection and timely intervention.

Keywords

Equine, Oral Tumor, Squamous Cell Carcinoma, Gingival Neoplasm, Mandibular Tumor

Number of Figures: 2
Number of Tables: 0
Number of References:: 16
Number of Pages: 5

Abbreviations

SCC: squamous cell carcinoma
OSCC: oral squamous cell carcinoma
EDTA: Ethylenediaminetetraacetic Acid
WBC: White Blood Cell
HCT: Hematocrit
H&E staining: haematoxylin and eosin staining

Corresponding author: *Omid Azari*
Email: Omid.azari@ut.ac.ir
Tel:+98(91)2318-5781

Introduction

Squamous cell carcinoma (SCC), characterized by the abnormal and rapid proliferation of stratified squamous epithelial cells [1], is the second most common tumor and the most frequently reported primary oral neoplasm in horses [2]. Although SCC generally exhibits a slow growth pattern, some cases may sometimes exhibit a more rapid clinical course [1]. Initially, these tumors exhibit a proliferative tendency but often evolve into highly destructive form, marked by ulceration and extensive infiltration of surrounding tissues [1,3]. Oral squamous cell carcinoma (OSCC) is a malignant neoplasm originating from the oral keratinocytes within the stratified squamous epithelium, predominantly impacting the oral mucosa. The present report describes the clinical presentation, histopathological characteristics, and imaging features of an invasive grade III OSCC in a 23-year-old Budyonny gelding, emphasizing the diagnostic difficulties and therapeutic limitations associated with this condition.

Case Presentation

A 23-year-old Budyonny gelding was brought to the Veterinary Teaching Hospital at the University of Tehran with a large, space-occupying soft tissue mass in the rostral mandible, which prevented complete oral examination. According to the owner, the mass developed after the extraction of a loose left lower canine tooth several months prior. The owner reported rapid and aggressive growth of the mass, accompanied by a persistent fetid odour, despite previous surgical and medical attempts at treatments. Initial treatments included cleaning the extraction site with salt, disinfecting with chlorhexidine and diluted betadine solution, and administration of co-trimoxazole. However, the mass proved resistant to all therapeutic interventions.

Results and Discussion

Clinical findings

On general clinical examination, vital parameters were within normal limits: rectal temperature 37.6°C, heart rate 35 beats/min, and respiratory rate 12 breaths/min .The horse was able to defecate and urinate without difficulty. Upon close inspection, a tumor was identified on the dental alveolus of the right mandible, accompanied by a large fistula connecting the oral cavity to the cutaneous aspect of the intermandibular space. Suppurative discharge was observed at the defect site, resulting in excessive drooling and lateral protrusion of the tongue (Figure1.A, B). Despite the oral pathology, the horse maintained good body condition, without significant weight loss or reduction in appetite.

Laboratory findings

Blood samples were obtained from the jugular vein using vacuum tubes containing 10% EDTA for the assessment of complete blood count and plasma protein concentrations. The results of the blood sample were as follows: Haemoglobin 8.6g/dL, Red blood cells 5.2× 106/µL, HCT 27%, WBC 12800 /µL, Band neutrophils 640/µL, segmented neutrophils 10800 /µL, lymphocyte 1280/µL, monocyte 128/µL, and Fibrinogen 0.4g/dL. The haematological profile indicated normocytic normochromic anaemia, likely cancer-related. Additionally, a relatively elevated band neutrophil count with a degenerative left shift

Figure 1.
Gross and radiographic images, (A) A prominent mass at the site of the labial gingiva in the oral cavity. (B) A discharging sinus tract with purulent material and pus underneath. (C) Lateral radiograph of the rostral aspect of the mandible, demonstrating severe osteolysis associated with squamous cell carcinoma.

was observed, suggesting a systemic inflammatory response [4].

Diagnostic imaging findings

Lateral and dorsoventral views of the mandible demonstrated severe mandibular bone lysis between the incisor and premolar check teeth, along with significant bone proliferation within the adjacent soft tissue mass (Figure1.C). These radiographic findings were highly suggestive of a neoplastic process.

Histopathological findings

A preliminary mass biopsy was performed with the horse standing under sedation (xylazine 2%,0.5mg/kg) and local analgesia (lidocaine 2%). The tissue samples were subsequently preserved in 10% neutral buffered formalin, processed accordingly, embedded in paraffin, sectioned to a thickness of 5µm, and stained with H&E. Slides were examined under a light microscope. (Olympus, CX33). Histopathological analysis of the specimens confirmed a diagnosis of grade III OSCC, characterized by tumor development originating from peripheral basal-like cells. This progression occurred through the layers of the stratified squamous epithelium, ultimately resulting in the formation of a central keratin pearl due to keratinization. (Figure2.A). Areas of viable tumor cells transitioned to zones of necrosis, characterized by a loss of structural integrity and replacement with eosinophilic proteinaceous material and cellular debris (Figure2.B). Additionally, small blood vessels were observed near the tumor nests, often with inflammatory cells marginating along the endothelial surfaces. The tumor cells displayed significant nuclear polymorphism, indicating a moderately to highly abundant number of mitotic cells, with the mitotic count ranging from 5 to 9 per high-power field. Furthermore, evidence of lymphovascular invasion was also observed, as tumor cells were identified within endothelial-lined spaces (lymphatics or blood vessels).

Outcome

Given the horse's condition, a rostral hemimandibulectomy was recommended as the treatment of choice. However, owner declined surgical intervention due to the poor prognosis, high financial costs, and emotional considerations. Follow-up revealed that the horse succumbed to the disease and died six months after presentation.

This study describes the clinical, laboratory, and histopathological features of an invasive case of OSCC in a 23-years-oldBudyonny horse, highlighting the challenges of managing and treating oral cavity neoplasia in equines.

SCC is a malignant tumor that originates from epithelial cells derived from either ectodermal or endodermal tissues [5]. OSCC has been documented in a variety of specious, including horses, cattle, sheep, goats, rats, hamsters, rabbits, ferrets, hedgehogs, and numerous other laboratory, domestic and wild animals [6]. In dogs, SCC ranks among the three most prevalent oral cancers, while in cats it is the most common [7]. In horses, SCC frequently arises in the genitalia, ocular and periocular tissues, and stomach. Less frequently, it appears in the oesophagus, skin, hard palate, arytenoid cartilage, guttural pouch, maxillary sinus, perineal tissues, peritoneal cavity, maxilla, lymph nodes, nasal cavity and mucosal surfaces such as gingiva, tongue, larynx, pharynx, and palate [3,8,9]. Although OSCC is the most prevalent primary oral neoplasm in horses, it remains relatively uncommon condition for only about 7% of all

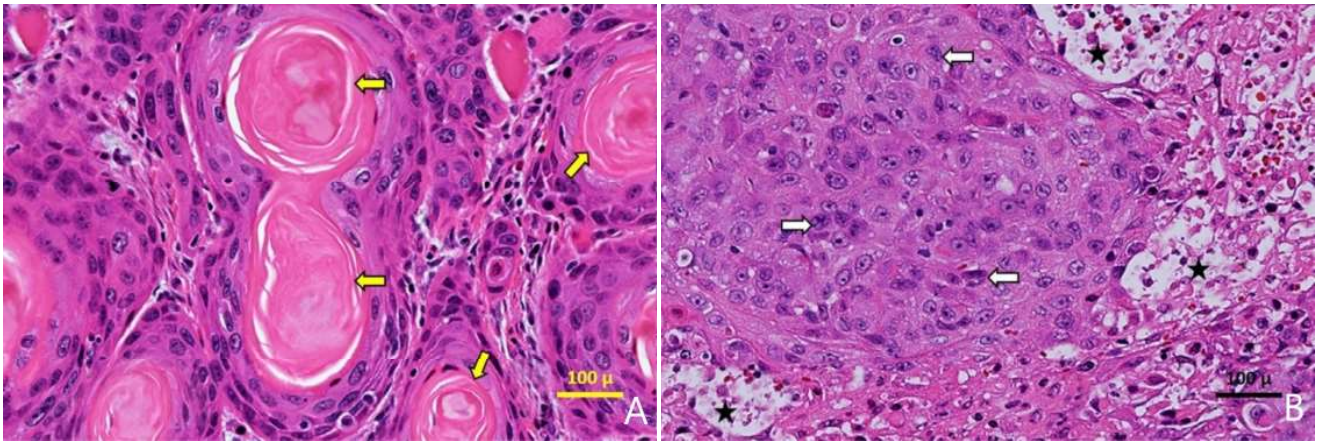

Figure 2.
Histopathological images, (A)clusters of well differentiated malignant squamous epithelial cells showing progression from peripheral basal like cells through stratified squamous epithelium with keratinization forming a central keratin pearl (yellow arrow) - H&E stain, 40X objective. (B) Tumour cells (white arrow) with mitotic figures and pleomorphism, areas of necrosis (*) characterized by loss of structure and replacement with eosinophilic (pink) proteinaceous material and cellular debris - H&E stain, 40X objective.

equine SCC cases [2,10].Nonpigmented skin regions, especially those with high exposure to light, exhibit a greater vulnerability to the development of OSCC. Mucocutaneous junctions are particularly vulnerable, even outside the oral cavity [11]. Age is also a factor and older horses have a higher susceptibility to OSCC. The horse in this case was 23 years old, placing it within a high-risk group. The exact pathogenesis of OSCC in horses remains unclear [1].

The simultaneous presence of long-standing infection or granulation tissue proliferation can complicate the accurate diagnosis of mandibular tumors [12]. Differential diagnoses for equines OSCC, include equine sarcoid, papilloma, mast cell tumor, exuberant granulation tissue, habronemiasis, phycomycosis, cutaneous lymphoma, melanoma, ossifying fibroma, hemangiosarcoma, myxomatous tumors, salivary adenocarcinoma, and basal cell carcinoma [11,12,14,15].

Radiography is useful for evaluating the tumor extent; though radiographic appearance can vary widely. In our study, severe mandibular bone lysis and irregular periosteal reactions suggested neoplasia. Other potential differential diagnoses for these radiographic findings include apical sepsis, osteomyelitis, and trauma [5]. Computed tomography can be helpful in differentiating various forms of SCC from other skull pathologies. Unfortunately, we were unable to perform computed tomography on our case, as the horse passed away at a considerably distant location from our facility.

Histopathological grading of SCC is based on the degree of cellular anaplasia in samples collected via biopsy or surgical excision. Well-differentiated SCC (grade I) exhibits minimal atypia in basal or parabasal cells, while poorly differentiated SCC (grade III) shows little to no architectural or cellular resemblance to normal tissue. Grade II tumors have features between the criteria for grade I and grade III [7]. In the case, the gelding presented with a large, destructive mandibular mass accompanied by infection, granulomatous tissue, and a purulent sinus tract.

Definitive diagnosis requires biopsy specimens from both the neoplastic tissue and the marginal zone, which are then prepared for histopathological examination. In the present case, histopathology confirmed grade III OSCC. It is advisable to perform fine needle aspiration (FNA) or biopsy of regional lymph nodes to assess the possibility of metastasis. However, mandibular lymphadenopathy in horses with oral neoplasia, often results by reactive inflammation rather than metastatic disease; thus, the results of lymph node biopsy or FNA are not always conclusive for metastases [1,11]. A retrospective study of 114 equine penile and preputial neoplasms reported metastasis most frequently in grade III tumors [13]. In our case, the owner declined any further diagnostic, so lymph node metastasis could not be assessed .

Treatment success depends on many factors but mostly related to mass including type, size and accessibility [8]. Multiple strategies have been suggested for the treatment of SCC, encompassing surgical intervention, cryotherapy, hyperthermia, radiotherapy, chemotherapy, and photodynamic therapy. The success of these treatment options varies by tumour aggressiveness, accessibility, and chronicity [11]. Tumors in the rostral oral cavity are often easier to treat since they are typically detected early and can be excised surgically or accessed for intralesional chemotherapy and radiotherapy. Although surgical excision has been shown effective in treating OSCC, achieving complete removal is often challenging, particularly in difficult-to-access locations, where complete excision may be impossible, leading to high consequently, recurrence rates [1,10]. In this case, the lesion's extensive nature, coupled with a secondary infection, significantly worsened the prognosis. The owner declined treatment owing to the associated risks and elected to keep the horse comfortable without active treatment, despite medical recommendations for pain management and surgical intervention. OSCC typically presents a challenging prognosis for resolution, particularly when metastasis to regional lymph nodes occurs, which significantly deteriorates the overall outlook and may impact the decision-making process regarding the commencement of treatment and even may affect the decision to commence treatment [8,11,16]. These tumours extensively infiltrate surrounding tissues, including bone, and may metastasize to local lymph nodes and the lungs, compounding the unfavourable prognosis for effective treatments.

Authors' Contributions

S.G and O.A performed clinical examination and conceived and planned the experiments. O.A and S.M performed review literature and manuscript writing. F.M and A.R performed paraclinical examinations.

Acknowledgements

We thank the staff of the Veterinary Hospital of the University of Tehran.

Competing Interests

The authors declare that there is no conflict of interest.

Reference

1. Knottenbelt DC, et al. Clinical equine oncology. 1st ed. Elsevier Health Sciences; 2015. 437-440.Doi:10.1016/c2009-0-61955-3.

2. Sundberg JP, Burnstein T, Page EH, Kirkham WW, Robinson FR. Neoplasms of Equidae. J Am Vet Med Assoc. 1977;170:150-2. Available from: https://europepmc.org/article/med/576219.

3. Schuh JCL. Squamous cell carcinoma of the oral, pharyngeal, and nasal mucosa in the horse. Vet Pathol. 1986;23:205-7. Doi:10.1177/030098588602300217.

4. Lambert JL, Fernandez NJ, Roy M-F. Association of presence of band cells and toxic neutrophils with systemic inflammatory response syndrome and outcome in horses with acute disease. J Vet Intern Med. 2016;30:1284–92. Doi:10.1111/jvim.13968.

5. Loftin P, Fowlkes N, McCauley C. Mandibular squamous cell carcinoma in a 5-year-old Tennessee Walking Horse. Equine Vet Educ. 2015;27(1):4-8. Doi:10.1111/eve.12231.

6. Gardner DG. Spontaneous squamous cell carcinomas of the oral region in domestic animals: A review and consideration of their relevance to human research. Oral Dis. 1996;2:146-54. Doi:10.1111/j.1601-0825.1996.tb00216.x

7. Van den Top JGB, Ensink JM, Barneveld A, van Weeren PR. Penile and preputial squamous cell carcinoma in the horse and proposal of a classification system. Vet Surg. 2011;23(12):636-48. Doi: 10.1111/j.2042-3292.2010.00216.x.

8. Auer JA, Stick JA, Kümmerle JM, Prange T. Equine surgery. 5th ed. Elsevier Health Sciences; 2018. 466. Doi:10.1016/C2015-0-05672-6.

9. Moore AS, Beam SL, Rassnick KM, Provost P. Long-term control of mucocutaneous squamous cell carcinoma and metastases in a horse using piroxicam: Case reports. Equine Vet J. 2003;35(7):715-8. Doi: 10.2746/042516403775696320.

10. Orsini JA, Nunamaker DM, Jones CJ, Acland HM. Excision of oral squamous cell carcinoma in a horse. Vet Surg. 1991;20:264-6. Doi: 10.1111/j.1532-950x.1991.tb01259.x.

11. Taylor S, Haldorson G. A review of equine mucocutaneous squamous cell carcinoma. Equine Vet Educ. 2013;25(7):374-8. Doi: 10.1111/j.2042-3292.2012.00457.x.

12. Monteiro S, Lemberger K, Gangl M. Mandibular squamous cell carcinoma in a young horse: Case report. Equine Vet Educ. 2009;21(8):406-10.Doi:10.2746/095777309x465512.

13. Van den Top JGB, De Heer N, Klein WR, Ensink JM. Penile and preputialtumours in the horse: A retrospective study of 114 affected horses. Equine Vet J. 2008;40:528-32. Doi: 10.2746/042516408x281180.

14. Luff J, Weingart S, May S, Murphy B. A subset of equine oral squamous cell carcinomas are associated with Equus-caballus papillomavirus 2 infection. J Comp Pathol. 2023;205:1–6. Doi: 10.1016/j.jcpa.2023.06.003.

15. Junge RE, Sundberg JP, Lancaster WD. Papillomas and squamous cell carcinomas of horses. J Am Vet Med Assoc. 1984;185:656-9. Doi:10.2460/javma.1984.185.06.656.

16. McGeachy TLEP, Jackson LAR. Veterinary oral and maxillofacial pathology. n.d. 137. Doi: 10.1002/9781119221296.fmatter.

How to cite this article
Ghamsari SM, Azari O, Moayer F, RostaeiA, Mortazavi SH. Oral Squamous Cell Carcinoma in a Budyonny horse: A case report Iran J Vet Sci Technol. 2025; 17(3): 69-73.
DOI: https://doi.org/10.22067/ijvst.2025.92011.1470
URL:https://ijvst.um.ac.ir/article_47075.html

Iranian Journal of Veterinary Science and Technology

Received: 2025- Sep- 01
Published online: 2025- Sep-10

ERRATUM

DOI: 10.22067/ijvst.2025.47340

Errata

The Iranian Journal of Veterinary Science and Technology publishes corrections when they are significant to scientific data, record-keeping, authorship, or patient care, whether the error was made by an author, editor, or staff during article processing. Errata also appear in the online version and are attached to files downloaded from ijvst.um.ac.ir.

In the article entitled "A comparison of bacteriological culture, serological and qPCR methods detecting Brucellosis in ewes with a history of abortion" by Aminzadeh M.J., Rahmani H.K., Hashemi K., Khaleghnia N., Azizzadeh M., and Mirshokraei P., published in Vol. 15, No. 4 (2023), DOI:10.22067/ijvst.2023.82928.1268, errors were identified in Figures 1, 2, and 3. These figures have now been replaced with the correct versions (https://ijvst.um.ac.ir/article_44331.html).

We apologize to the readers for this error. The article has been updated online to reflect the corrected figures.

Correct Figures:

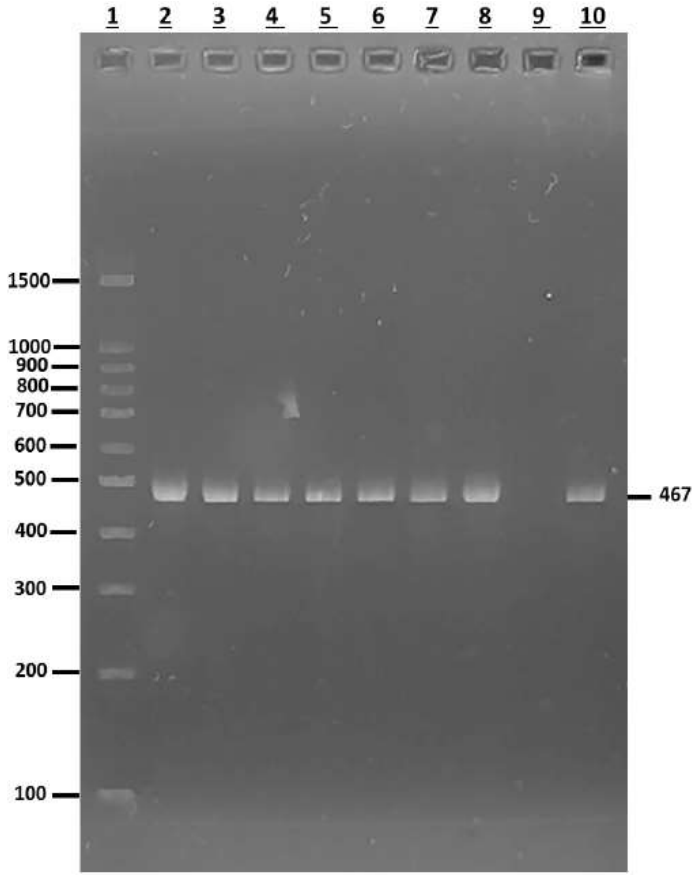

Figure 1.
PCR product of GAPDH gene. Lane 1: 100-bp DNA size marker (100-1500 bp); Lane 2-8: GAPDH gene; Lane 9: Negative control; Lane 10: Positive control.

Corresponding author:
Pezhman Mirshokraei
Email: mirshokraei@um.ac.ir
Tel+98(91)5512-0392

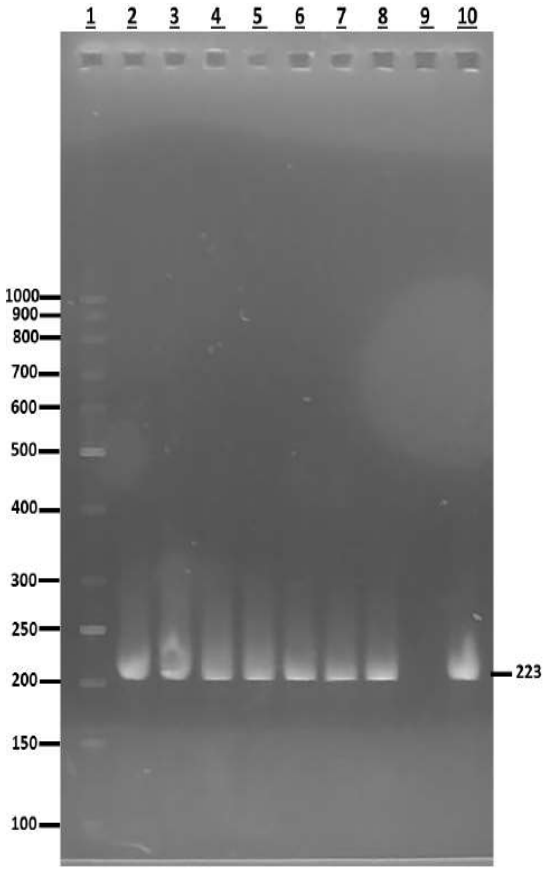

Figure 2.
PCR product of Brucella spp. Lane 1: 50-bp DNA size marker (50-1k bp); Lane 2-8: Brucella spp.; Lane 9: Negative control; Lane 10: Positive control.

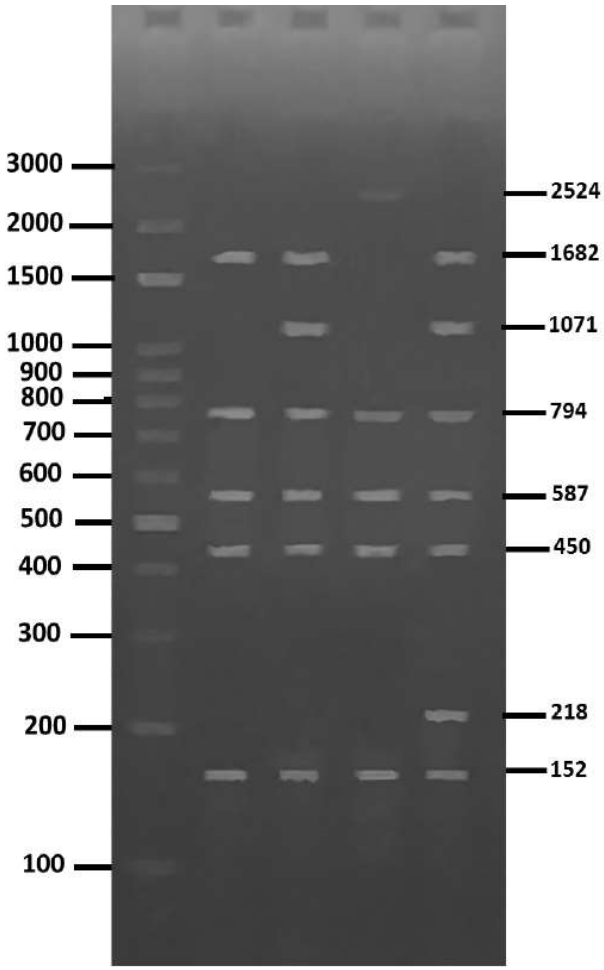

Figure 3.
Differentiation of B. abortus, B. melitensis, RB51, and Rev.1 vaccine strains by Bruce-ladder multiplex PCR. Lane 1: 100 bp Plus DNA size marker (100-3k bp); Lane 2: B. abortus; Lane 3: B. melitensis; Lane 4: B. abortus RB51 vaccine strain; Lane 5: B. melitensis Rev.1 vaccine strain.

Iranian Journal of Veterinary Science and Technology

Received: 2025- Jan-05
Accepted after revision: 2025- Jun-02
Published online: 2025- Jun- 03

Abstract in Persian

تاثیر مهاری عصاره گیاه اسپند، بر اثر کشنده زهر مار افعی جعفری در موش‌ها

سهیلا شیرخانی، بهروز فتحی هفشجانی*

گروه علوم پایه، دانشکده دامپزشکی، دانشگاهفردوسی مشهد، مشهد، ایران.

چکیده

دراین مطالعه تأثیرات آنتاگونیستی احتمالی عصاره گیاه اسپند (Peganum harmala) براثر کشنده زهر مار جعفری E. cari-natus ارزیابی شده است. هفتاد و دو موش آلبینو به ۱۲ گروه مساوی در ۶ پروتکل آزمایشی تقسیم شدند. روش تزریق، داخل صفاقی بود. در پروتکل اول، به موش های گروه A (کنترل) به میزان ۱۰ میلی‌گرم بر کیلوگرم زهربه تنهایی تزریق شد، آنها به طور میانگین بعد از ۸۰ دقیقه تلف شدند. در پروتکل دوم، به گروه‌های B۱ و B۲ به ترتیب با ۱۵ و ۳۰ میلی‌گرم بر کیلوگرم عصاره گیاه اسپند با ۱۰ میلی‌گرم بر کیلوگرم زهربطور همزمان تزریق شد. زمان زنده مانی آنها به ترتیب به ۲۳۲ و ۲۱۰ دقیقه افزایش یافت. در پروتکل سوم، به گروه‌های C۱ و C۲ ابتدا زهربا دوز ۱۰ میلی‌گرم بر کیلوگرم تزریق شد و بعد از ۱۵ دقیقه به ترتیب عصاره گیاه اسپند به میزان ۱۵ و ۳۰ میلی‌گرم بر کیلوگرم دریافت کردند. زمان مرگ آنها به ترتیب به ۲۴۶ و ۲۲۰ دقیقه افزایش یافت. در پروتکل چهارم، به گروه‌های D۱ و D۲ محلول حاصل از انکوباسیون عصاره گیاه اسپند با زهربه مدت ۳۰ دقیقه با دوزهای قبلی تزریق شد، زمان زنده مانی آنها به ترتیب به ۲۱۱ و ۱۹۵ دقیقه افزایش یافت. در پروتکل پنجم، گروه‌های E۱ و E۲ فقط عصاره گیاه اسپند را به میزان ۱۵ و ۳۰ میلی‌گرم بر کیلوگرم بصورت داخل صفاقی دریافت کردند. در پروتکل ششم، گروه‌های F۲ ،F۱ و F۳ فقط عصاره گیاه اسپند را به صورت خوراکی را و با دوزهای ۱۵، ۳۰ و ۶۰ میلی‌گرم بر کیلوگرم به ترتیب دریافت کردند. آنها همه زنده ماندند. دراین مطالعه، گیاه اسپند به طور معنی‌داری ($p < 0.05$) زمان زنده مانی موش ها را افزایش داد و بنابراین، دارای اثر آنتاگونیستی علیه اثر کشنده زهر مار جعفری می باشد و می‌تواند به عنوان یک کاندیدای ضد زهر برای تحقیقات بیشتر در نظر گرفته شود.

واژگان کلیدی

مار گزیدگی، مار جعفری، زهر، اسپند، اثرمخالف، موش ها

* **نویسنده مسئول:** بهروز فتحی هفشجانی
b-fathi@um.ac.ir

Iranian Journal of Veterinary Science and Technology

Received: 2024- Oct-02
Accepted after revision: 2025- Jun-19
Published online: 2025- Jun-20

Abstract in Persian

مطالعه رادیوآناتومیکی سر طوطی طوق قرمز (*Psittacula krameri*) بر پایه یافته‌های توموگرافی کامپیوتری

سیامک علیزاده[۱*]، محمدرضا حسین چی[۲]، رامان اسماعیل نژاد[۳]

۱گروه علوم درمانگاهی، دانشکده دامپزشکی، واحد نقده، دانشگاه آزاد اسلامی، نقده، ایران.
۲گروه علوم پایه، دانشکده دامپزشکی، واحد ارومیه، دانشگاه آزاد اسلامی، ارومیه، ایران.
۳ دانش آموخته دکترای حرفه‌ای دامپزشکی، دانشکده دامپزشکی، واحد ارومیه، دانشگاه آزاد اسلامی، ارومیه، ایران.

چکیده

سی‌تی اسکن یکی از کاربردی‌ترین و دقیق‌ترین روش‌های تصویربرداری تشخیصی می‌باشد که می‌تواند برای ارزیابی ناحیه سر در پرندگان استفاده شود. هدف از این مطالعه ارائه اطلاعات آناتومیکی نرمال سر طوطی طوق قرمز (*Psittacula krameri*) به روش توموگرافی کامپیوتری بود. در این تحقیق ویژگی‌های سر این پرنده از نظر استخوان‌ها، مفاصل، عضلات، سینوس‌ها و سایر بافت‌های تشکیل دهنده آن بررسی گردید. در این مطالعه توصیفی - مقطعی از لاشه ۶ طوطی طوق قرمز بالغ (۳ طوطی نر و ۳ طوطی ماده) با میانگین سنی ۱-۵ سال و با متوسط وزنی ۱۱۵-۱۲۵ گرم استفاده شد. پس از تهیه تصاویر توموگرافی کامپیوتری، سر هر طوطی تحت مطالعات آناتومیکی قرار گرفت. بر اساس نتایج این مطالعه اغلب ساختارهای سر طوطی طوق قرمز (*Psittacula krameri*) به وسیله تصاویر توموگرافی کامپیوتری بازسازی شده قابل شناسایی هستند. در تصاویر CT استخوان‌های آهیانه، فک پایین، پس‌سری، ماگزیلاری، پری‌ماگزیلاری، کامی، بالی، چهارگوش، گیجگاهی، غشاهای اپیتلیال، مجرای خارجی گوش و لابیرنت استخوانی، استخوانچه‌های گوش و آنتوگلوسوم، قسمت‌های مختلف سینوس تحت حدقه‌ای، نیم‌کره‌های مغز و قسمت‌های مختلف حدقه چشم و کانکاهای حفرات بینی بررسی گردیدند. مطالعه همزمان ارزیابی توموگرافی کامپیوتری و بررسی آناتومیکی سر طوطی ملنگو همبستگی بالایی از یافته‌ها را فراهم کرد. نتایج این تحقیق می‌تواند در شناسایی خصوصیات آناتومیکی و بررسی گونه‌های مختلف طوطی‌های طوق قرمز (Psittacula krameri)، آموزش علوم آناتومی و تفسیر تصاویر CT اسکن و نیز در معاینات بالینی و امور درمانی این نوع از طوطی مورد استفاده قرار گیرد.

واژگان کلیدی

توموگرافی کامپیوتری، آناتومی، سر، (*Psittacula krameri*) طوطی طوق قرمز

* **نویسنده مسئول:** سیامک علیزاده
Si.Alizadeh@iau.ac.ir

Iranian Journal of Veterinary Science and Technology

Received: 2024- Sep-28
Accepted after revision: 2025- Jul-16
Published online: 2024- Jul-17

Abstract in Persian

توافق اندک بین آزمایش های مولکلوی و سرولوژی برای تشخیص بروسلوز گاوی

مهران قائمی*[1]، محمدصادق گلواجوئی[2]

۱گروه پاتوبیولوژی، دانشکده دامپزشکی، دانشگاه فردوسی مشهد، مشهد، ایران.
۲ گروه پاتوبیولوژی، دانشکده دامپزشکی، دانشگاه شیراز، شیراز ، ایران.

چکیده

بروسلوز گاوی که بیشتر بوسیله بروسلا آبورتوس ایجاد می شود، یک بیماری مهم در گاو می باشد. این بیماری مشترک بین انسان و دام بوده و مشکلات زیادی برای سلامت عمومی ایجاد می کند. هم اکنون تشخیص بروسلوز گاوی بر اساس آزمایش های سرولوژی انجام می شود. در این مطالعه، تلاش گردید که آزمایش های سرولوژیک بروسلوز گاوی رایج در ایران را آزمایش های ردیابی انتی ژن مقایسه کنیم. همچنین نرخ آلودگی به یرسینیا انتروکولیتیکا 9O به عنوان یک عامل مداخله کننده احتمالی در آزمایش های سرولوژیک گونه های بروسلا ارزیابی شد. ۹۶ نمونه از غدد لنفاوی فوق پستانی گاوهای راکتور مثبت در استان فارس اخذ گردید. کشت باکتریایی و آزمایش های مولکولی بر روی این نمونه ها انجام گردید. باکتری بروسلا تنها از ۸/۳ ٪ از نمونه های کشت شده جداسازی گردید و نیز در۱۵.۳ ٪ و۲۱.۴ ٪ نمونه ها با روش های PCR معمولی و بی درنگ ردیابی گردید. تمامی بروسلاهای ردیابی شده از گونه بروسلا آبورتوس بودند. اینکه در اغلب گاوهای راکتور مثبت، باکتری بروسلا ردیابی نشد نشانگر نرخ بالای مثبت کاذب آزمایش های سرولوژی رایج می باشد که نیاز به بازنگری در آزمایش های مورد استفاده برای شناسائی گاوهای آلوده را نشان می دهد. در نهایت، آزمایش PCR بی درنگ اطلاعات ارزشمندی درباره گونه های بروسلای در حال گردش هر ناحیه فراهم می کند.

واژگان کلیدی

بروسلا آبورتوس، یرسینیا انتروکولیتیکا، تست سرولوژی ، پی درنگ PCR

* **نویسنده مسئول:** مهران قائمی
m.ghaemi@um.ac.ir

Iranian Journal of Veterinary Science and Technology

Received: 2025- Feb-20
Accepted after revision: 2025- Jun-08
Published online: 2025- Jun-10

Abstract in Persian

کارسینوم سلول سنگفرشی دهان در اسب بودیونی: گزارش موردی

سید مهدی قمصری[۱]، امید آذری*[۱]، فریبرز معیر[۲]، علی روستایی[۱]، سیده حورا مرتضوی[۳]

۱ گروه جراحی و تصویربرداری تشخیصی، دانشکده دامپزشکی دانشگاه تهران، تهران، ایران.
۲ گروه پاتوبیولوژی، دانشکده دامپزشکی دانشگاه آزاد اسلامی، واحد کرج، کرج، ایران.
۳ دانشجوی دکتری حرفه‌ای، دانشکده دامپزشکی دانشگاه تهران، تهران، ایران.

چکیده

کارسینوم سلول-سنگفرشی (*Squamous Cell Carcinoma*) یک نئوپلازی بدخیم است که از اپیتلیوم سنگفرشی مطبق ناشی می‌شود و به‌عنوان شایع‌ترین تومور دهان در اسب‌ها شناخته می‌شود. این گزارش موردی، ویژگی‌های بالینی و بافت‌شناسی یک کارسینومای سلول سنگفرشی لثه را در یک اسب بودیونی ۲۳ ساله با سابقه درمان‌های ناموفق متعدد، از جمله تلاش ناموفق برای برداشت تومور توسط جراحی ، توصیف می‌کند. این اسب با یک توده نرم وسیع، ترشح بیش از حد بزاق و بیرون افتادن زبان به جانب به بیمارستان ارجاع شد. یافته‌های آزمایشگاهی حاکی از آنمی مرتبط با سرطان بود و بررسی های تصویربرداری تشخیصی، تخریب استخوان فک پایین و ماهیت مخرب توده را نشان داد. بررسی بافت‌شناسی تشخیص کارسینومای سلول سنگفرشی لثه را تأیید کرد که با تشکیل مرواریدهای کراتینی و شاخص میتوتیک بالا مشخص می‌شود. صاحب اسب به دلیل پیش آگهی ضعیف و هزینه‌های بالای درمان، از مداخلات درمانی بیشتر صرف‌نظر کرد و این اسب ۶ ماه پس از مراجعه تلف شد. در این گزارش، به چالش‌های مدیریت کارسینومای سلول سنگفرشی پیشرفته لثه در اسب‌ها و اهمیت تشخیص زودهنگام این عارضه و مداخله درمانی مناسب را مورد بررسی قرار می‌گیرد.

واژگان کلیدی

اسب، محوطه دهانی، تومور، کارسینوم سلول سنگفرشی

* نویسنده مسئول: امید آذری
Omid.azari@ut.ac.ir

Author Index

Author index

A

Abubakar, Yusuf 1
Agbeniyi, Opeyemi 38
Akinlade, Jelili Akinwole 38
Akinjogunla, Victoria Folakemi 1
Alizadeh, Siamak 47
Atabo, Shaibu Mohammed 29
Azari, Omid 69

B

Babelhadj, Baaissa 8
Boukerrou, Maya 8

D

Djeghar, Alaa Eddine 8

E

Esmaeilnejad, Raman 47
Evin, Allowen 8

F

Fathi, Behrooz 21
Furo, Nathan Ahmadu 29

G

Ghaemi Mehran 61
Ghamsari, Seyed Mahdi 69
Golvajouei, Mohammad Sadegh 61
Guintard, Claude 8

H

Hammed, Opeyemi Oladipupo 38
Hassan, Khalid Shuaibu 1
Hosseinchi, Mohammadreza 47

I

Ibrahim, Abdulganiu Olawale 29

J

Jaji, Alhaji Zubair 29

K

Kigir, Esther Solomon 29

L

Lawal, Abdulrazak 1

M

Moayer, Fariborz 69
Mortazavi, Seyedeh Houra 69
Muazu, Tuaheed Abubakar 1

O

Olaseni, Christian Anuoluwapo 1
Ojoawo, Olubunmi Titilayo 38
Onwuama, Kenechukwu Tobechukwu 29
Ozohu Abdulkarim, Latifah 29

R

Ridouh, Rania 8
Rom-Kalilu, Fiwasade Adejoke 38
Rostaei, Ali 69

S

Salako, Jamiu Olatoye 1
Salami, Sulaiman Olawoye 29
Shirkhani, Soheila 21

Author Index

T

Tekkouk - Zemmouchi, Faiza 8

U

Usman, Mannir Dahiru 1

W

Wanmi, Nathaniel 29

Y

Yah, Clarance Suh 1

Guide for authors

SCOPE

Iranian journal of Veterinary Science and Technology (IJVST) publishes important research advances in veterinary medicine and subject areas relevant to veterinary medicine including anatomy, physiology, pharmacology, bacteriology, biochemistry, biotechnology, food hygiene, public health, immunology, molecular biology, parasitology, pathology, virology, large and small animal medicine, poultry diseases, diseases of equine species, and aquaculture. Articles can comprise research findings in basic sciences, as well as applied veterinary findings and experimental studies and their impact on diagnosis, treatment, and prevention of diseases. IJVST publishes four kinds of manuscripts: Research Article, Review Article, Short Communication, and Case Report.

Guide for Authors

GENERAL GUIDELINES

1. Submitted manuscripts should not be previously published elsewhere and should not be under consideration by any other journal.
2. The corresponding author should provide all co-authors with information regarding the manuscript, and obtain their approval before submitting any revisions.
3. The submitted manuscript should be accompanied by a written statement signed by the corresponding author on behalf of all the authors that its publication has been approved by all co-authors, stating that the whole manuscript or a part of it has not been published.
4. Ethics: Authors must state that the protocol for the research project has been approved by the Ethics Committee of the institution within which the work was undertaken. Authors are responsible for animal welfare and all statements made in their work.

OPEN ACCESS POLICY

Iranian Journal of Veterinary Science and Technology is a fully Open Access journal in which all the articles are available Open Access. There is no cost to the reader or author. All costs are covered by the Ferdowsi University of Mashhad Press.

COPYRIGHT

Copyright on any open access article in the Iranian Journal of Veterinary Science and Technology, published by Ferdowsi University of Mashhad Press is retained by the author(s).

- Authors grant Ferdowsi University of Mashhad Press a license to publish the article and identify itself as the original publisher.
- Authors also grant any third party the right to use the article freely as long as its integrity is maintained and its original authors, citation details, and publisher are identified.

The Creative Commons Attribution License 4.0 formalizes these and other terms and conditions of publishing articles. The Copyright assignment form can be downloaded from the IJVST website.

SUBMISSION

Copyright on any open access article in the Iranian Journal of Veterinary Science and Technology, published by Ferdowsi University of Mashhad Press is retained by the author(s).

- Authors grant Ferdowsi University of Mashhad Press a license to publish the article and identify itself as the original publisher.
- Authors also grant any third party the right to use the article freely as long as its integrity is maintained and its original authors, citation details, and publisher are identified.

The Creative Commons Attribution License 4.0 formalizes these and other terms and conditions of publishing articles. The Copyright assignment form can be downloaded from the IJVST website.

Copyright assignment form (can be downloaded from IJVST website)

Conflict of interest and author agreement form (can be downloaded from the IJVST website)

Guide for Authors

For further information, please contact the Editorial Office:
Iranian Journal of Veterinary Science and Technology
Email: ijvst@um.ac.ir;
Tel: +98 51 3880-3742

PREPARATION OF MANUSCRIPT

Manuscripts submitted to IJVST should neither be published previously nor be under consideration for publication in another journal. The main article types are as follows:

Research Articles should contain Title page, Abstract, Keywords, List of Abbreviations, Introduction, Results, Discussion, Materials and methods, References, and Figure legends. Tables and figures should be appended as individual files.

Review Articles should contain Title page, Abstract, Keywords, List of Abbreviations, Introduction, appropriate sections dependeing to the subject, Conclusions and future directions. Tables and figures should be appended as individual files. The review article should provide an update on recent advances in a particular field. Authors wishing to submit review articles should contact the Editor with an outline of the proposed paper prior to submission.

Case Reports should include Title page, Abstract, Keywords, List of Abbreviations, Introduction, Case Presentation, Results and Discussion, and References. Case reports should not exceed 2000 words (excluding the references) and should include no more than two tables or figures. Tables and figures should be appended as individual files.

Short Communications should not exceed 2000 words (excluding the references) and include no more than two tables or figures. They should include Title page, Abstract, Keywords, List of Abbreviations, the text summarizing results with no other divisions, and References. Tables and figures should be appended as individual files.

Submission Process

Manuscripts for IJVST should be submitted online at https://ijvst.um.ac.ir/ .

The submitting author, who is generally the corresponding author, is responsible for the manuscript during the submission and peer-review process. The submitting author must ensure that all eligible co-authors have been included in the tittle page and that they have all read and approved the submit-

ted version of the manuscript.

To submit your manuscript, register and log in (https://ijvst.um.ac.ir/contacts?_action=loginForm). All co-authors can see the manuscript details in the submission system, if they register and log in using the e-mail address provided during manuscript submission.

Reviewer Suggestions: During the submission process, please suggest three potential reviewers with the appropriate expertise to review the manuscript. The editors will not necessarily approach these referees. Please provide detailed contact information (address, homepage, phone, e-mail address). The proposed referees should neither be current collaborators of the co-authors nor have published with any of the co-authors of the manuscript within the last three years. Proposed reviewers should be from different institutions to the authors. You may identify appropriate Editorial Board members of the journal as potential reviewers. You may suggest reviewers from among the authors that you frequently cite in your paper. For detailed information regarding the qualifications and responsibilities of the reviewers, please visit Review Guide.

Ethics: Authors must state that the protocol for the research project has been approved by the Ethics Committee of the institution within which the work was undertaken. Authors are responsible for animal welfare and all statements made in their work.

Accepted file format

Authors are encouraged to use the Microsoft Word template to prepare their manuscript. Using the template file will substantially shorten the time to complete copy-editing and publication of accepted manuscripts. The total amount of data for all files must not exceed 120 MB. If this is a problem, please contact the Editorial Office ijvst@um.ac.ir. Accepted file formats are:

Microsoft Word: Manuscripts prepared in Microsoft Word must be written in English, with Abstract in both English and Persian (where applicable), typewritten in MS Word program, double-spaced, in 12-point "Times New Roman" font on A4 paper size. Authors are requested to reserve margins of 2.5 cm all around the pages. Manuscript should also have line numbers. All pages of the manuscripts should also be enumerated.Templates can be downloaded from the following links:

Template MS Word file for Title page (https://ijvst.um.ac.ir/page_3.html).
Template MS Word file for Original articles (https://ijvst.um.ac.ir/page_3.html).
Template MS Word file for Short Communication (https://ijvst.um.ac.ir/page_3.html).
Template MS Word file for Case Report (https://ijvst.um.ac.ir/page_3.html).
Template MS Word file for Tables (https://ijvst.um.ac.ir/page_3.html).
Template MS Word file for Persian Abstract (https://ijvst.um.ac.ir/page_3.html).

Tables: Please submit tables as individual files and editable text and not as images. Place all table notes below the table body. Each table should have a title which is followed by explanation of results shown in the table. Use of vertical rules must be avoided. Tables should be self-explanatory, and

clearly arranged. Tables should provide easier understanding and not duplicate information already included in the text or figures. Each table should be typewritten with double spacing on a separate file and numbered in order of citation in the text with Arabic numerals. Each table should have a concise heading that makes it comprehensible without reference to the text of the article. Explain any non-standard abbreviations in a footnote to the table.

Figures: Figures must be submitted in individual files (format: TIFF, Dimensions: Width: 789 – 2250 pixels at 300 dpi Height maximum: 2625 pixels at 300 dpi, Resolution: 300 – 600 dpi, file size: less than 10 MB, Text within figures: Arial or Symbol font only in 8-12 point). The text and other labels should be placed in the figure as un-compressed layers. Each figure should have a title which is followed by explanation of results shown in the figure. Figures should be numbered in order of citation in the text with Arabic numerals. If a published figure is used, the publisher's permission needs to be presented to the office, and the figure should be referenced in its legend.

diagrams : For the use of bar diagrams the following publication should be consulted:

Weissgerber TL, Milic NM, Winham SJ, Garovic VD. Beyond bar and line graphs: time for a new data presentation paradigm. PLoS Biol. 2015 Apr22;13(4):e1002128. The bar diagrams should be provided in color and in a well-designed and professional format. Please do not use different shades of gray. The axes of diagrams should have titles and units. Also, the source file of the image (Excel etc.) should be provided for typesetting.Illustrations should be numbered as cited in the sequential order in the text, with a legend at the end of the manuscript. Color photographs are accepted at no extra charge. The editors and publisher reserve the right to reject illustrations or figures based upon poor quality of submitted materials.

Title Page information

Full Title Page should include title (concise and informative), author(s) (including the complete name, department affiliation, and institution), running head (condensed title) (≤ 50 characters, including spaces), name and address of the authors to whom correspondence and reprint requests should be addressed, Acknowledgements, Author contributions, and Conflict of interest.

Acknowledgements: Personal acknowledgement, sources of financial support, contributions and helps of other researchers and everything that does not justify authorship should be mentioned in this section, if required.

Author contributions: Authors are required to include a statement to specify the contributions of each author. The statement describes the tasks of individual authors referred to by their initials. Listed below is an example of author contributions statement:

" Conceived and designed the experiments: HD, SS. Performed the experiments: SS. Analyzed the data: HD, SS, MMM, ARB.

Research space and equipment: HD, MMM, ARB. Contributed reagents/materials/analysis tools: HD. wrote the paper: SS, HD."

Conflict of interest: All authors must disclose any financial and personal relationships with other people or organizations that could inappropriately influence (bias) their work. Examples of poten-

tial conflicts of interest include employment, consultancies, stock ownership, honoraria, paid expert testimony, patent applications/registrations, and grants or other funding. If there are no conflicts of interest then please state 'The authors declare that there is no conflict of interest'. This form can be downloaded from the IJVST website.

Abstract: Abstract (in English and Persian) no more than 250 words should contain the purpose of the study, findings and the conclusion made on the basis of the findings. Authors who are not native Persian speakers may submit their manuscript with an abstract in English only. Abbreviations and reference citations may not be used in the abstracts.

Keywords: For indexing purposes, each submitted manuscript should include three to seven keywords, following the abstract and preferably chosen from the Medical Subject Headings (MESH). Keywords should express the precise content of the manuscript.

Abbreviations: Define abbreviations that are not standard in this field in a list to be placed on the tittle page. Such abbreviations that are unavoidable in the abstract must be defined at their first mention there, as well as in the tittle page. Ensure consistency of abbreviations throughout the article.

Main Text

Introduction: Introduction should be as concise as possible, and clearly explain the main objective and hypothesis of the investigation.

Results: Results indicate the results of an original research in a clear and logical sequence. Do not repeat data that are already covered in tables and illustrations. In manuscripts describing more than one animal, all animals should be assigned a case number.

Discussion: Discussion should include the answer to the question proposed in the introduction and emphasize the new and important aspects of the study and the conclusions that follow from them. It could include the implication, application, or speculation of the findings and their limitations, relate the observations to other relevant studies, and links the conclusions with the goals of the study. Recommendations, when appropriate, may be included.

Materials and Methods: Materials and methods should be described in sufficient details to allow other researchers to reproduce the results. Specify any statistical computer programs used .The methods of data collection and use of statistical analysis will be checked by the referees and if necessary, a statistician. Drugs and therapeutic agents, reagents, softwares and equipments should be given in the format: name (trade name, manufacturer name, city, country), e.g. Statview 5 (SAS Institute, Inc., Cary, NC, USA).

Animals: All animal experiments should comply with the ARRIVE guidelines and the authors should clearly indicate in the manuscript the ethical code of the study.

Gene names: The standard gene names, as provided by HGNC should be used. Gene names must be italicized. If the case of mammalian species and if gene names refer to rodent species, they must be upper case; if they refer to non-rodent species they must be written in capitals. If they refer to other species, they must written lower case. Protein names are written in capitals and are not italicized. As

an example:

Mouse beta actin gene: Actb

Bovine beta actin gene: ACTB

Chicken beta actin gene: actb

Beta actin protein: ACTB

Quantitative PCR: If the quantitative PCR method has been used, the related section in Materials and Methods and Results must be written following the reference:

Bustin SA, Benes V, Garson JA, Hellemans J, Huggett J, Kubista M, Mueller R, Nolan T, Pfaffl MW, Shipley GL, Vandesompele J, Wittwer CT. The MIQE guidelines: minimum information for publication of quantitative real-time PCR experiments. Clin Chem. 2009 Apr;55(4):611-22.

Protocol for DNA/RNA extraction, including quantification and determination of purity.

Reverse transcription (if used): amount of RNA, concentration of all reagents: primers conce ntration (either random primers or oligonucleotides), reverse transcriptase and master mix components.

qPCR: sequence of forward and reverse primers, probes, amplicon size, accession number of Genebank;

thermocycler parameters (i.e. denaturation, annealing and extension steps, number of cycles, melting curves);

validation of PCR products; non-template controls for reverse transcription and qPCR should be included in all reactions; and

Data analysis: details for the quantitative or relative analysis.

Use of antibodies: Authors must show that the antibodies are validated and their specificity sis confirmed.

References: Must be up-to-dated and limited to those that are necessary. Lists of references should be given in numerical order in the text, and in the reference list. Please use Vancouver style. To download the Vancouver Style follow the link in the IJVST website which could be used in the Endnote software.

Example piece of text and reference list :
An unhealthy diet, obesity and physical inactivity play a role in the onset of type 2 diabetes, but it has been shown that increased physical activity substantially reduces the risk [1], and participation in regular physical activity is one of the major recommendation of the evidence based guidelines for the primary prevention of diseases [2]. According to the 2004-05 National Health Survey, more than half a million Australians (3.5% of the population) have diabetes mellitus which had been medically diag-

nosed and most of these people have the Type 2 condition [3]. Gestational diabetes is also on the increase, rising steadily between 2000-01 and 2005-06 [4]. Approximately two thirds of those with diabetes have been prescribed medication [3], but it is of concern that a recent review of the literature found that many people do not take their medication as prescribed [5]. Many patients also self monitor the disease by measuring their blood glucose levels with a glucose meter but Song and Lipman [6] have concerns about how well this is managed.

References for the above example:

1. Hull J, Forton J, Thompson A. Paediatric respiratory medicine. Oxford: Oxford University Press; 2015.
2. Eckerman AK, Dowd T, Chong E, Nixon L, Gray R, Johnson S. Binan goonj: bridging cultures in Aboriginal health. 3rd ed. Chatswood, NSW: Elsevier Australia; 2010.
3. Johnson C, Anderson SR, Dallimore J, Winser S, Warrell D, Imray C, et al. Oxford handbook of expedition and wilderness medicine. Oxford: Oxford University Press; 2015.
4. McLatchie GR, Borley NR, Chikwe J, editors. Oxford handbook of clinical surgery. Oxford: Oxford University Press; 2013.
5. Petitti DB, Crooks VC, Buckwalter JG, Chiu V. Blood pressure levels before dementia. Arch Neurol. 2005 Jan;62(1):112-6. Doi: 10.1001/archneur.62.1.112 .
6. Liaw S, Hasan I, Wade, V, Canalese R, Kelaher M, Lau P, et al. Improving cultural respect to improve Aboriginal health in general practice: a multi-perspective pragmatic study. Aust Fam Physician. 2015;44(6):387-92.Doi: 10.1001/archneur.62.1.112 .

Use of Italics

Gene symbols, Latin terms (i.e. in vivo, in vitro, ex vivo, in utero, in situ, and etc.) and species scientific names (using the binomial nomenclature), should be typed in italics, while the first letter of the genus name must be capitalized (i.e. Homo sapiens).

Copyright

Accepted manuscripts in IJVST will be Open-Access articles distributed under the terms and conditions of the Creative Commons Attribution License (CC BY). The copyright is retained by the author(s). The publisher will insert the following note at the end of the published text:

PUBLICATION ETHICS

Iranian Journal of Veterinary Science and Technology is a member of the Committee on Publication Ethics (COPE), best practice guidelines for dealing with ethical issues in journal publishing and adopts the COPE guidelines. The journal members (editor, editorial board and the journal manager) have agreed to meet the purposes and objectives of the Journal.

Ethical guidelines for authors:

- Manuscripts must be submitted with the understanding that they have not been previously published and are not currently under consideration by another journal.

- Authors are expected to submit manuscripts with enough detail and references to enable others to replicate the work.

-Authors may be requested to provide the original data from their study for editorial review and should be ready to make the data publicly available if feasible.

-The corresponding author is responsible for ensuring that all co-authors have approved the manuscript prior to submission.

- Only individuals who meet the authorship criteria should be listed as authors in the manuscript, as they are expected to take public responsibility for the content. The "Conflict of interest declaration and author agreement form" must be signed and completed by all authors. This statement and signatures certifies that all authors have seen and approved the manuscript being submitted. Also, the authors by signing this form warrant that the article is the Authors' original work, that the article has not received prior publication and is not under consideration for publication elsewhere, and that the corresponding author shall bear full responsibility for the submission.

Before submission, all authors are required to review the Article Submission Checklist.

- Authors should disclose any conflicts of interest that might be perceived as influencing the results or their interpretation in the manuscript at the earliest stage possible. This can be done by uploading the Conflicts of Interest Form along with the manuscript submission.

-The authors are responsible for ensuring that the submitted manuscript is a complete and original work, free from any form of plagiarism. All authors are advised to use plagiarism prevention software to check for similarities.

-Authors are required to identify in their manuscript if their work involves chemicals, procedures, or equipment that have any inherent unusual hazards.

- All researchers should have a written and signed informed consent form from whom voluntarily participate in their researches. This signed form shows obviously the consent of the subject to participate. All steps of the experiment were carried out based on the Guidelines for Animal Care at Ferdowsi University of Mashhad in Iran that are approved by the Committee of Biological Ethics, Faculty of Veterinary Medicine, Ferdowsi University of Mashhad, Iran (https://ethics.research.ac.ir/docs/pages/Guideline-En.pdf). The experiments that are carried outside the university should have a written and

signed informed consent form related to ethic protocols of university or institute that they are carried.

- If the decision is 'Needs Revision,' authors are expected to respond systematically and promptly to the reviewers' comments, addressing point by point, and revising their manuscript accordingly. The revised manuscript should then be submitted to the journal within the given deadline.

- Authors are requested to clearly identify who financially supported the research and/or preparation of the manuscript and briefly describe the role of the founder/ sponsor in any part of the work at the end of their manuscript under "Acknowledgements" section.

-It is a condition for submission of a manuscript that the authors permit editing of the paper for readability.

- All authors agree to allow the corresponding author to serve as the correspondent with the Journal's editorial office, to review the edited manuscript and proof.

-Under open access license, authors retain ownership of the copyright for their content, but allow anyone to download, reuse, re-print, modify, distribute, and/or copy the content as long as the original authors and source are cited properly.

- When author(s) discover(s) a significant error or inaccuracy in his/her own published work, it is the author's obligation to promptly notify the Journal editor or publisher to retract or correct the manuscript.

- All authors must know that the submitted manuscripts under review with the IJVST are subject to screening, using Plagiarism Prevention Software. Plagiarism is a serious violation of publication ethics and in all its forms constitutes unethical publishing behavior and is unacceptable.

- Editors and members of editorial board as authors should be excluded from publication decisions when they are authors or have contributed to a manuscript.

-The artificial intelligence (AI) tools such as ChatGPT or Large Language Models cannot meet the requirements for authorship. Authors who use AI tools in the writing of a manuscript, production of images or graphical elements of the paper, or in the collection and analysis of data, must be transparent in disclosing in the Materials and Methods (or similar section) of the paper how the AI tool was used and which tool was used. Authors are fully responsible for the content of their manuscript, even those parts produced by an AI tool, and are thus liable for any breach of publication ethics(Authorship and AI tools).

Ethical guidelines for Peer reviewers

- Reviewers are expected to provide insightful comments that assist the editors in making a decision about whether or not to publish the submitted manuscript.

- Reviewers are expected to maintain the confidentiality of the manuscripts they are invited to review.

-Reviewers are expected to disclose any conflicts of interest they have with the authors, companies, or institutions associated with the manuscripts they are invited to review. If a conflict of interest exists, reviewers should immediately notify the Editor-in-Chief, decline the invitation to review, and suggest alternative reviewers.

- If reviewers feel unqualified to review an assigned manuscript or are unable to provide a timely review, they should inform the Editor-in-Chief and excuse themselves from the review process. If they know of any other expert reviewers, they may suggest them to the Editor-in-Chief through the dedicated email/comments section in the Reviewer Dashboard.

- Reviewers are expected to maintain the confidentiality of the manuscripts they review and not discuss any information from the manuscript with anyone other than the Editor-in-Chief, unless they have obtained explicit permission to do so. This also applies to invited reviewers who decline the review invitation.

- Reviewers are obligated to treat the manuscripts they receive for peer review as confidential and must not use any information obtained through this process for personal gain.

-Reviewers are expected to provide technical, professional, and objective comments on the manuscripts they are invited to review.

-Reviewers are expected to avoid personal biases in their comments and judgments, and express their views clearly with supporting arguments that assist the author in improving the manuscript.

-Reviewers are expected to identify any relevant published work that has not been cited by the authors. If a statement has been previously reported elsewhere, it should be accompanied by the appropriate citation.

-Reviewers should also bring to the attention of the Editor-in-Chief any significant similarity or overlap between the manuscript under consideration and any other publications of which they are personally aware.

The process has been explained in the section "Peer Review Process".

Ethical guidelines for Editor

-The editors should evaluate submitted manuscripts to determine if they fall within the scope of the journal. Additionally, the editors should recommend expert reviewers based on their integrated recognition of specialized reviewers.

-The Editor-in-Chief is responsible for deciding whether to accept or reject submitted manuscripts for the journal. This decision takes into consideration several factors, such as the judgment of the editorial board members, the validation of the work in question, its significance to researchers and readers, as well as any feedback from reviewers. Furthermore, the decision must also comply with legal requirements regarding libel, copyright infringement, and plagiarism, which are currently in force. The Editor-in-Chief works closely with other editors and reviewers to ensure that all submissions are fairly evaluated.

-The editors ought to uphold the anonymity of both reviewers and authors.

-The editors should disclose any potential conflicts of interest and make efforts to avoid them. If such circumstances arise, they are expected to delegate the handling of the manuscript to another member of the editorial board.

-The editors, particularly the Editor-in-Chief, should demonstrate a willingness to investigate cases

of plagiarism and fraudulent data. When ethical concerns are raised about a submitted manuscript or published paper, the editors will take appropriate measures in response. Any reported incidents of unethical publishing behavior will be thoroughly examined, even if they come to light years after publication.

-When dealing with cases of suspected misconduct, the Editor-in-Chief follows the COPE Flowcharts. If an investigation supports the ethical concern, the journal will publish a correction, retraction, expression of concern, or any other relevant note.

-The editors must not share any information about submitted manuscripts with anyone until they are published, as appropriate.

-The Editor-in-Chief and members of the editorial board will not use unpublished materials disclosed in a submitted paper for their own research purposes without obtaining explicit written consent from the author.

-Editors are expected to give fair consideration to all manuscripts submitted for publication, evaluating each on its own merits and without prejudice based on the author(s)' country, race, religion, nationality, sex, seniority or institutional affiliation. Decisions about editing and publishing are made solely based on the quality and relevance of the manuscript and are not influenced by external policies of governments or other agencies beyond the scope of this journal.

-The Editor-in-Chief has complete authority over the editorial content of the journal as well as the timing of its publication.

Ethical guidelines for Publisher

"Ferdowsi University of Mashhad press (FUM)" is promising to ensure that the decision on manuscript submissions is only made based on professional judgment and will not be affected by any commercial interests.

- FUM is committed to maintain the integrity of academic and research records.

- FUM is monitoring the ethics by Editor-in-Chief, Associate Editors, Editorial Board Members, Reviewers, Authors, and Readers.

- FUM, together with the Journal's editors, shall take reasonable steps to identify and prevent the publication of manuscripts where research misconduct has occurred, and under no circumstances encourage such misconduct or knowingly allow taking place.

- FUM is always checking the plagiarism and fraudulent data issues involving in the submitted manuscripts and willing to publish corrections, clarifications and retractions involving its publications as and when needed.

-FUM as the publisher supports the Journal for each published issue by paying a defined budget according to its published annual rank in the Portal of Scientific Journals of Iranian Ministry of Science, Research and Technology for costs including those pertaining to setup and maintenance of the publication infrastructure, routine operation of the Journal, processing of manuscripts through peer-reviews, editing, publishing, maintaining the scholarly record, and archiving.

Publication Ethics

Violation of Publication Ethics

The Editorial board of IJVST acknowledges that plagiarism is unacceptable in any of its forms:

Plagiarism:

Plagiarism is intentionally using someone else's ideas or other original material as if they are one's own. Copying even one sentence from someone else's manuscript, or even one of your own that has previously been published, without proper citation is considered by the JAM as plagiarism. All manuscripts under review or published with JAM are subject to screening using plagiarism prevention software (e.g. iThenticate). Thus, plagiarism is a serious violation of publication ethics.

Simultaneous Submission:

Care should be taken to ensure that the work has not been published elsewhere, in any language and is not simultaneously submitted to other journals.

Duplicate Publication:

Duplicate publication occurs when two or more articles, without full cross referencing, share essentially the same hypotheses, data, discussion points, and conclusions.

Redundant Publications:

Redundant publications involve the inappropriate division of study outcomes into several articles, most often consequent to the desire to plump academic vitae.

Data Fabrication:

Data fabrication means the researcher did not really carry out the study, but made up data or results and had recorded or reported the fabricated information. Data falsification means the researcher did the experiment, but manipulated, changed, or omitted data or results from the research findings.

Citation Manipulation:

Citation Manipulation implies excessive citations in the submitted manuscript that do not contribute to the scholarly content of the article and have been included solely for the purpose of increasing citations to a given author's work, or to articles published in a particular journal. This leads to misrepresenting the importance of the specific work and journal in which it appears and is thus a form of scientific misconduct.

Improper Author Contribution or Attribution:

All listed authors must have made a significant scientific contribution to the research in the manuscript and approved all its claims. Do not forget to list everyone who made a significant scientific contribution, including students and laboratory technicians.

Handling Misconduct Cases

The Editorial board of IJVST takes the necessary measures to examine the incoming papers on their originality, reliability of contained information and correct use of citations.

-If any of the unethical publishing behavior is detected by the Journal Editorial board or by one of the reviewers, the first action is to inform the Editor-in-chief by supplying copies of the relevant material and a draft letter to the corresponding author asking for an explanation in a nonjudgmental

manner.

- If the infraction is less severe, the Editor, upon the advice of the Committee on Publication Ethics, sends the author a letter of reprimand and reminds the JAM publication policies; if the manuscript has been published, the Editor may request the author to publish an apology in the journal to correct the record.

- If the author's explanation is unacceptable and it seems that serious unethical conduct has taken place, the matter is referred to the Publication Committee via Editorial board. After deliberation, the Committee will decide whether the case is sufficiently serious to warrant a ban on future submissions.

Post-Publication Discussions and Corrections

This journal allows debate post publication on journal's site, through "Send comment about this article" section to the editor up to one month before final publication. Our mechanisms for correcting, revising or retracting articles after publication depends on the content of the received comment and if the sent comments are useful and applicable for readers/authors, they will be showed under reference section of the articles pages.

Complaint Policy

If the authors disagree with the editorial decision on their manuscripts, they have a right to appeal. Authors who wish to appeal an editorial decision should contact the Editor-in-Chief of the Iranian Journal of Veterinary Science and Technology. In such cases the Editor-in-Chief will review the manuscript, the editorial and peer reviewers' comments and gives his/her decision for accepting or rejecting a manuscript. Editor-in-Chief may, if so required, send the manuscript to a new handling editor for a fresh editorial review and to new reviewer for further peer reviewing. In such case, the final decision maker will be the Editorial board of the journal.

How to Make a Complaint

The procedure to make a complaint is quite simple. The complaint can be made by writing an e-mail to: ijvst@um.ac.ir. All complaints will be acknowledged within a week.

PEER REVIEW PROCESS

Iranian Journal of Veterinary Science and Technology peer reviews all submitted manuscripts with contents within the scope of the journal.

Initial assessment

The submitted manuscript will be subjected to a primary review by the editor or a member of the editorial board for suitability and relevance of the findings to the scope of the journal and quality of the science presented in the paper (sufficient originality, having a message that is important to the general field of Veterinary Medicine, quality of data, novelty, English language, and overall manuscript quality) within two weeks. If the paper is evaluated to be relevant to the scope of the journal and having enough scientific rigor and novelty, it will be sent for the next stage. Otherwise, those manuscripts which are evaluated as not-appropriate in the initial review will be rejected at this stage.

Initial screen

The initial screen will be performed by the editorial office for the structure and format of the manuscript.

Peer review (double-blind)

The manuscripts which are found to be appropriate after the initial screen will be sent for external review by experts in the related field. We have prepared a checklist for reviewers that summarizes their evaluation of the manuscript. The items in this checklist are:

1. TITLE is clear and adequate
2. ABSTRACT clearly presents objects, methods, and results.
3. INTRODUCTION well-structured and provides a rationale for the experiments described.
4. MATERIALS AND METHODS are sufficiently explained and is detailed enough to be reproduced.
5. RESULTS are clearly presented and supported by figures and tables.
6. DISCUSSION properly interprets the results and places the results into a larger research context, and contains all important references.
7. Conclusions are logically derived from the data presented.
8. English Language/style/grammar is clear, correct, and unambiguous.
9. Figures and tables are of good quality and well-designed and clearly illustrate the results of the study.
10. References are appropriate.
11. Regarding this article are you concerned about any issues relating to author misconduct such as plagiarism and unethical behavior.
12. Comments on the importance of the article.

Final Decision

Based on the reviewers' recommendations a final decision is made by the editor and if needed the help of a member of the editorial board (depending on the field of study). Decisions will include accept, minor revision, major revision with and without re-review, and reject. We aim to reach a final decision on each manuscript as soon as their review results are available.

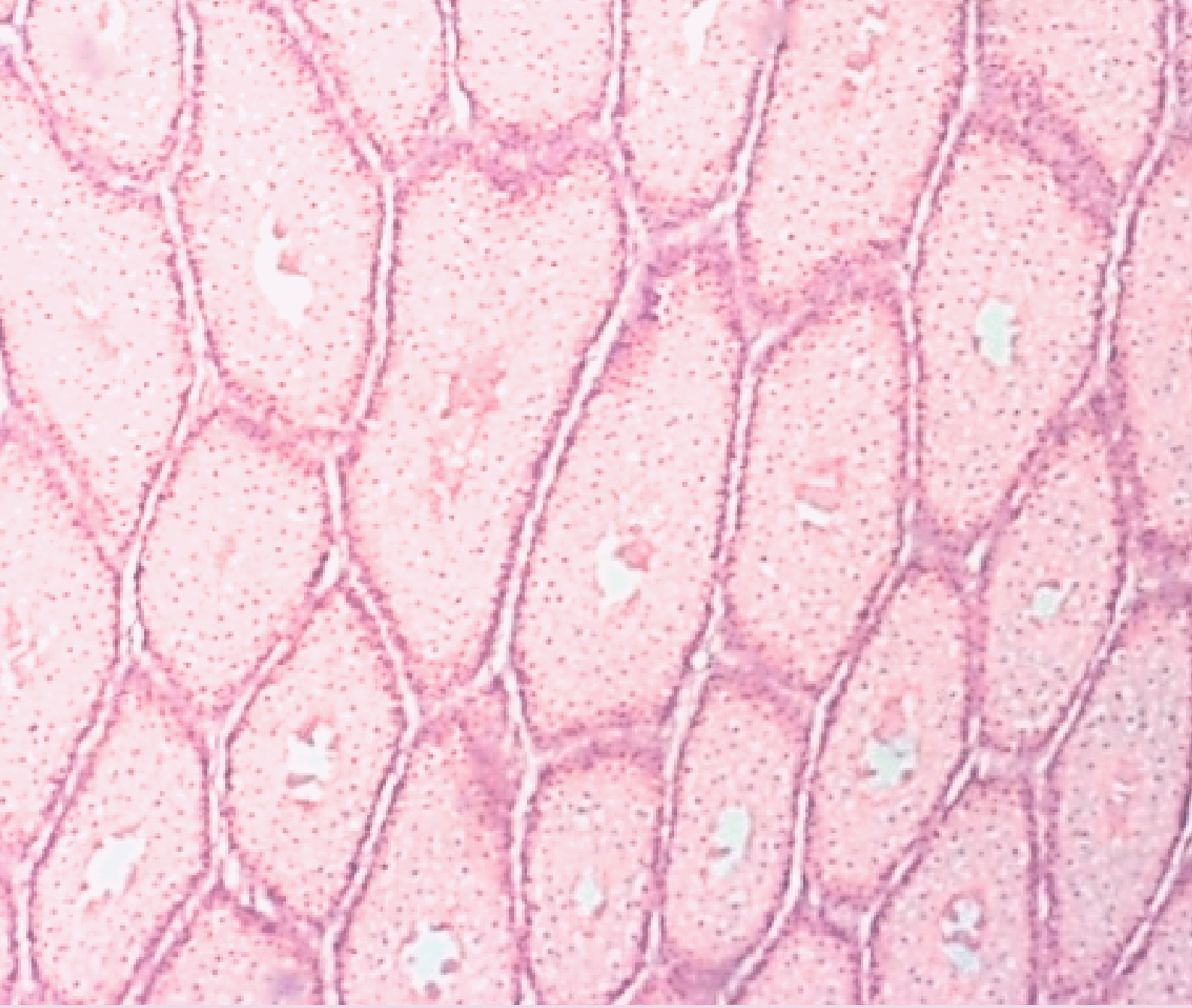

Iranian Journal of Veterinary Science and Technology

Faculty of Veterinary Medicine, Ferdowsi University of Mashhad,
Azadi Square, Mashhad, IRAN
P.O. Box: 1793; Postal Code: 9177948974

Tel: 0098 51 3880 3742
Fax: 0098 51 3876 3852

Web: ijvst.um.ac.ir
Email: ijvst@um.ac.ir